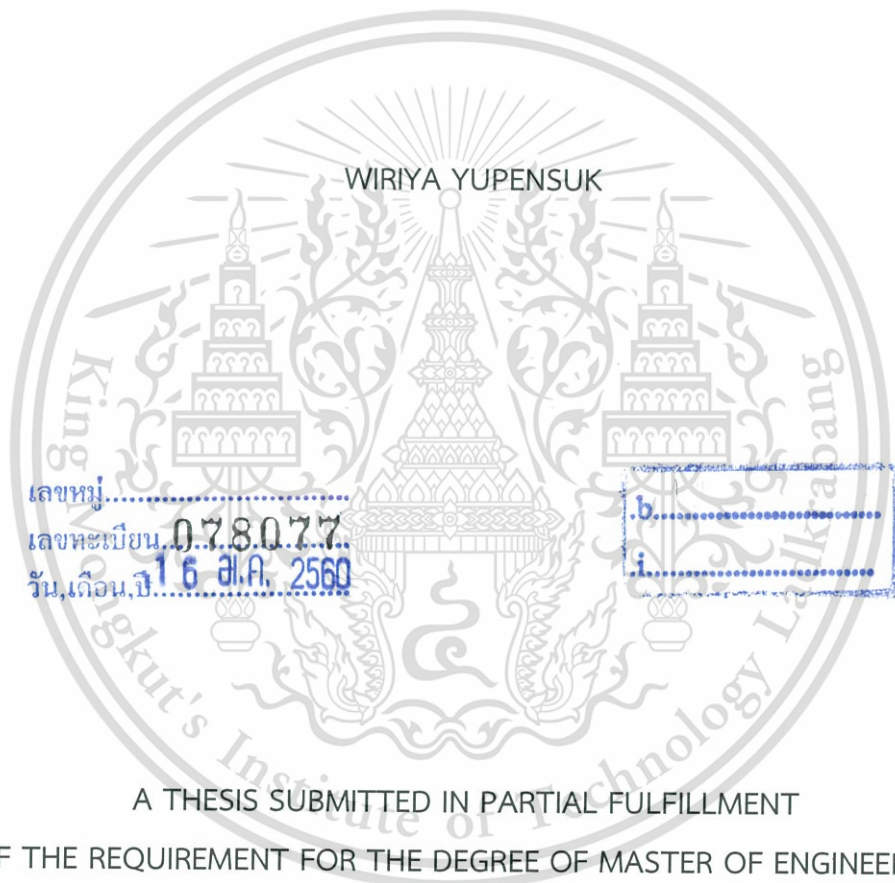


สำนักหอสมุดกลาง พระจอมเกล้าลาดกระบัง

PARAMETRIC STUDY OF SHIPPING COMB
ON INSERTION AND REMOVAL FORCES



E078077



เลขหมู่.....
เลขทะเบียน 078077
วัน,เดือน,ปี 16 ต.ค. 2560



A THESIS SUBMITTED IN PARTIAL FULFILLMENT
OF THE REQUIREMENT FOR THE DEGREE OF MASTER OF ENGINEERING
IN DATA STORAGE TECHNOLOGY
INTERNATIONAL COLLEGE
KING MONGKUT'S INSTITUTE OF TECHNOLOGY LADKRABANG
2016
KMITL-2016-IC-M-005-005



COPYRIGHT 2016

INTERNATIONAL COLLEGE

KING MONGKUT'S INSTITUTE OF TECHNOLOGY LADKRABANG

This material is reserved for educational use only, not allowed for commercial use.

Forbidden to modify the content, and cite the document when use.

หัวข้อวิทยานิพนธ์	การศึกษาเชิงพารามิเตอร์ต่อแรงในการใส่และถอดหวีป้องกันหัวอ่าน
นักศึกษา	นายวิริยะ อยู่เป็นสุข
รหัสประจำตัว	54600701
ปริญญา	วิศวกรรมศาสตรมหาบัณฑิต
สาขาวิชา	เทคโนโลยีการบันทึกข้อมูล
พ.ศ.	2559
อาจารย์ที่ปรึกษาวิทยานิพนธ์	ผศ.ดร.มนต์ศักดิ์ พิมสาร

บทคัดย่อ

หวีป้องกันหัวอ่านเป็นชิ้นส่วนหนึ่งในหัวอ่านฮาร์ดดิสก์ที่ประกอบเข้ากับหัวอ่านจนกระทั่งหัวอ่านถูกประกอบเข้าไปในฮาร์ดดิสก์ แรงที่ใช้ในการใส่และถอดหวีป้องกันนี้หากมากเกินไปจะมีผลกับเครื่องมืออัตโนมัติในสายการผลิต ความแตกต่างของขนาดลิ้มยึดของหวีจากแต่ละแท่นฉีด ส่งผลให้แรงในการใส่และถอดของหวีจากแต่ละแท่นฉีดแตกต่างกัน จุดประสงค์ของการศึกษานี้เพื่อหาความสัมพันธ์ระหว่างมิติของลิ้มยึดซึ่งประกอบด้วยความสูงของปุ่มยึด ความกว้างของฐานลิ้ม และความหนาของก้านยึด กับแรงในการใส่และถอดของหวีป้องกัน แล้ววิเคราะห์ว่าตัวแปรใดส่งผลกับแรงเหล่านี้มากกว่ากัน เพื่อนำผลที่ได้ไปใช้ในภาคการผลิตหวีป้องกันที่เหมาะสม และแจ้งไปยังผู้ผลิตหวีป้องกันหัวอ่านให้ทำการปรับปรุงแม่พิมพ์ฉีดให้ได้ขนาดตามที่ระบุ เพื่อให้หวีป้องกันหัวอ่านที่ได้มาจากการปรับหุ้มีค่าแรงในการใส่และถอดหวีป้องกันตามที่ต้องการ การศึกษาพฤติกรรมของหวีป้องกันหัวอ่านนี้ใช้วิธีการวิเคราะห์ด้วยไฟไนต์เอลิเมนต์ ผลจากการวิเคราะห์แสดงให้เห็นว่า ความสูงของปุ่มยึดส่งผลกับแรงการใส่และถอดหวีมากที่สุด แต่ก่อนที่จะตัดสินใจแก้ไขในส่วนของความสูงของปุ่ม ทางผู้ออกแบบหวีป้องกันจะต้องทำการตรวจสอบความสูงของปุ่มยึดจากกลุ่มตัวอย่างของหวีป้องกันก่อน ว่ามีค่าของความสูงอยู่ใกล้เคียงกับค่ากลางตามที่ออกแบบไว้หรือไม่ หากความสูงของปุ่มยึดอยู่ที่ค่ากลางตามที่ออกแบบไว้ก็ไม่ควรจะทำ การแก้ไขค่าความสูงของปุ่ม แต่ควรเลือกแก้ไขที่ความกว้างของฐานลิ้ม หรือความหนาของก้านยึดแทน ประโยชน์ที่ได้จากการศึกษานี้คือ ลดเวลาในการออกแบบหวีป้องกันและลดค่าใช้จ่ายในการแก้ไขแม่พิมพ์ฉีดของหวีป้องกัน

Thesis Title	Parametric Study of Shipping Comb on Insertion and Removal Forces
Student	Wiriya Yupensuk
Student ID	54600701
Degree	Master of Engineering
Program	Data Storage Technology
Year	2016
Thesis Advisor	Asst.Prof.Dr.Monsak Pimsarn

ABSTRACT

Shipping comb is a component in Head Stack Assembly (HSA) which is assembled in HSA until the HSA is merged into a hard disk drive. The insertion and removal forces of shipping comb are critical for automation tooling. The variation of latch dimension from different mold results in force varying and sometimes also leads to out of specification. Thus, this thesis aims to study the sensitivity of shipping comb latch dimensions, namely, bump height, base width and bar thickness, and to predict appropriate dimensions for mold modification in order to meet insertion and removal force requirement. The transient structural of Finite Element Analysis (FEA) is employed to simulate the behavior of the shipping comb model. From the simulated results, it is found that the bump height is provided highest sensitivity for both of insertion and removal forces, but before making decision to modify the mold, shipping comb designer must review on dimension of shipping comb from the first lot. If the bump height is equal to nominal design, the bump height should be maintained and select to adjust on base width or bar thickness instead. Benefits of this thesis are to reduce design process time and to save cost of the mold modification.

This material is reserved for educational use only, not allowed for commercial use.

Forbidden to modify the content, and cite the document when use.

ACKNOWLEDGEMENTS

This thesis would not be accomplished if it was without the guidance and the support of several persons who contributed and extended their appreciated assistance in the completion of this research.

First, I would like to sincerely thank for scholarship, financial, equipment and technical expertise support under the collaboration development of Seagate Technology (Thailand) Ltd., National Electronics and Computer Technology Center (NECTEC, National Science and Technology Development Agency (NSTDA) and College of Data Storage Innovation, King Mongkut's Institute of Technology Ladkrabang.

I am utmost gratitude to my advisor Asst.Prof.Dr.Monsak Pimsarn, who provided valuable advices , always encouraged, gave time and chances to help me go over all the obstacles in the completion this research.

Finally, I would like to express my deepest appreciation and sincere gratitude to family and my friends for their love, moral support, and encouraging for the entire of my study.

Wiriya Yupensuk

CONTENTS

	Page
บทคัดย่อ.....	I
ABSTRACT.....	II
ACKNOWLEDGEMENTS.....	III
CONTENTS.....	IV
LIST OF FIGURES.....	VII
LIST OF TABLES.....	X
LIST OF ABBREVIATIONS.....	XI
CHAPTER 1 INTRODUCTION.....	1
1.1 Background.....	1
1.2 Objectives.....	4
1.3 Scope of work.....	4
1.4 Expected benefits.....	5
CHAPTER 2 LITERATURE REVIEWS.....	6
CHAPTER 3 RELATED THEORY.....	15
3.1 Mechanical problem.....	15
3.2 Finite element method.....	16
3.3 Definition and purpose of transient dynamic analysis.....	16
3.4 Transient analysis method.....	18
3.4.1 Nonlinearities in transient analysis.....	18
3.4.2 Three sources of structural nonlinearity.....	19
3.3.2.1 Changing status.....	19
3.3.2.2 Geometric nonlinearities.....	20
3.3.2.3 Material nonlinearities.....	20
3.3.3 Contact Types.....	21
3.5 Newton-raphson technique.....	23

This material is reserved for educational use only, not allowed for commercial use.

Forbidden to modify the contents, and cite the document when use.

CONTENTS (CONT.)

	Page
3.6 Analysis settings in full transient analysis.....	25
3.6.1 Time step size.....	25
3.6.2 Solver controls – solver type.....	26
3.6.3 Damping control.....	26
CHAPTER 4 RESEARCH METHODOLOGY.....	28
4.1 Assumption.....	29
4.2 Material property	29
4.2.1 Friction coefficient.....	28
4.2.2 Stress-strain curve	31
4.3 Model creation.....	33
4.4 Model setting in ANSYS.....	34
4.5 Parametric study.....	38
CHAPTER 5 RESULT AND DISCUSSION.....	40
5.1 Friction identification result	40
5.2 Stress-Strain result	41
5.3 Model validation result.....	43
5.4 Experimental result.....	54
5.4.1 Effect of the bump height	54
5.4.2 Effect of the base width	58
5.4.3 Effect of the bar thickness	62
5.5 Discussion.....	67
CHAPTER 6 CONCLUSIONS AND SUGGESTION.....	69
6.1 Conclusions.....	69
6.2 Suggestions	71
References.....	72

This material is reserved for educational use only, not allowed for commercial use.

Forbidden to modify the content, and cite the document when use.

CONTENTS (CONT.)

	Page
APPENDIX A.....	73
Publication.....	73
APPENDIX B.....	80
ANSYS Setting.....	80
AUTHOR BIOGRAPHY.....	98



LIST OF FIGURES

Figures	Page
1.1 Shipping comb in HSA	1
1.2 HSA process flow	2
1.3 Shipping comb in HDA	3
2.1 FEA Model of HGA components and shipping comb	6
2.2 Mesh models of HGA components and shipping comb	7
2.3 HGA condition (a) before mounted (b) after mounted)	7
2.4 Gramload data of each spreader pin size	8
2.5 Graph relationship of maximum load and wash cycle	9
2.6 FEM Model of shipping comb and fixture	10
2.7 Position and direction of force applied	11
2.8 Mesh model of shipping comb and fixture	12
2.9 Results comparison	12
2.10 FEM model and mesh model of shipping comb and actuator	13
2.11 Interesting parameters	14
3.1 Force diagram of mass in nonlinear equation	17
3.2 Graph force (F) and displacement (u) in linear analysis.....	19
3.3 Graph force (F) and displacement (u) in nonlinear analysis	19
3.4 Changing status of mesh in structural nonlinear analysis	19
3.5 Example of deformation in structural nonlinear analysis	20
3.6 Graph stress-strain of nonlinear material	20
3.7 Enforce contact and not enforce contact.....	21
3.8 Penalty-based	22
3.9 Iteration step in newton-raphson method	23
3.10 Iteration substep in newton-raphson method	24
3.11 Time sequence from auto time stepping	25

LIST OF FIGURES (CONT.)

Figures	Page
4.1 Study flow	28
4.2 Tool and force diagram	30
4.3 Specimen of comb material and Universal Testing Machine.....	31
4.4 Engineering Stress-Strain and True Stress-Strain	31
4.5 (a) Actual model (b) Simplified model	33
4.6 Model shipping comb and actuator	34
4.7 Discretized model of shipping comb and actuator.....	35
4.8 Fixed support on actuator	35
4.9 Cylindrical support on shipping comb	36
4.10 Cylindrical support on probe	36
4.11 Plane for displacement and force sensor	37
4.12 Interesting dimension	38
5.1 Engineering stress-strain curve of shipping comb material	41
5.2 True Stress-Strain curve of shipping comb material	42
5.3 Comparison of simulation result and Measurement result.....	43
5.4 Probe reaction force in x direction variation from simulation	44
5.5 Force diagram between shipping comb and actuator at first contact state.....	45
5.6 Simulation model at first contact state.....	45
5.7 Force diagram between shipping comb and actuator at negative peak.....	46
5.8 Simulation model at negative peak.....	46
5.9 Force diagram between shipping comb and actuator at steady in negative.....	47
5.10 Simulation model at steady in negative zone.....	47
5.11 Force diagram between shipping comb and actuator at force trends to zero..	48
5.12 Simulation model at force trends to zero	48
5.13 Force diagram between shipping comb and actuator at zero force.....	49
5.14 Simulation model at zero force	49
5.15 Force diagram between shipping comb and actuator at positive peak.....	50
5.16 Simulation model at positive peak.....	50

This material is reserved for educational use only, not allowed for commercial use.

Forbidden to modify the content, and cite the document when use.

LIST OF FIGURES (CONT.)

Figures	Page
5.17 Force diagram between shipping comb and actuator at steady in positive.....	51
5.18 Simulation model at force steady in positive.....	51
5.19 Force from experiment	52
5.20 Comparison of simulation result and measurement result	53
5.21 Force from increasing the bump height	54
5.22 Force from decreasing the bump height	55
5.23 Simulation result bump height variation	56
5.24 Linear regression of bump height	57
5.25 Force from increasing the base width	58
5.26 Force from decreasing the base width	59
5.27 Simulation result base width variation	60
5.28 Linear regression of base width	61
5.29 Force from increasing the bar thickness	62
5.30 Force from decreasing the bar thickness	63
5.31 Simulation result of bar thickness variation	64
5.32 Linear regression of bar thickness	65
5.33 Normalized data of insertion forces	66
5.34 Normalized data of removal forces	66
5.35 Surface of simulation model and experiment	67
5.36 Sensitivity of all parameters	68
6.1 Mold insert of shipping comb latch	70

LIST OF TABLES

Tables	Page
3.1 Contact type in nonlinear analysis	21
4.1 Material of friction test component	30
4.2 Percent variation of each parameter	39
5.1 Measurement data and friction coefficient	40



LIST OF ABBREVIATIONS

ANSYS	Commercial finite element software name
EDM	Electrical discharge machining
ESD	Electro static discharge
FEM	Finite element method
FOS	Flex on suspension
HDA	Hard disk drive assembly
HGA	Head gimbal assembly
HHT	Hilber-Hughes-Taylor
HSA	Head stack assembly
MAC	Mini auto collimator
MARPOSS	Company name of machine
OCR	Optical character reader
PCG	Preconditioned conjugate gradient

CHAPTER 1

INTRODUCTION

1.1 Background

Shipping comb is a component in head stack assembly (HSA) which is assembled in HSA, as shows in Figure 1.1, until the HSA is merged into a hard disk drive assembly (HDA). In HSA process flow, as shown in Figure 1.2, the shipping comb is inserted and removed in many operations in order to measure the HSA parameters.

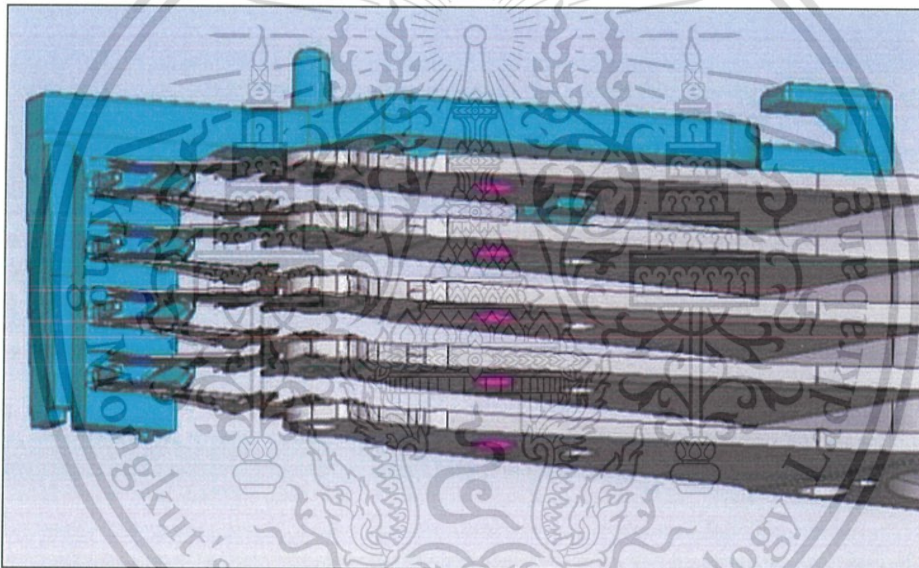


Figure 1.1 Shipping comb in HSA

The insertion and removal forces of shipping comb are critical property for many machines because HSA will be damaged if the machine cannot remove the shipping comb before measurement or immobile it back into the HSA. Especially in drive assembly process, the shipping comb is removed in complicate method, as shown is Figure 1.3. These forces are complex properties that are contributed from many parameters such as shape, material property, contact condition etc.

This material is reserved for educational use only, not allowed for commercial use.

Forbidden to modify the content, and cite the document when use.

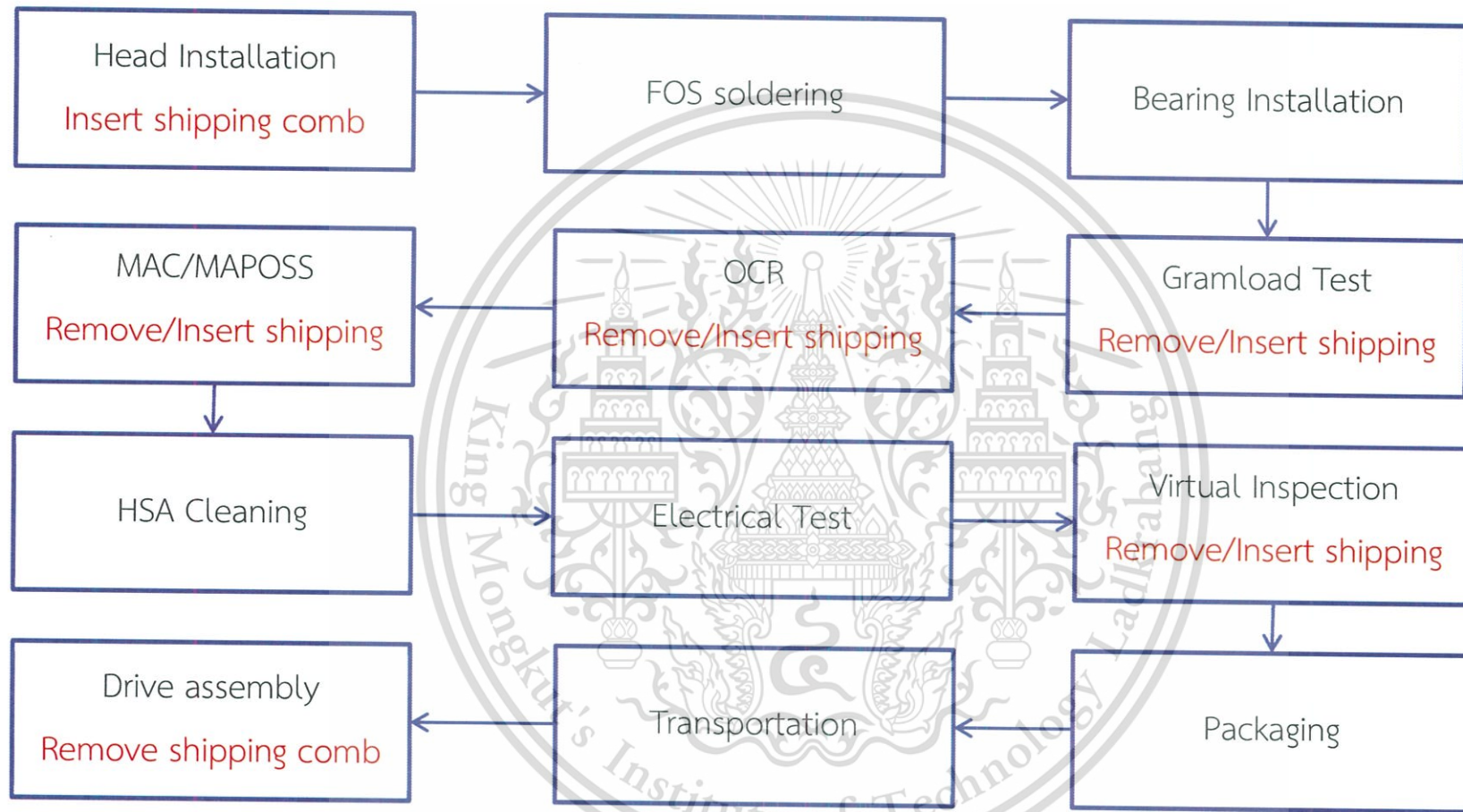


Figure 1.2 HSA process flow

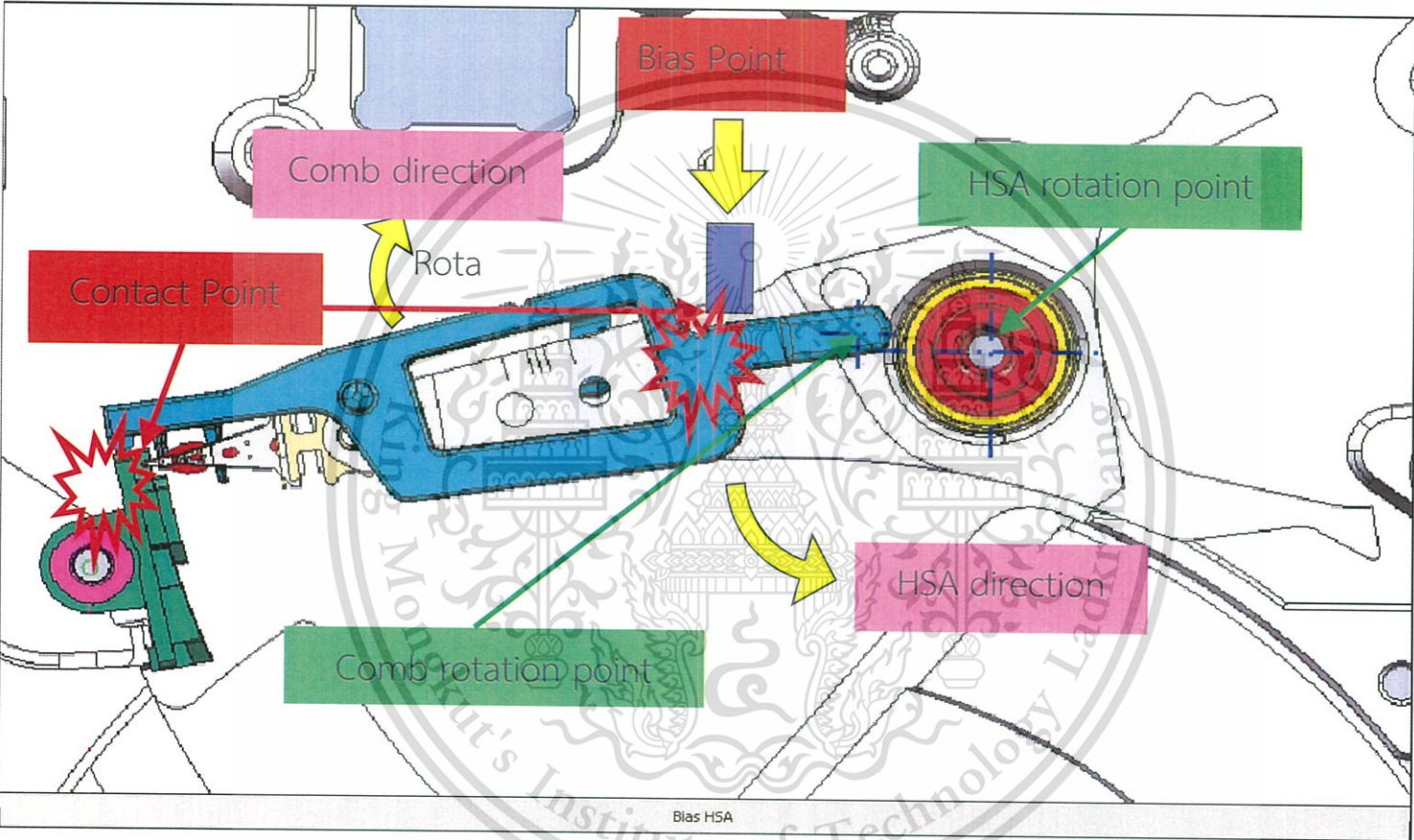


Figure 1.3 Shipping comb in HDA

Once new HSA design was launched, shipping comb designer has to design the shipping comb to support new HSA design. After design of the shipping was completed, the 3D model and drawing will be sent to mold supplier to start mold fabrication then mold supplier will shift the shipping first lot to shipping comb designer to review design and to measure shipping comb insertion and removal force. In the past the shipping comb has to be modified several times before meet the insertion and removal force specification.

1.2 Objectives

1.2.1 To study the behavior of shipping comb insertion and removal forces from simulation and validate with experimental result.

1.2.2 To study the parameters that effect to the shipping comb insertion and removal forces.

1.2.3 To identify the most affected parameter on those forces.

1.3 Scope of Work

1.3.1 Shipping comb in this thesis is the shipping comb of one product in 3.5 inch products of hard disk drive.

1.3.2 Numerical study of shipping comb insertion and removal force behavior will be analyzed using finite element method in ANSYS program [1].

1.3.3 Parameters used in the simulation study are based on current data use.

1.3.4 All surface of simulation model are assumed to be smooth.

1.4 Expected Benefits

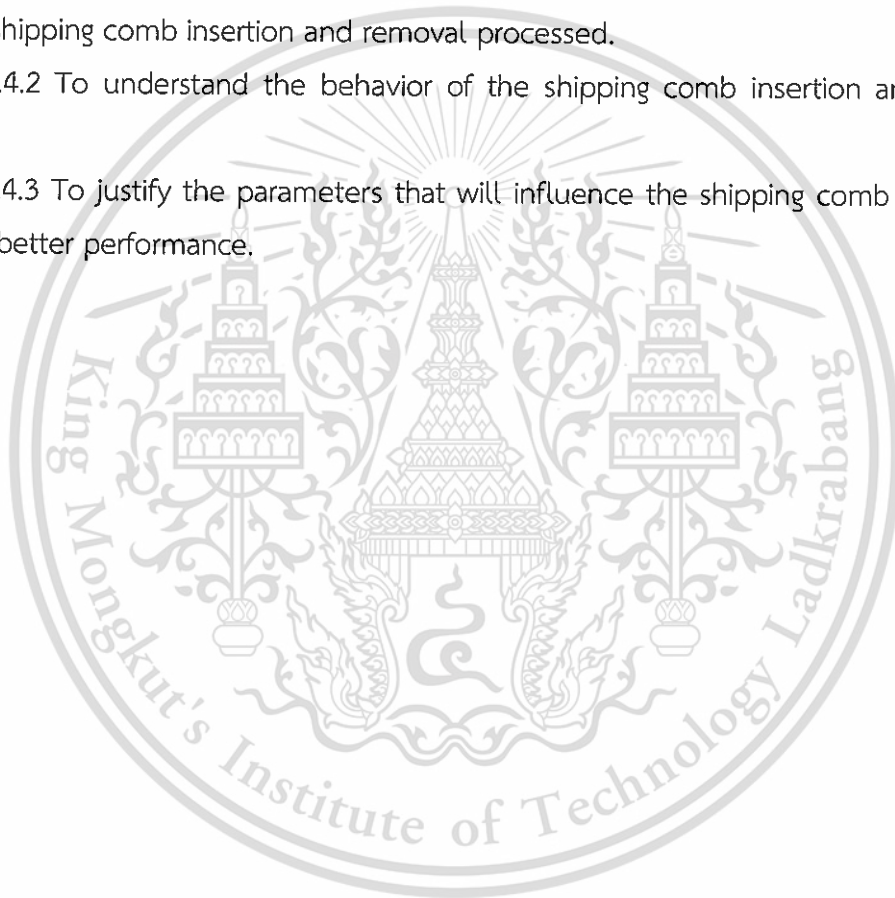
1.4.1 Time to design the shipping comb can be reduced if we can reduce time to modify the shipping comb mold to make the shipping comb insertion and removal force to meet requirement.

1.4.2 The cost of mold modification can be reduced if we can reduce time to modify the mold.

1.4.1 To be able to use the finite element method to simulate dynamic problem such as shipping comb insertion and removal processed.

1.4.2 To understand the behavior of the shipping comb insertion and removal forces.

1.4.3 To justify the parameters that will influence the shipping comb design and leads to better performance.



CHAPTER 2

LITERATURE REVIEWS

In recent years, many researchers have used the finite element to study on HSA component but just few researchers have studied on the shipping comb.

In 2009, Kajornsak and Vissawat [2] studied HGA behaviors after mounted with shipping comb. In HSA process shipping comb is mounted to HSA adjacent the HGA area, at the end of suspension. Shipping is purposed to prevent the vibration of the slider when transfer in HSA process. Component of HGA and shipping comb are created for finite element method (FEM), as shown in Figure 2.1 and the model are meshed to be shell mesh, as shown in Figure 2.2. The study model is started from condition before mounted the shipping come to condition after mounted the shipping comb, as shown in Figure 2.3 and then measuring gramload on this condition.

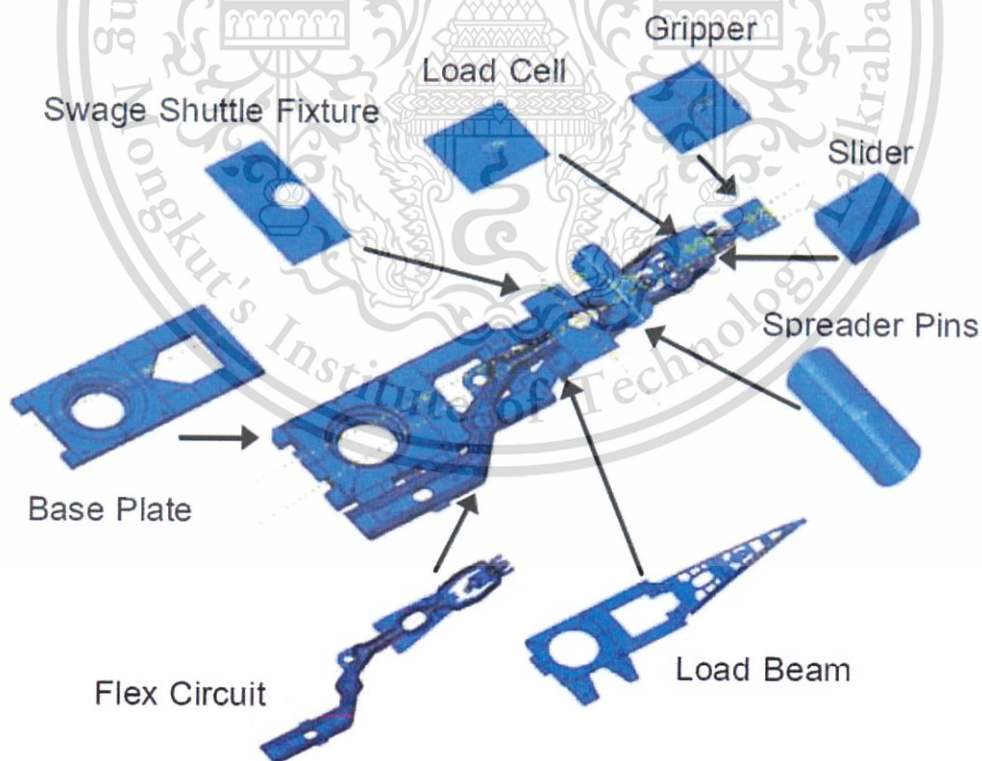


Figure 2.1 FEM Model of HGA components and shipping comb



The spreader comb is a representative of shipping comb finger. In this study, the holder positions of spreader pin and spreader pin diameter are varied to study the gramload force. The gramload data of each pin size and holding position are compared and analyzed, as shown in Figure 2.4. The result showed that the spreader pin size has a great effect on gramload force.

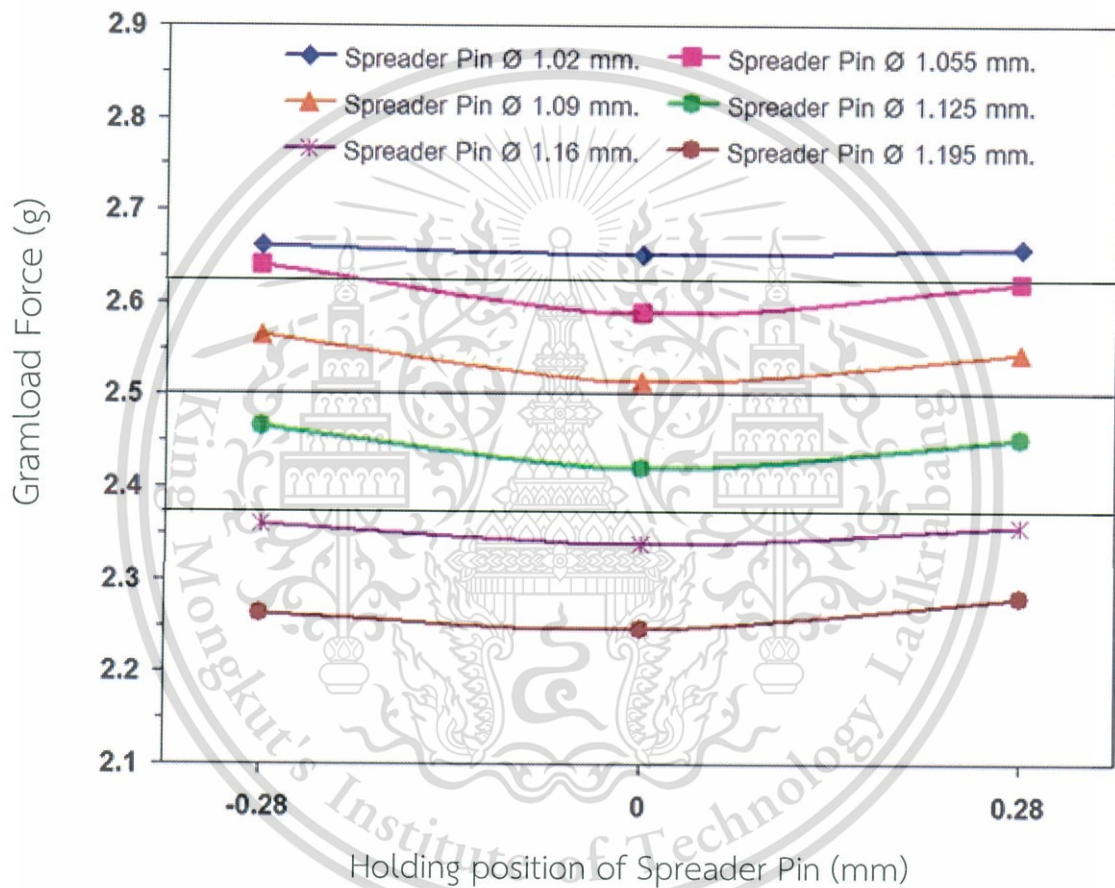


Figure 2.4 Gramload data of each spreader pin size.

In 2010, Chalermchai [3], studied effect of temperature and time to properties of polycarbonate composite which is a material of the shipping comb. The specimens of polycarbonate are grouped by number of time of washing and baking. The temperature and treatment time is result to changing the polycarbonate composite from ductile to brittle material. The strength of shipping comb is reduced after past washing process and will be stable after 7-15 cycles, as shown in Figure 2.5.

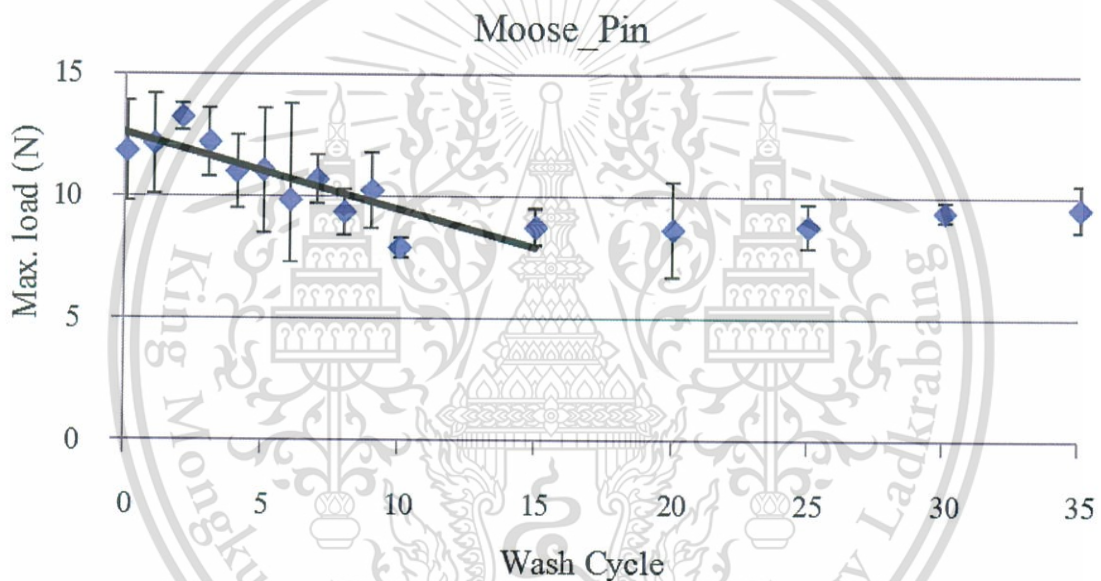


Figure 2.5 Graph relationship of maximum load and wash cycle.

In 2010, Thawisanee [4] analyzed the failure of polycarbonate part by using finite element method (FEM). The shipping comb part is selected to study force from tensile test and force from FEM program. FEM model is created for force applied on many positions and directions, as shown in Figure 2.6 and Figure 2.7.

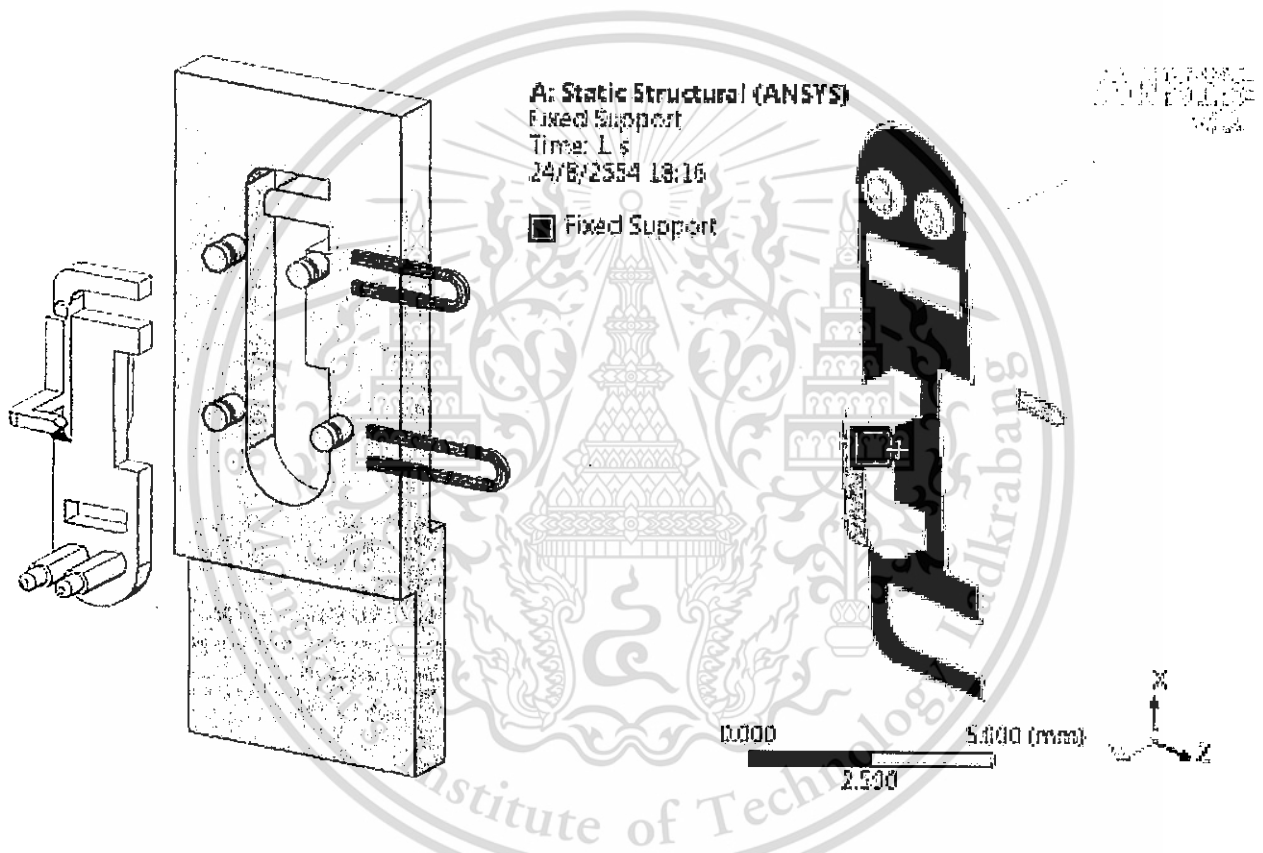


Figure 2.6 FEM Model of shipping comb and fixture.

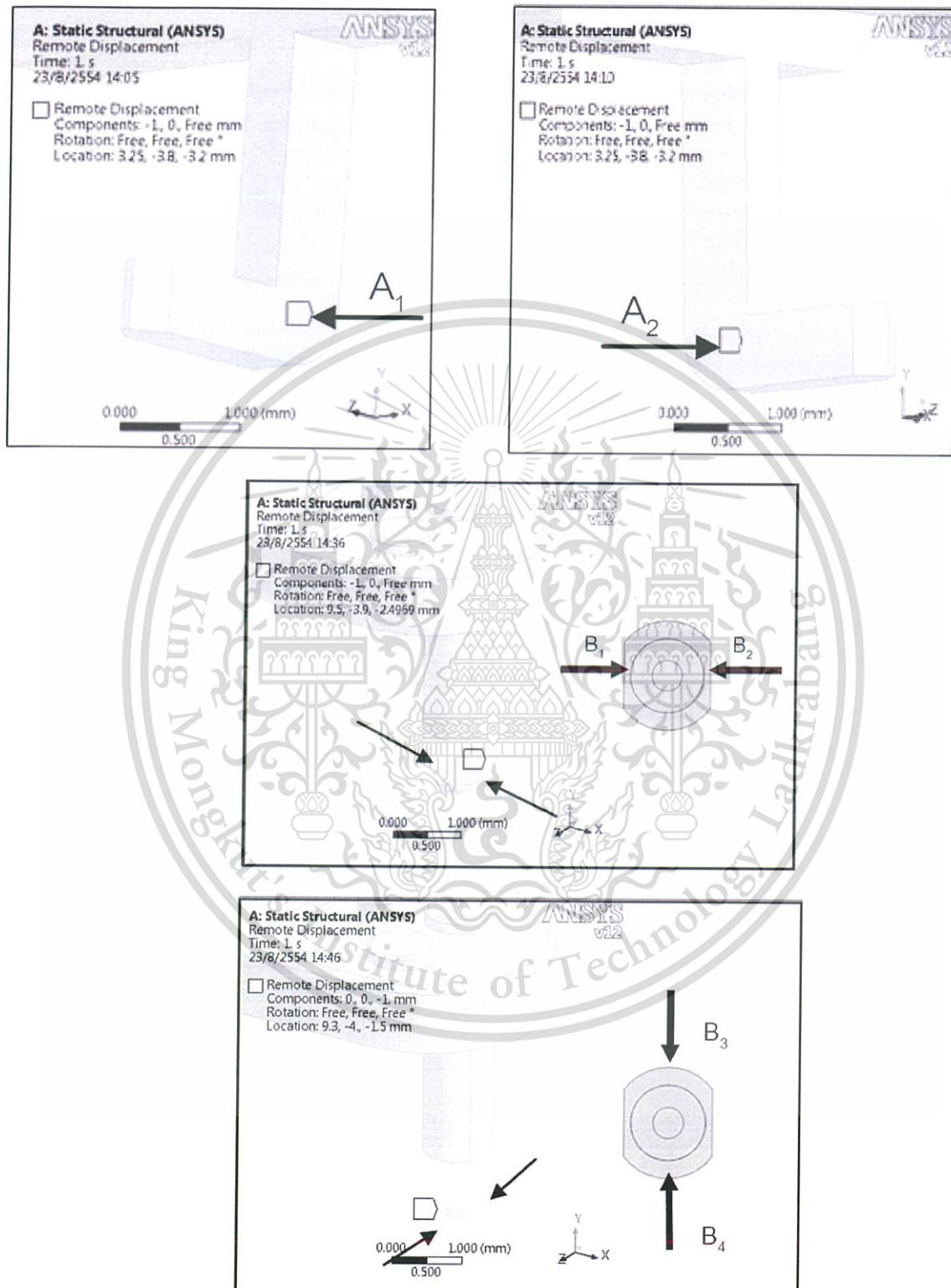


Figure 2.7 Position and direction of force applied.

In this study, hex dominant is mesh type that selected for analysis, as shown in Figure 2.8, and the model are analyzed in the static condition.

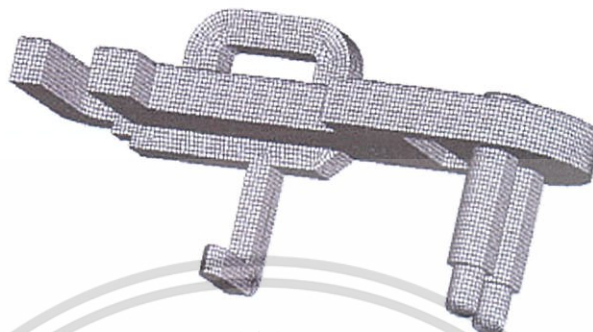


Figure 2.8 Mesh model of Shipping comb and fixture.

The force comparison between experiment and simulation, referred to Figure 2.9, showed that the force from simulation is lower than experiment about 10% or approximately 90% of accuracy. It implies that simulation model and software are verified.

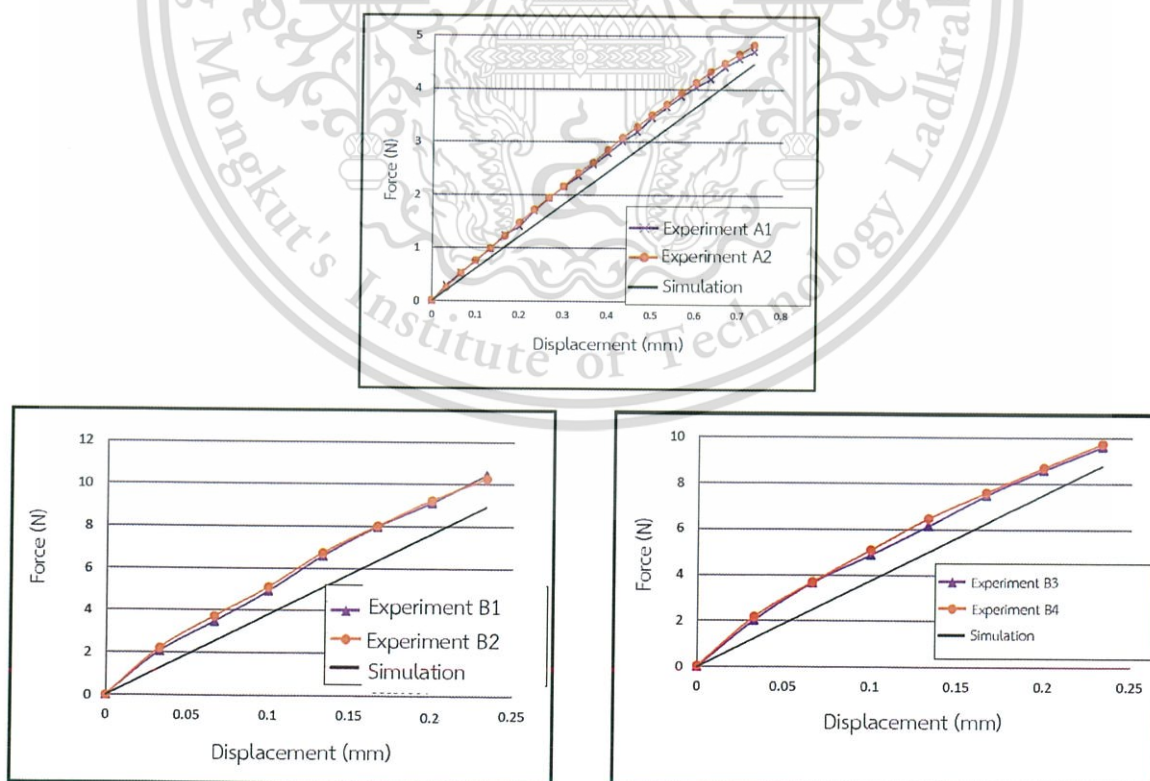


Figure 2.9 Comparison of force from simulation and experiment for all models

This material is reserved for educational use only, not allowed for commercial use.

Forbidden to modify the content, and cite the document when use.

In 2011, Suriya [5] studied the shape of shipping comb concerning with shipping comb insertion and removal forces by using finite element method. This research studies on 3 parameters such as insertion chamfer angle, symmetry gap and fillet radius.

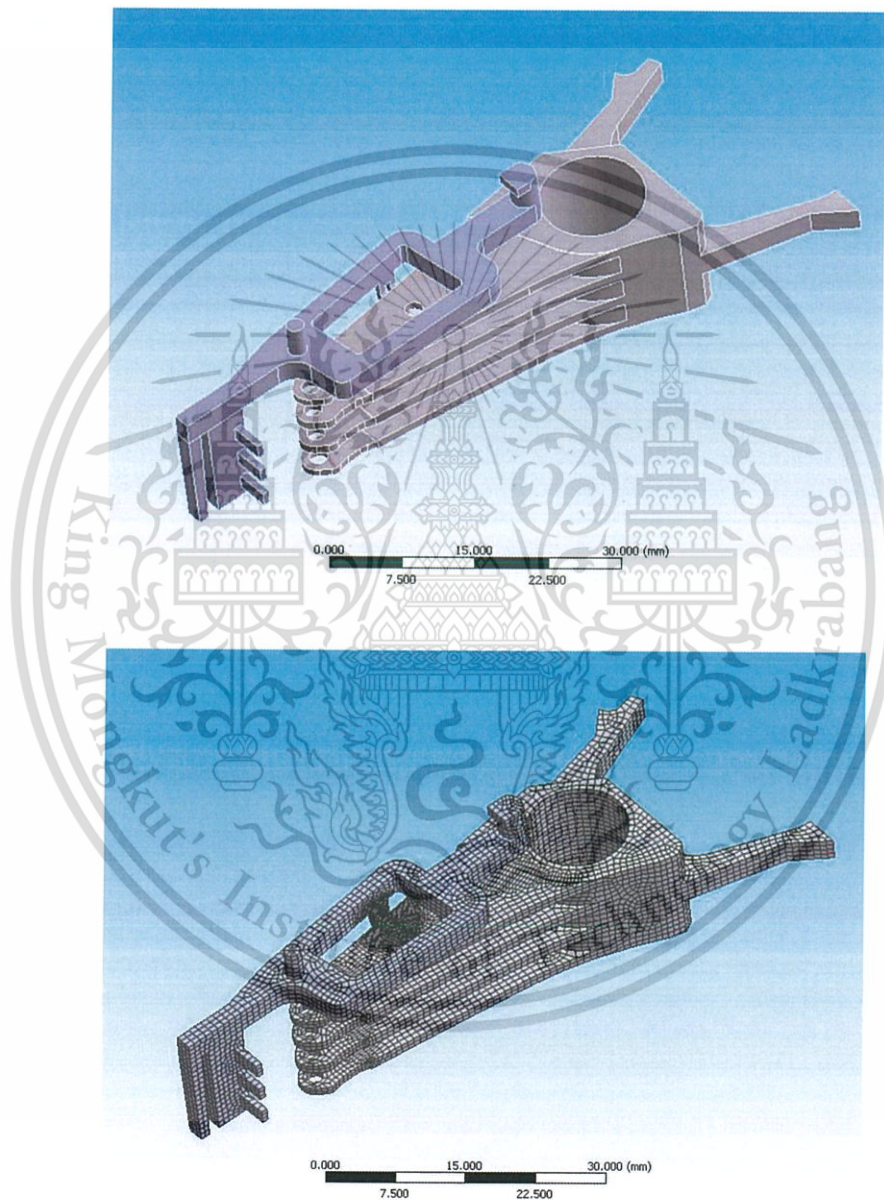


Figure 2.10 FEM model and mesh model of shipping comb and actuator.

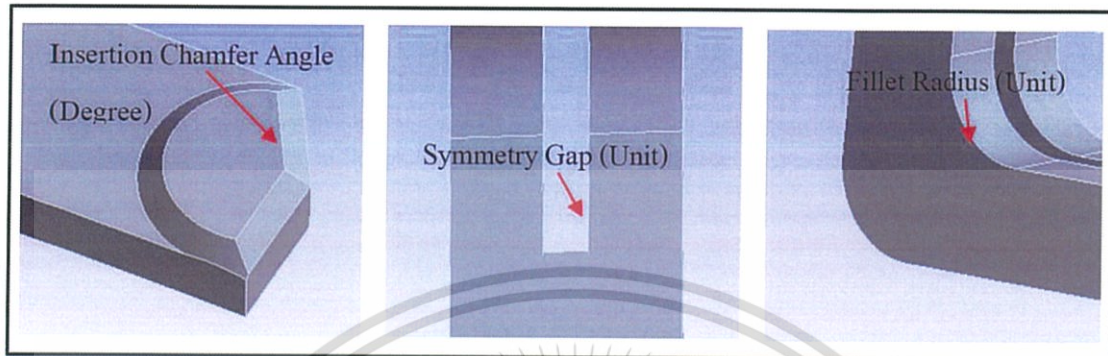


Figure 2.11 Interested parameters.

The result showed that chamfer on latch is the major contributor to shipping comb insertion and removal forces. He suggested shipping comb designers to focus on the chamfer when they design the shipping comb

However, in case modification shipping comb, the chamfer is not the good parameter to adjust because chamfer is very difficult to measure and control because the complexity of shipping comb mold [6], especially on the chamfer. The process to modify mold insert on the chamfer is electrical discharge machining (EDM) which is difficult to control the dimension of part. The precise dimension of chamfer is required very high investment for high-precision EDM machine.

CHAPTER 3

RELATED THEORIES

3.1 Mechanical Problem

The behavior of mechanical is the description of how loads cause deformation. The relationship between an object's deformations and the forces that are applied are called the mechanical properties of the object. The mechanical properties are sometimes called constitutive laws because the mechanical properties describe how an object is constituted. When solving mechanics problems one has to make assumptions and idealizations about the constitutive laws applicable to the parts of a system. The set of assumptions about the mechanical behavior of the system is sometimes called the constitutive model.

Elementary mechanics is traditionally partitioned into three courses named "statics", "dynamics", and "strength of materials". These subjects vary in how much they emphasize material properties, geometry, and Newton's laws.

Statics is mechanics with the idealization that the acceleration of mass is negligible in Newton's laws. Statics is generally about things that do not much move. The material properties used as examples in elementary statics are very simple. The constitutive law is generally introduced into statics problems by the assumption of rigidity. Because things do not much move or deform in statics, the geometry of deformation and motion are ignored. Despite the commonly applied vast simplifications, statics is useful, for example, for the analysis of structures, slow machines or the light parts of fast machines.

Dynamics concerns motion associated with the non-negligible acceleration of mass thus concerns the two words kinematics and kinetics. Kinematics concerns geometry with no mention of force and kinetics concerns the relation of force to motion. Once one has mastered statics, the hard part of dynamics is the kinematics. Dynamics is useful for the analysis of, for example, fast machines, vibrations, and ballistics.

Strength of materials expands statics to include material properties and also pays more attention to distributed forces, lightly on strength of materials topics like stress, strain, and linear elasticity. Strength of materials gives equal emphasis to all three pillars of mechanics. Strength of materials is useful for predicting the amount of deformation in a structure or machine and whether or not it is likely to break with a given load.

To solve the problem in mechanical, if the problem can be defined in term of function, generally mathematic operation or well-known constants or variables, the closed form solution can be used to solve it but if the problem has unknown that have to produce the sequence to approximate the value and repeat the procedure again and again, the numerical analysis is to be involved to solve that problem.

3.2 Finite Element Method

Finite Element Method (FEM) is the one of numerical method that is used to simulate and analysis behavior of the mechanical model. ANSYS is the famous program for FEA which is used to study the nonlinear model. The shipping comb insertion and removal force have to use Transient Structural System of nonlinear module [4] in ANSYS program because this force is related to part deformation, friction coefficient and time in very short moment.

3.3 Definition and Purpose of Transient Dynamic Analysis

Transient dynamic analysis is a technique used to determine the dynamic response of a structure under the action of any general time-dependent loads, also known as time-history analysis or transient structural analysis. This analysis can include inertia and/or damping effects and nonlinear effects. The non-linear governing equation for the Transient Dynamic Analysis is showed as following.

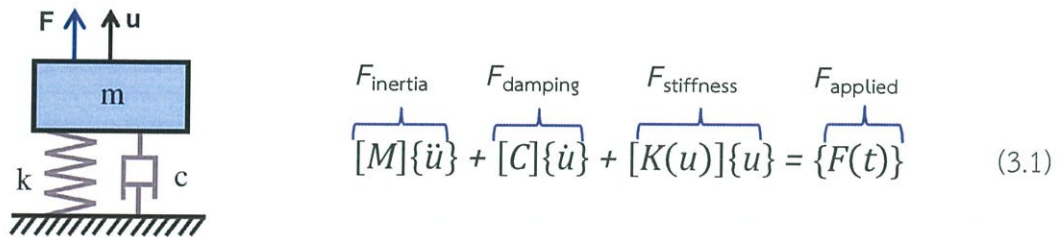


Figure 3.1 Force diagram of mass in nonlinear equation

- $[M]$: is structural mass matrix $\{\ddot{u}\}$: is nodal acceleration vector
- $[C]$: is structural damping matrix $\{\dot{u}\}$: is nodal velocity vector
- $[K]$: is structural stiffness matrix $\{u\}$: is nodal displacement vector
- $\{F\}$: is the load vector (t) : is time

At any given time t , these equations are thought of as a set of "static" equilibrium equations that take into account inertia forces $[M]\{\ddot{u}\}$ and damping forces $[C]\{\dot{u}\}$. To solve these equations ANSYS uses the Newmark time integration method or an improved method called HHT. The Integration time step is the time increment between successive time points.

$$\Delta t = t_n - t_{n-1} \tag{3.2}$$

The *Newmark method* uses finite difference expansions in the time interval Δt , with a primary aim of computing displacements $\{u_{n+1}\}$.

$$\{\dot{u}_{n+1}\} = \{\dot{u}_n\} + [(1-\delta)\{\ddot{u}_n\} + \delta\{\ddot{u}_{n+1}\}]\Delta t \tag{3.3}$$

$$\{u_{n+1}\} = \{u_n\} + \{\dot{u}_n\}\Delta t + [(0.5-\alpha)\{\ddot{u}_n\} + \alpha\{\ddot{u}_{n+1}\}]\Delta t^2 \tag{3.4}$$

$\{u_{n+1}\}$ can be obtained such that

$$(a_0[M] + a_1[C] + [K])\{u_{n+1}\} = \{F^a\} + [M](a_0\{u_n\} + a_2\{\dot{u}_n\} + a_3\{\ddot{u}_n\}) + [C](a_1\{u_n\} + a_4\{\dot{u}_n\} + a_5\{\ddot{u}_n\}) \tag{3.5}$$

The integration constants a_0 through a_5 as functions of γ and Δt . (γ represents numerical damping and can be directly input in the analysis settings) In ANSYS Mechanical, the Newmark parameters α , and δ are calculated using equation below.

$$\alpha = \frac{1}{4} (1+\gamma)^2 \quad (3.6)$$

$$\delta = \frac{1}{2} + \gamma \quad (3.7)$$

γ is a numerical damping value (amplitude decay factor). The value that use in this study is showed in appendix B.

3.4 Transient Analysis Method

The full method technique is selected to analysis model in this paper. This method allows all types of nonlinearities, accepts most load types such as nodal forces, non-zero displacements, element loads, tabular boundary condition, full matrices properties, etc. The important thing for this method is the mesh should be fine enough to resolve the highest mode of interest.

3.4.1 Nonlinearities in Transient Analysis

The different between linear analysis and nonlinear analysis in transient analysis are force and displacement in linear analysis are linearly related as shown in figure xxx and structural stiffness (K) is constant while the force and the displacement in nonlinear analysis are not linearly related as shown in figure xxx and stiffness K_T is not constant, it changes through the load path. *Newton-Raphson* method is used to solve nonlinear analysis.

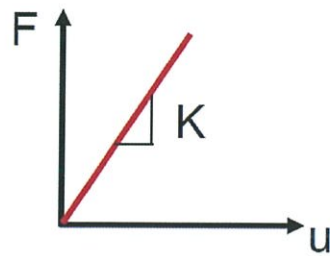


Figure 3.2 Graph force (F) and displacement (u) in linear analysis [7]

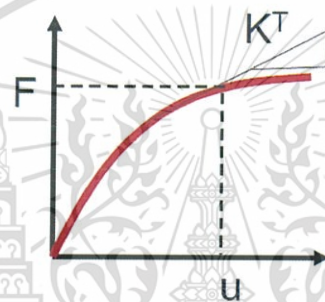


Figure 3.3 Graph force (F) and displacement (u) in nonlinear analysis [7]

3.4.2 Three sources of structural nonlinearity

3.4.2.1 Changing status

Contact pair either in or out of contact status, tension-only cable is either slack or taut, frictional contact, etc.

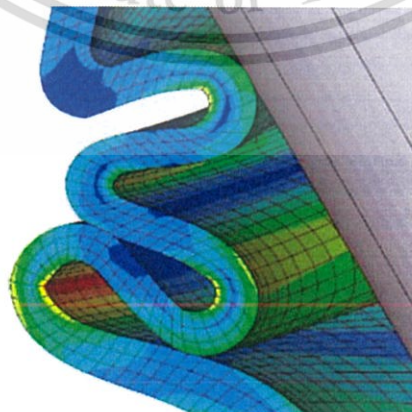


Figure 3.4 Changing status of mesh in structural nonlinear analysis [7]

This material is reserved for educational use only, not allowed for commercial use.

Forbidden to modify the content, and cite the document when use.

3.4.2.2 Geometric nonlinearities

Changing geometric configuration (large deformation) causes structure to respond nonlinearly (classic fishing pole behavior)

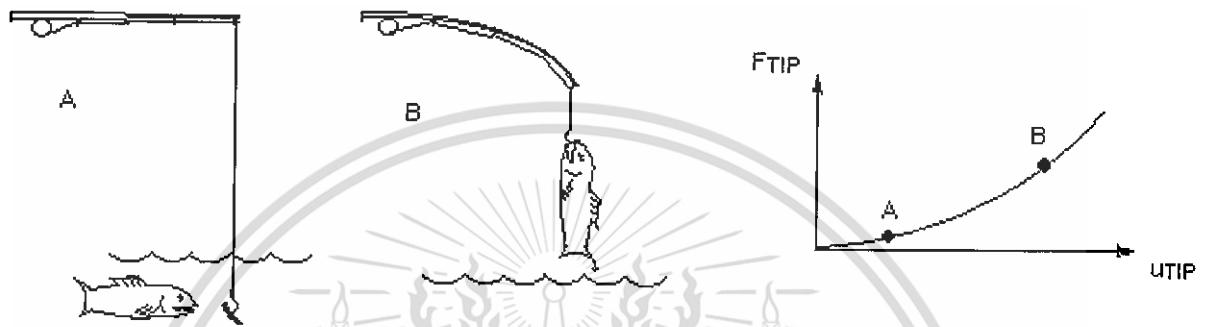


Figure 3.5 Example of deformation in structural nonlinear analysis [7]

3.4.2.3 Material nonlinearities

Nonlinear stress-strain relationships (metal plasticity, creep, hyperelasticity, etc.)

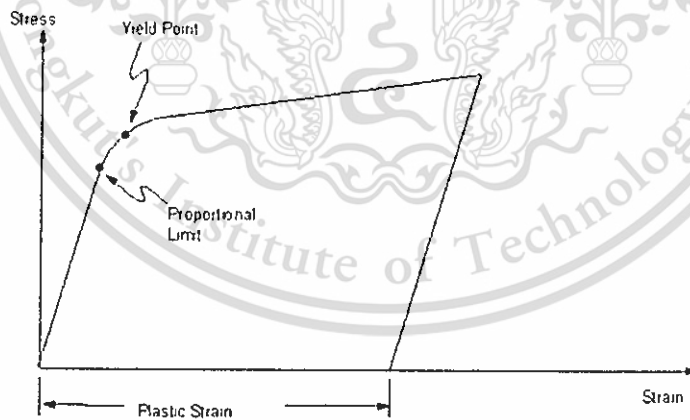


Figure 3.6 Graph stress-strain of nonlinear material [7]

3.4.3 Contact Types

Contact is called of two separate surface touched each other such that they become mutually tangent, do not interpenetrate. The contact can transmit compressive normal forces and tangential friction forces but do not transmit tensile normal forces. Contact is a nonlinearity changing status. That is the stiffness of the system depends on the contact status, whether parts are touching or separated. The available types of contact behaviors are showed in table 3.1.

Table 3.1 Contact type in nonlinear analysis

Contact Type	Iterations	Normal Behavior (Separation)	Tangential Behavior (Sliding)
Bonded	1	No Gaps	No Sliding
No Separation	1	No Gaps	Sliding Allowed
Frictionless	Multiple	Gaps Allowed	Sliding Allowed
Rough	Multiple	Gaps Allowed	No Sliding
Frictional	Multiple	Gaps Allowed	Sliding Allowed

Bonded are no penetration, no separation and no sliding between faces of edges. No Separation is similar to bonded, except frictionless sliding can occur along contacting faces. Frictionless is no penetration allowed, but surfaces are free to slide and separate without resistance. Rough is similar to the frictionless setting except no sliding allowed. Frictional allows sliding with resistance proportional to user defined coefficient of friction, with freedom to separate without resistance.

Generally, the physical contacting bodies do not interpenetrate. Therefore, the program must establish a relationship between the two surfaces to prevent them from passing through each other in the analysis. When the program prevents interpenetration, we say that it enforces contact compatibility, Figure 3.7. Mechanical offers several different contact formulations to enforce compatibility at the contact interface.

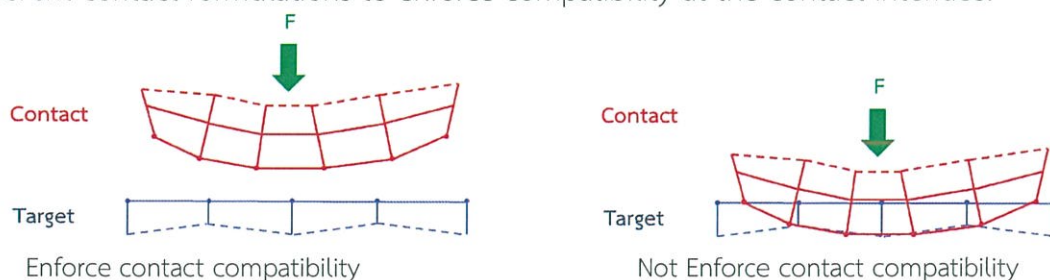


Figure 3.7 Enforce contact and not enforce contact

This material is reserved for educational use only, not allowed for commercial use.

Forbidden to modify the content, and cite the document when use.

Formulation of contact in ANSYS is Penalty-Based.

$$F_{normal} = k_{normal}X_{penetration} \quad (3.8)$$

For a finite contact force F_{normal} , is a concept of contact stiffness k_{normal} . The higher the contact stiffness, the lower the penetration $X_{penetration}$, as shown in the Figure 3.8, for an infinite k_{normal} , one would get zero penetration. This is not numerically possible with penalty-based methods, but as long as $X_{penetration}$ is small or negligible, the solution results will be accurate.

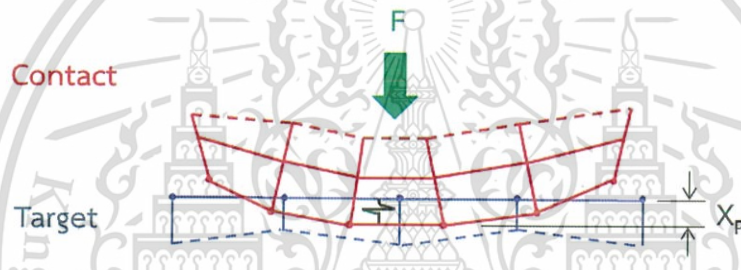


Figure 3.8 Penalty-based

In ANSYS, the contact method is defined to 2 method such as *Pure Penalty* and *Augmented Lagrange* methods. The main difference is that the latter augments the contact force (pressure) calculations. Formulation for Augmented Lagrange is showed in equation 3.9.

$$F_{normal} = k_{normal}X_{penetration} + \lambda \quad (3.9)$$

Because of the extra term λ (Lagrange multipliers), the augmented Lagrange method is less sensitive to the magnitude of the contact stiffness k_{normal} . Augmented Lagrange is the default formulation used for *Program Controlled* option.

3.5 Newton-Raphson Technique

In a nonlinear analysis, relationship between load and displacement cannot be determined with a single solution based on initial stiffness. This method uses a series of linear approximations with corrections.

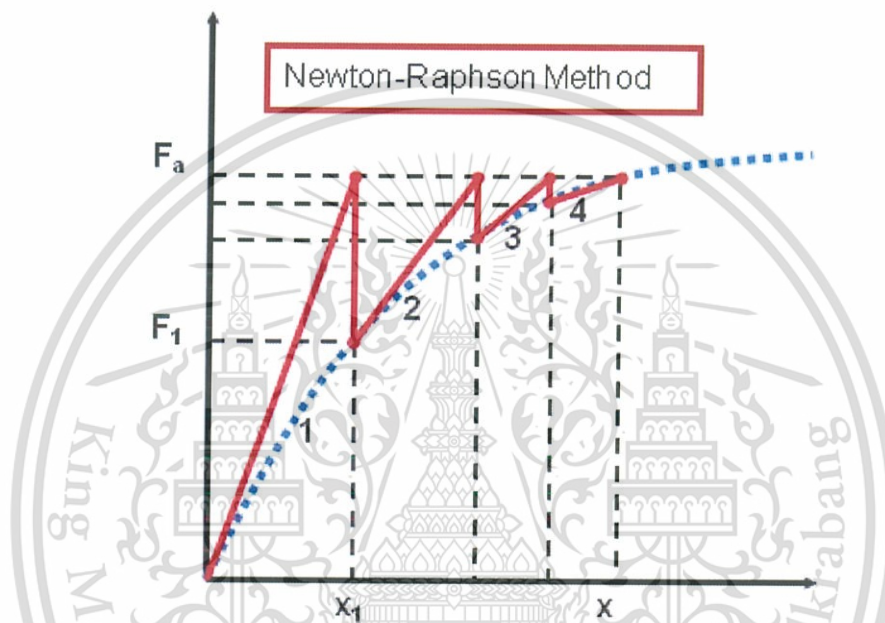


Figure 3.9 Iteration step in newton-raphson method

Total external load F_a is applied in iteration 1 and displacements (x_i) are calculated. Using x_i then internal forces F_i at iteration 1 are calculated. If the system $F_a - F_i$ is not in equilibrium. The difference of between applied external and calculated internal forces, ($F_a - F_i$) are the *out-of-balance* or *residual forces*. If residual forces are within an acceptable tolerance, the solution is converged. If residual forces are outside an acceptable tolerance, the solution is not converged, so a new stiffness matrix is assembled and the process is repeated. In this example, the system achieves convergence after iteration 4.

Each solution point is defined in terms of a unique monotonically increasing time and a unique load step and substep combination. *Load steps* are typically used to differentiate changes in general loading. F_a and F_b are loadsteps. *Substeps* are typically used to increment loading within load steps. It was desired to incrementally apply the load because of the complex response. For example, F_{a1} may be near 50% of the F_a load. After F_{a1} is converged, full F_a load is applied. F_a has 2 substeps while F_b has 3 substeps in this example.

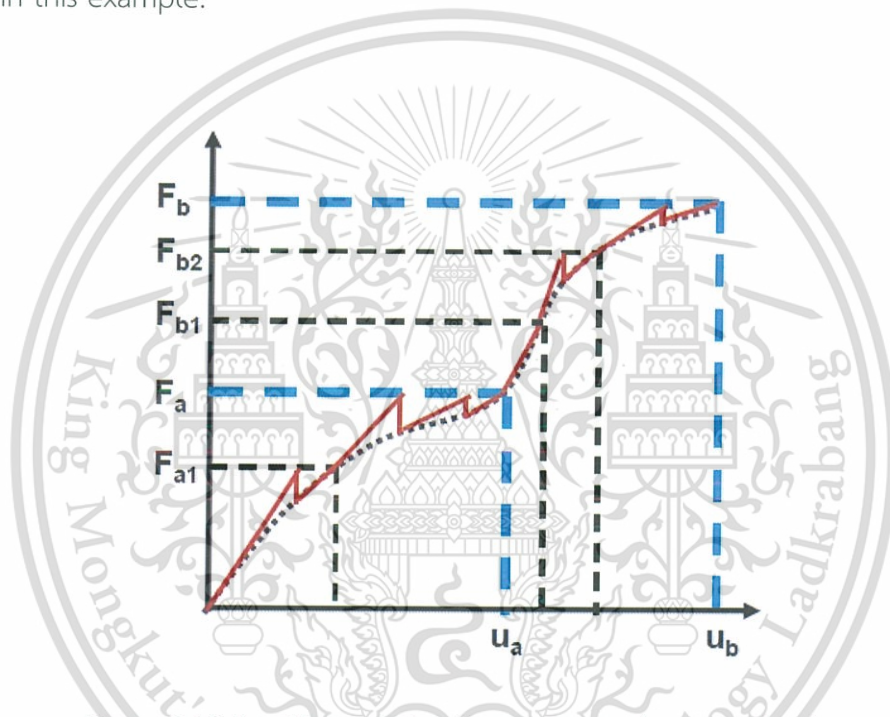


Figure 3.10 Iteration substep in Newton-Raphson method

In a nonlinear solution, equilibrium iterations are corrective solutions needed for convergence using the Newton-Raphson method. Equilibrium iterations occur at the same time point (and same load step and substep). In this example, the iterations between the dotted lines indicate equilibrium iterations.

3.6 Analysis in Transient Analysis

In a full transient analysis, the control options are set under “*Analysis Settings*”. It consists of Step Controls, Solver Controls, Restart Controls, Nonlinear Controls, Output Controls, Damping Controls and Analysis Data Management.

3.6.1 Time Step Size

Integration time step Δt , is time increment between successive time points. It is one of the most important parameters in a transient structural analysis. It must be small enough to correctly describe the time-varying loads, capture the dynamic response, running a preliminary modal analysis is suggested. Time step size controls the accuracy and convergence behavior of nonlinear systems. By default, transient structural analysis uses automatic time-stepping. Proper selection of the initial, minimum, and maximum time steps is important. Auto Time Stepping automatically adjusts the time step size (hence the load increment) throughout the solution. Smaller increments when convergence is difficult, larger increments when convergence is easy. Transient structural analysis uses implicit time integration (*time step is usually large*). It is recommended to use automatic time-stepping (default). The maximum time step can be chosen based on accuracy concerns. The minimum time step is input to prevent Mechanical from solving indefinitely, (*1/100 or 1/1000 of the initial time step*). A general suggestion for selection of the initial time step is to use the following equation.

$$\Delta t_{initial} = \frac{1}{20f_{response}} \quad (3.10)$$

$f_{response}$ is the frequency of the highest mode of interest (obtained from *Modal Analysis*).

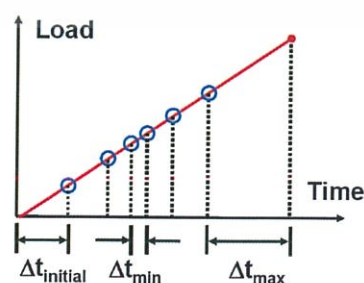


Figure 3.11 Time sequence from auto time stepping

This material is reserved for educational use only, not allowed for commercial use.

Forbidden to modify the content, and cite the document when use.

For Auto Time Stepping or Program Controlled (Default), *Mechanical* will automatically set specifications depending on the nature of the nonlinearity in the model. User should always verify that these values are adequate by checking the *Solution Information* folder at the beginning of the run and watching for bisections.

Time Integration: indicates whether a solution step should include transient effects (e.g., structural inertia). Transient effects can be turned “off” to set up the Initial Conditions for a transient analysis. Do not include structural inertia or thermal capacitance in solving this step. Mechanical does not compute velocity results. Therefore, damping forces, which are derived from velocity will equal zero.

3.6.2 Solver Controls – Solver Type

Solver Type reference to the way ANSYS builds the stiffness matrix for each newton-raphson equilibrium iteration. Direct (Sparse) is more robust, it recommended for challenging nonlinear models with non-continuum elements (shells and beams). Iterative (PCG) is more efficient, it recommended for large bulk solid models dominated by linear elastic behavior. The default “Program Controlled” is automatically selects a solver based on the problem. Weak Springs: to prevent numerical instability, while not having an effect on real world engineering loads. Large Deflection: If set to “ON”, Stiffness matrix is adjusted over multiple iterations to account for changes such as large deflection, large rotation and large strain. Stress stiffening effect and Spin softening effect are included.

3.6.3 Damping Control

Alpha and Beta damping are used to define Rayleigh damping constants α and β . $[C]$ is calculated using α and β to multiply the mass matrix $[M]$ and stiffness matrix $[K]$. They can be input via directly as global damping value (*Details section of Analysis Settings*) or material-dependent damping value (Mass- Matrix Damping Multiplier, and k-Matrix Damping Multiplier)

$$[C] = \alpha[M] + \beta[K] \quad (3.11)$$

$$\xi_i = \frac{\alpha}{2\omega_i} + \frac{\beta\omega_i}{2} \quad (3.12)$$

Problems involving rigid body translational motion, dissipative mechanisms like plasticity or friction typically require smaller values for numerical damping. Larger numerical damping values are usually necessary for problems involving rigid body rotational motion, elastic collisions and large deformations with frequent changes in sub-step. A sensible value to try initially is 0.1. Use the lowest possible value that damps out nonphysical response without significantly affecting the final solution.



CHAPTER 4

RESEARCH METHODOLOGY

This research studies parameters of shipping comb that relate to the force when insert and remove the shipping on actuator arm and investigates the sensitivity of each parameter to suggest shipping comb designer which one should be selected to modify in order to get the shipping comb insertion and removal forces meeting the required specification. The study flow of this research is shown in Figure 4.1.

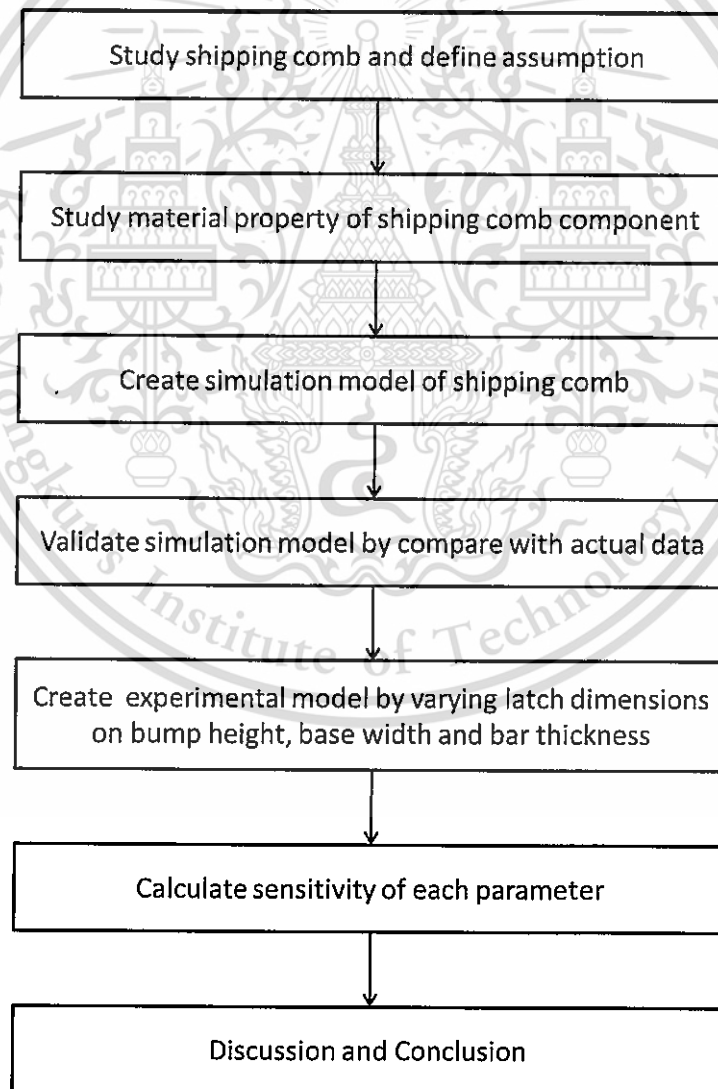


Figure 4.1 Study flow

This material is reserved for educational use only, not allowed for commercial use.

Forbidden to modify the content, and cite the document when use.

4.1 Assumption

4.1.1 The shipping comb insertion and removal forces are friction force between the shipping comb and the actuator surface.

4.1.2 Shipping comb is moved by the probe then reaction force on the probe can represent the insertion and removal forces acting on shipping comb.

4.1.3 Simulation begins with static condition. Then the probe is moved very slowly in order to reduce effect from dynamic force.

4.1.4 The deformation of shipping comb should be under elastic region in order to prevent shipping comb damage when re-use in production line.

4.1.5 Assume that the shipping comb insertion and removal forces are changed linearly when latch dimension is changed in small value.

4.2 Material Property

Polycarbonate is material of shipping comb that is developed to support specific requirement such as high wear resistant, ESD safe and low particle shading [8]. Some properties may not provide in public such as friction coefficient and stress-strain curve which are important properties for FEA.

4.2.1 Friction Coefficient

The friction coefficient [7] is the required material property for FEM. The wrong value can be made the result different from actual. A simple method to find out friction coefficient is calculated from friction force or push force. Figure 4.1 shows equipment for push force measurement such as plastic plate, actuator, mass and force gauge. Materials of all components are showed in Table 4.1. The testing is start from fixed the plastic plate on the ground. Stick the mass on actuator and put them on the plastic plate. Use the probe of force gauge, Chatillon DFS II, push on the side of actuator until it moved. The force gauge will capture the highest force of pushing and shows on display then the friction coefficient can be calculated by simple equation as showed in Eq. (4.1).

$$\mu = \frac{F_{probe}}{F_{mass}} \quad (4.1)$$

This material is reserved for educational use only, not allowed for commercial use.

Forbidden to modify the content, and cite the document when use.

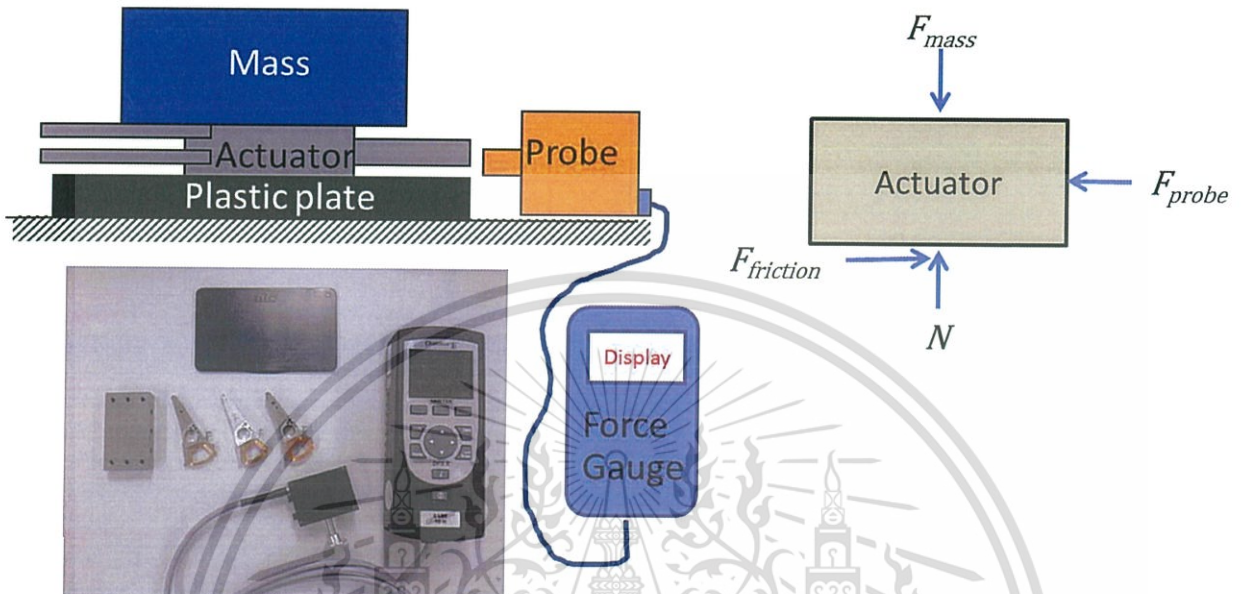


Figure 4.2 Friction parameter testing and free body diagram

Table 4.1 Material of friction test component

Component	Material type
Plastic plate	Polycarbonate RTP 399x82852A
Actuator	Aluminum AL-6061
Mass	Stainless SST-440C
Probe	Aluminum AL-6061

4.2.2 Stress-Strain curve

One important material property for FEA in non-linear is stress-strain curve [8]. The Universal Testing Machine 5560 at Suranaree University is chosen to generate stress-strain curve for shipping comb material.

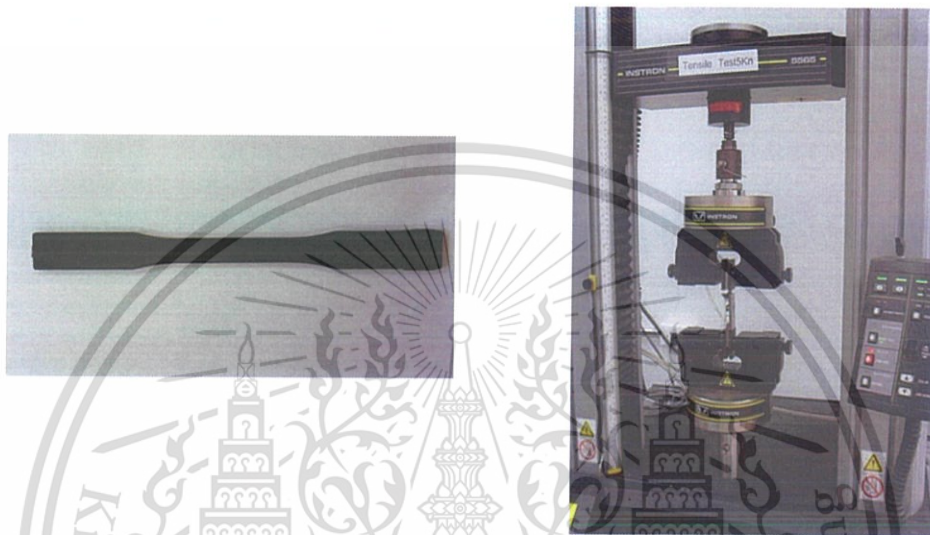


Figure 4.3 Specimen of comb material and universal testing machine 5560

Data from testing machine is engineering stress-strain which can be used for small-strain analyses but for plasticity must be used true stress-strain, as they are more representative measures of the state of the material.

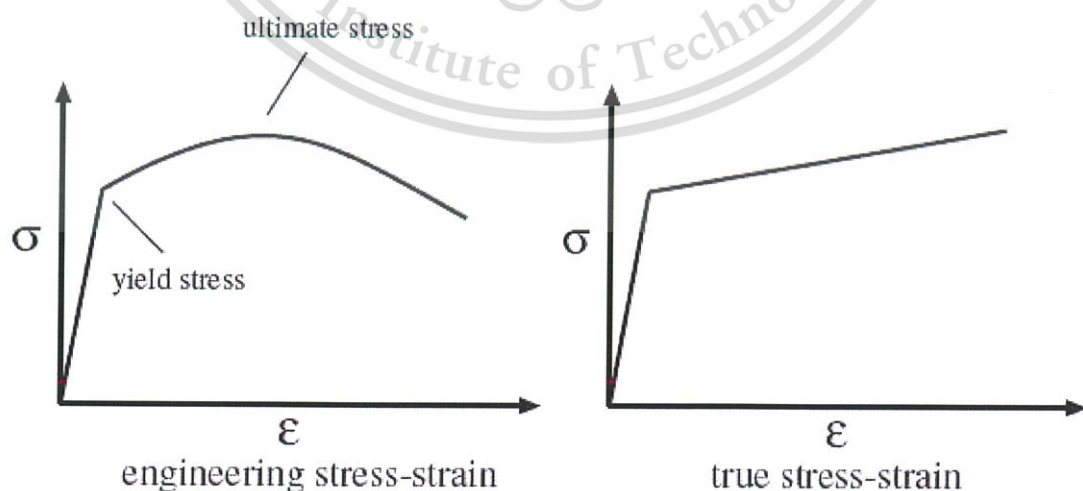


Figure 4.4 Engineering stress-strain and true stress-strain

This material is reserved for educational use only, not allowed for commercial use.

Forbidden to modify the content, and cite the document when use.

Figure 4.4 illustrated curves of engineering stress-strain value and true stress-strain value, while ϵ in x-axial is percent deformation or strain of specimen and σ in y-axial is tensile force or stress of specimen.

The engineering stress and engineering strain can be done calculated from equation 4.2 and 4.3

$$\sigma_{eng} = \frac{F}{A_0} \quad (4.2)$$

$$\epsilon_{eng} = \frac{l-l_0}{l_0} \quad (4.3)$$

F is the external axial tensile load

A_0 is the original cross-sectional area of the specimen

l_0 is the original length of the specimen

l is the final length of the specimen

Definition of the true stress is the ratio of the applied load to the instantaneous cross-sectional area. The relationship between the true stress and engineering stress once no volume change is assumed in the specimen. The engineering stress-strain values can be converted to true stress-strain with the following approximations.

The point at which yielding occurs.

$$\sigma_T = \sigma_{eng} \quad (4.4)$$

$$\epsilon_T = \epsilon_{eng} \quad (4.5)$$

The point at which necking occurs.

$$\sigma_T = \sigma_{eng}(1 + \epsilon_{eng}) \quad (4.6)$$

$$\epsilon_T = \ln(1 + \epsilon_{eng}) \quad (4.7)$$

4.3 Model Creation

The assembly model of shipping comb, actuator and probe are created in SolidWorks program then converted to general file type in order to analyze by ANSYS program. The model is simplified by removing non touching arm and the shipping comb finger in order to reduce number of elements. The fillet and the chamfer are also removed in order to reduce the calculation time

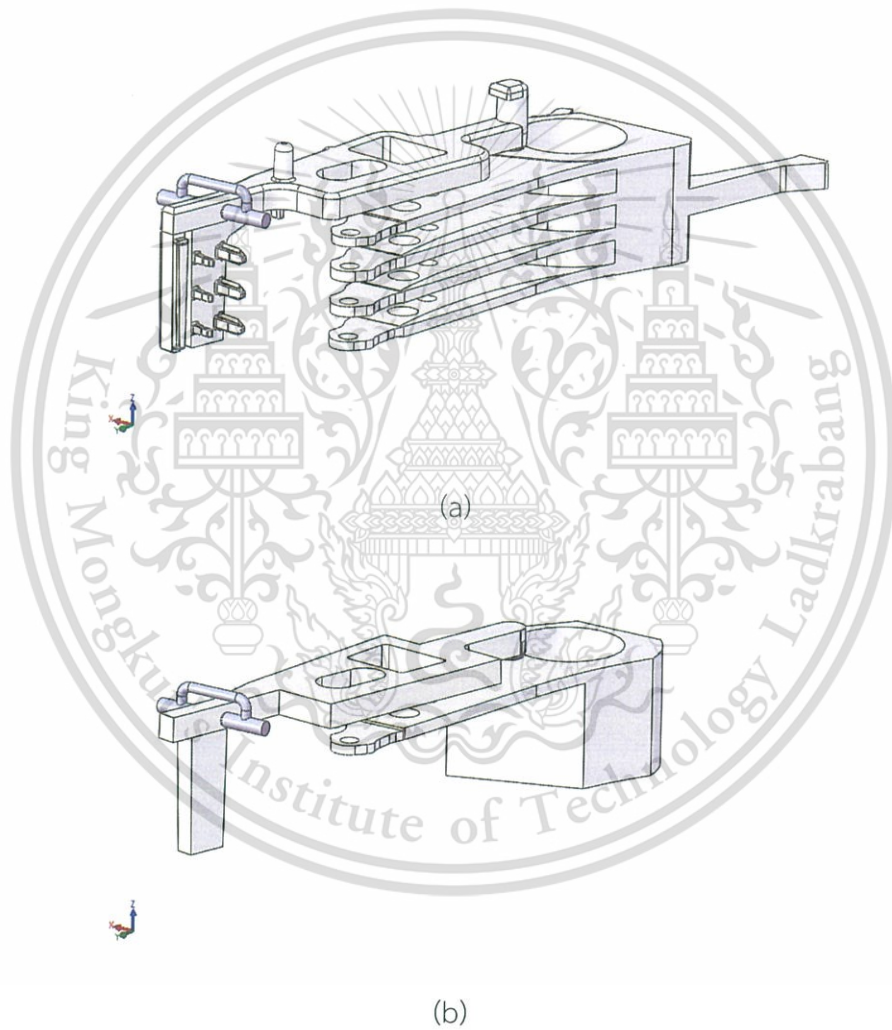


Figure 4.5 (a) Actual model. (b) Simplified model.

4.4 Model Setting in ANSYS

The transient structural analysis in ANSYS is selected to simulate the action of shipping comb insertion and removal because it can determine the dynamic response of the model under action of time-dependent loads. The movement of shipping comb is split into small time steps to capture the reaction force on the measurement probe in each time steps. The reaction force on the measurement probe in Figure 4.6 is the value that used to represent the shipping comb insertion and reaction force.

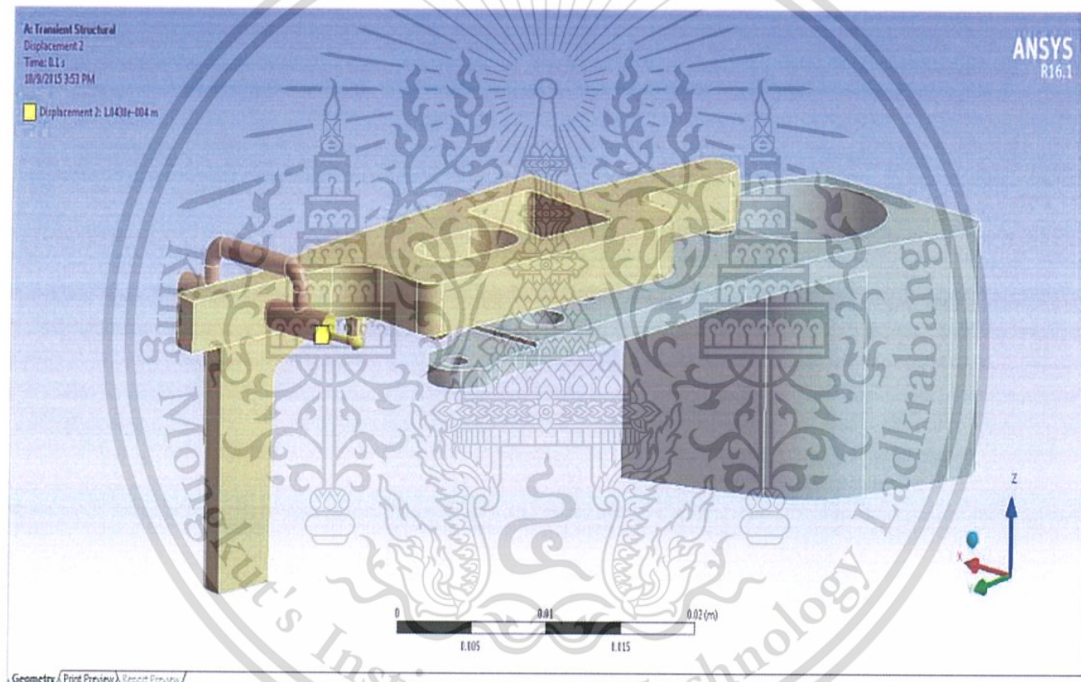


Figure 4.6 Model shipping comb and actuator

The Hex Dominant method is selected to create mesh for the mode. The model with hexagonal elements [9] is enabled to deform in a lower strain energy state, thus it produced lower error than tetrahedron elements.

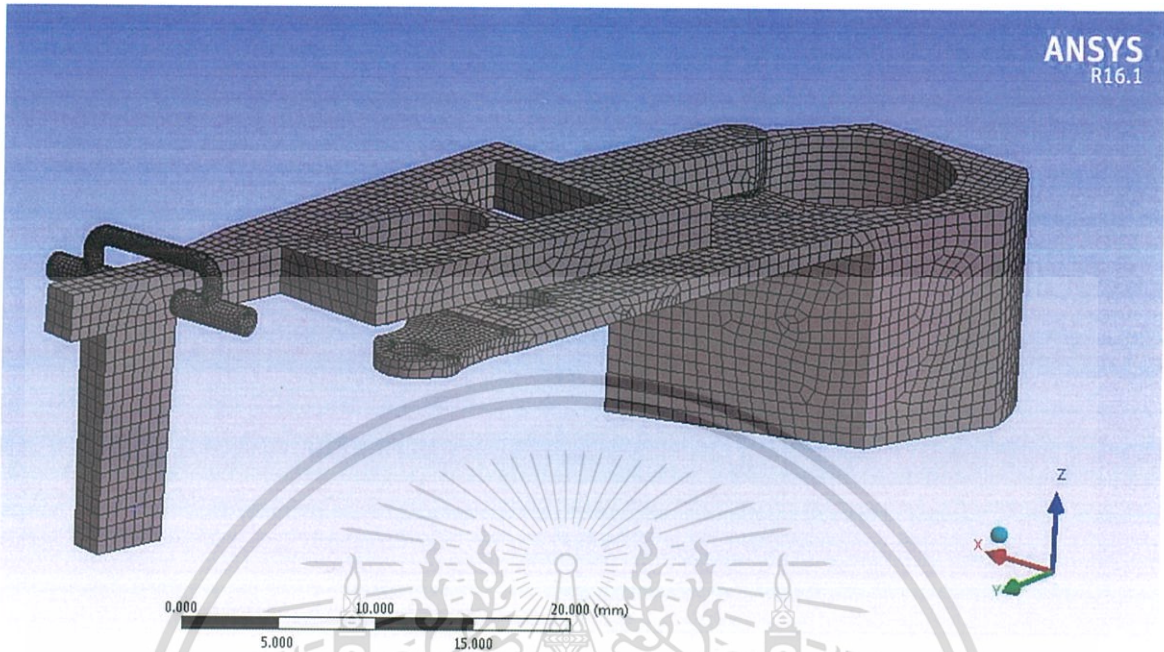


Figure 4.7 Discretized model of shipping comb and actuator

The hole in actuator as shows in Figure 4.8 is assigned to be a fixed support in order to fix the actuator.

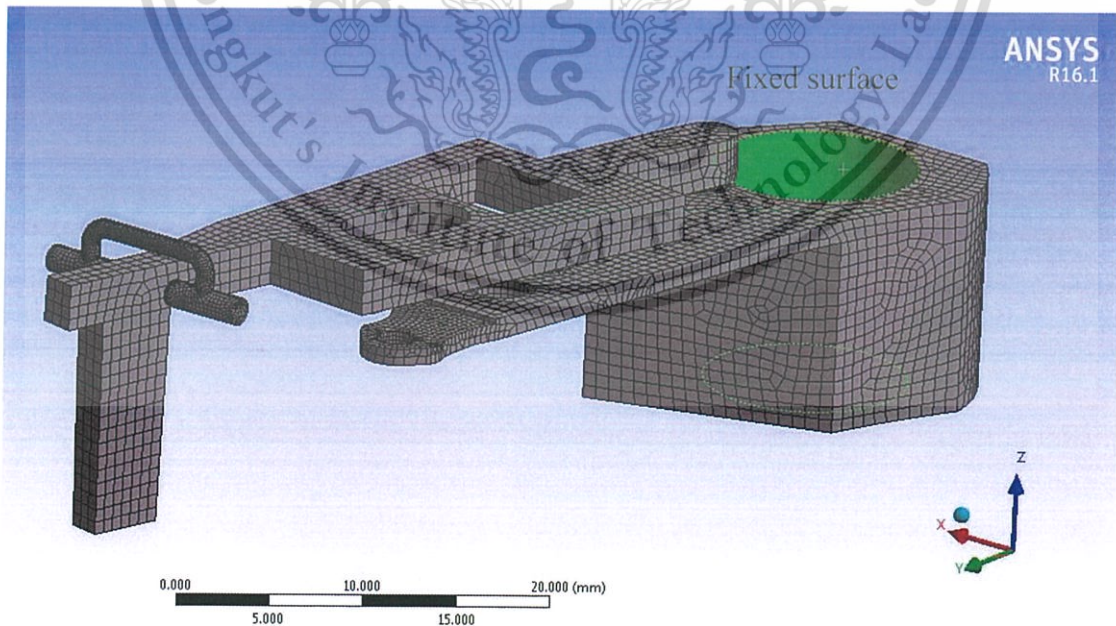


Figure 4.8 Fixed support on actuator

This material is reserved for educational use only, not allowed for commercial use.

Forbidden to modify the content, and cite the document when use.

The pivot pin of shipping comb as shows in Figure 4.9 is assigned to be cylindrical support by free in tangential in order to allow the shipping comb can only rotate.

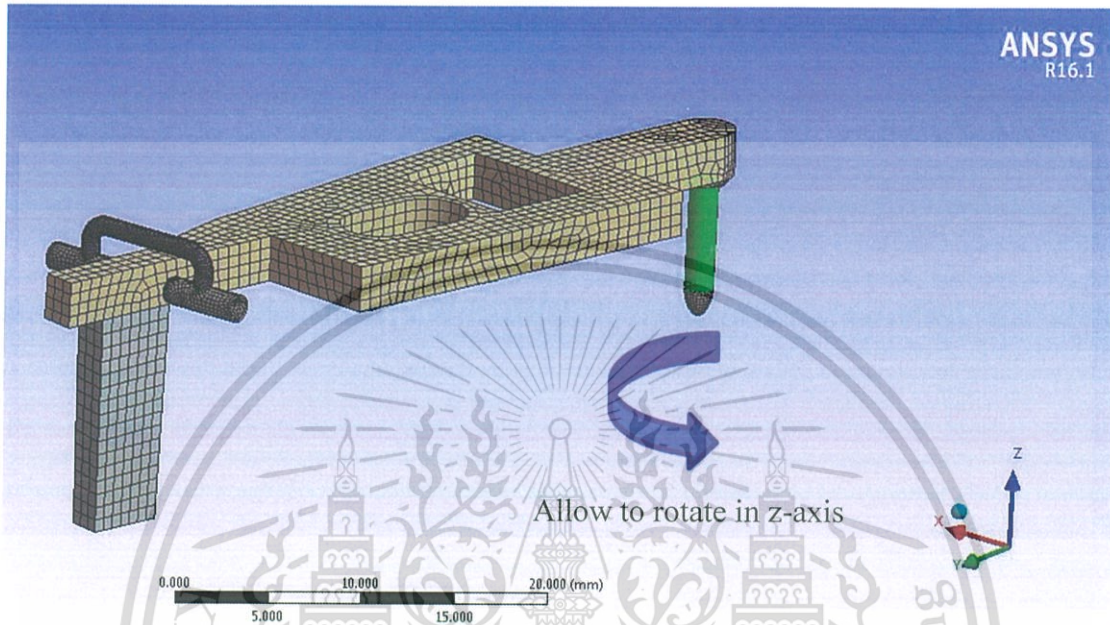


Figure 4.9 Cylindrical support on shipping comb

The rod of probe as shows in Figure 4.10 is assigned to be cylindrical support by free in axial in order to allow the probe can move in x-axis only.

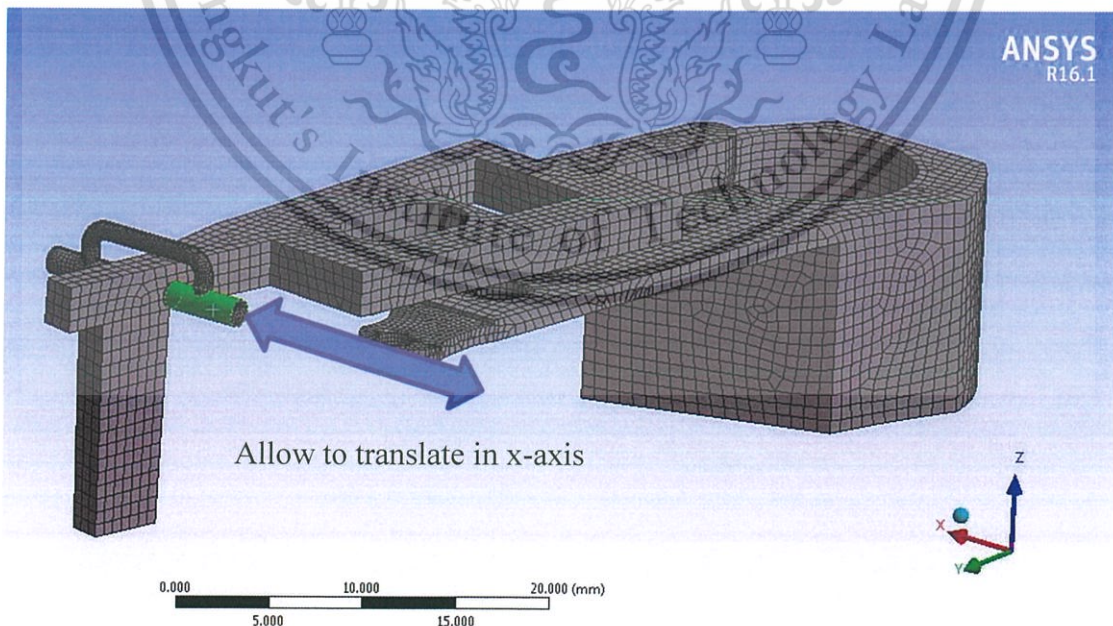


Figure 4.10 Cylindrical support on probe

This material is reserved for educational use only, not allowed for commercial use.

Forbidden to modify the content, and cite the document when use.

The flat plane on probe is assigned to be displacement in order to apply the moving distance of the probe. This plane is also assigned to be sensor plan to record the reaction force for insertion and removal force definition.

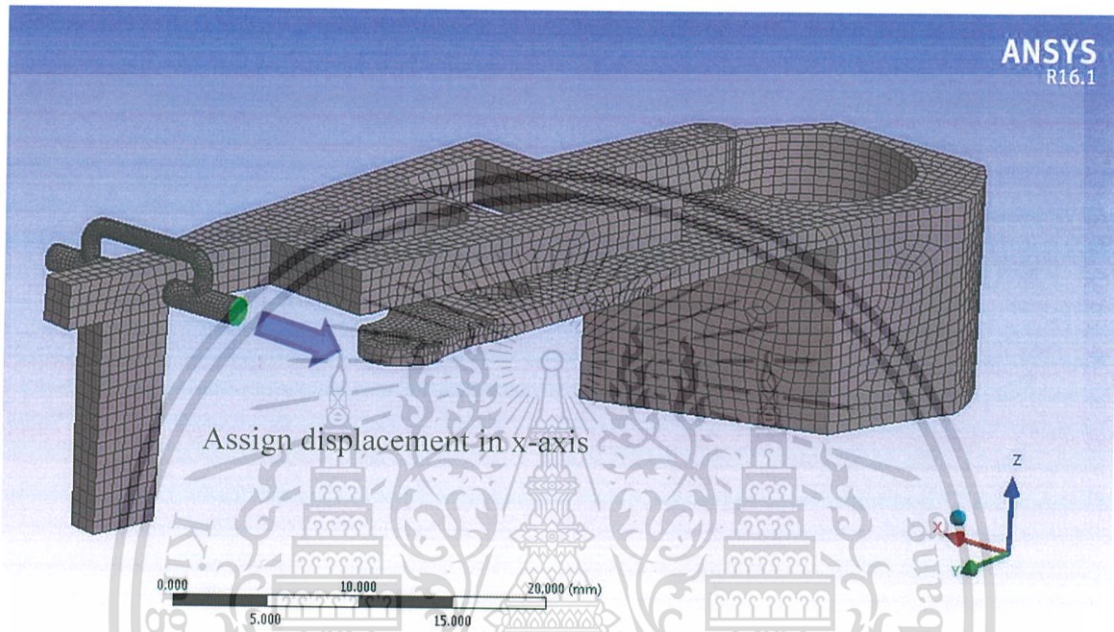
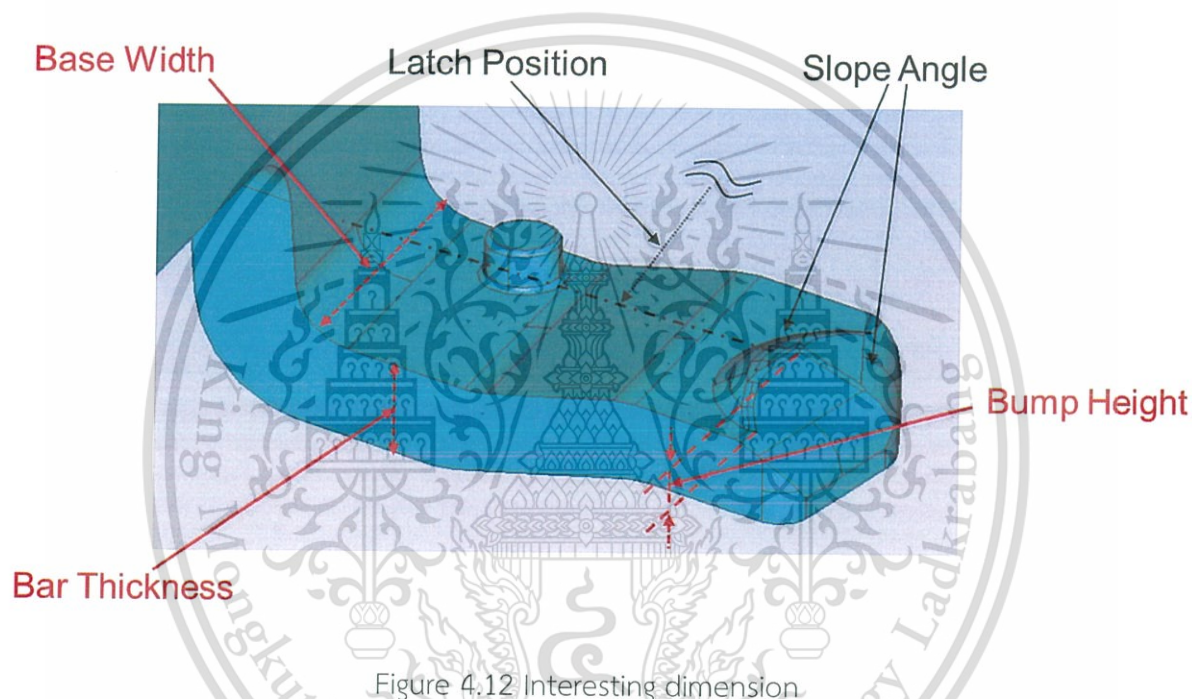


Figure 4.11 Plane for displacement and force sensor

4.5 Parametric Study

The dimensions on latch are defined in order to vary to study the relationship of each dimension to the shipping comb force. The dimensions in Figure 4.8 are the interesting dimensions. The bump height is fixed dimension for all design. The latch position and radius are the rarely change dimension. The base width, the base thickness, the bar thickness and the slope angle are always change dimension.



The variation in this study is scope into tolerance of each parameter in order to focus on the result when target to modify the existing mold to get the force per the specification.

The value of variation is tried to vary cover the tolerance of each dimension. The bump height is varied by increase and decrease height by 0.02 mm. The base width is varied by increase width by 0.12 mm and decrease width by 0.14mm. The bar thickness is varied by increase and decrease the thickness by 0.1 mm.

The variation of each parameter comparing to the nominal value are showed in Table 4.2

Table 4.2 Percent variation of each parameter

Parameter	Nominal (mm)	Decrease (mm)	Increase (mm)	%Decrease (%)	%Increase (%)
Bump height	0.203	0.02	0.02	9.85	9.85
Base width	2.263	0.14	0.12	6.2	5.3
Bar thickness	0.747	0.1	0.1	13.4	13.4

Because of percent variation of each parameter are quite low and the variation point is only three points, the linear regression is select to analyze the sensitivity of each parameter. The polynomial is the optional in case the R-squared from linear regression is very low.

Due to different variation value, the sensitivity and variation value from all parameters have to be normalized before comparing. The normalize value can be calculate per equation 4.8.

$$\text{Normalized} = \frac{\text{Actual} - \text{Midvalue}}{\text{Range}/2} \quad (4.8)$$

Midvalue and *Range* can be found as equation 4.9 and 4.10

$$\text{Midvalue} = (\text{Maximum} + \text{Minimum})/2 \quad (4.9)$$

$$\text{Range} = \text{Maximum} - \text{Minimum} \quad (4.10)$$

CHAPTER 5

RESULT AND DISCUSSION

5.1 Friction Identification Result

The measurement data from three head stack assemblies (HSA), ten repeat on each head stack assembly had been averaged and calculated to be friction coefficient as shown in Table 5.1.

Table 5.1 Measurement data and Friction coefficient

	HSA1	HSA2	HSA3
	0.658	0.763	0.716
	0.615	0.807	0.705
	0.654	0.764	0.781
	0.709	0.722	0.713
	0.681	0.773	0.824
	0.688	0.668	0.668
	0.597	0.860	0.688
	0.628	0.736	0.727
	0.656	0.749	0.710
	0.613	0.772	0.707
Push Force (N)	0.650	0.761	0.724
Weight (N)	2.331	2.354	2.382
Friction	0.279	0.323	0.304

From the obtained data, the average friction coefficient is 0.3. This value is input into material property table in ANSYS program.

5.2 Stress-Strain Result

The result of stress in mega Pascal (MPa) from tensile test of specimen has been plotted along the strain (mm/mm) in x-axial. This result is engineering stress-strain of shipping comb material RTP 399 x 82852A.

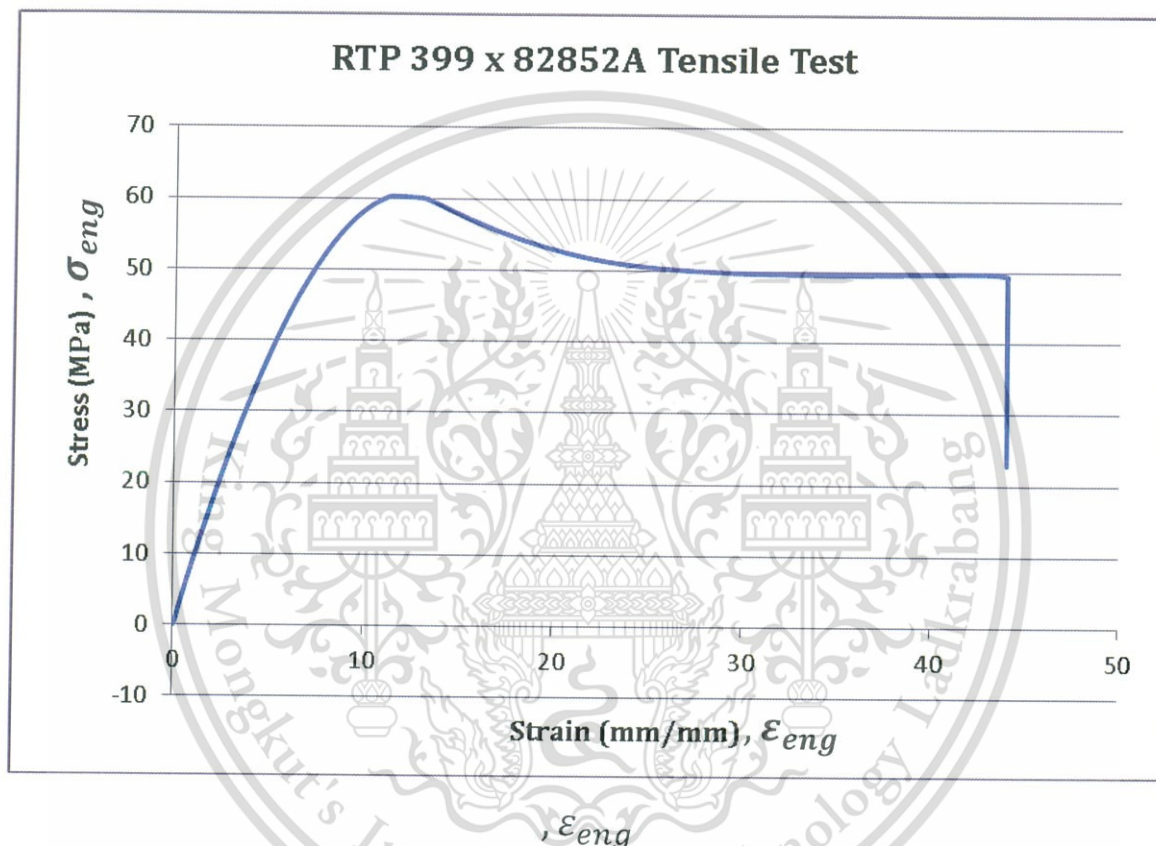


Figure 5.1 Engineering Stress-Strain curve of shipping comb material

From graph in Figure 5.1, the stress increases when strain increases, length of the specimen is increased from pulling, the relationship between stress and strain is close to linear until the specimen start to permanent deform stress is start to be curve, stress at this point is yield strength. As deformation continues, the stress increases on account of strain hardening until it reaches the ultimate tensile stress. After this point the cross-sectional area decreases uniformly and randomly the engineering stress shows decreasing until the specimen is fractured.

The engineering stress-strain from tensile test is converted to true stress-strain as shown in Figure 5.2. This data is to be input into material table in ANSYS program.

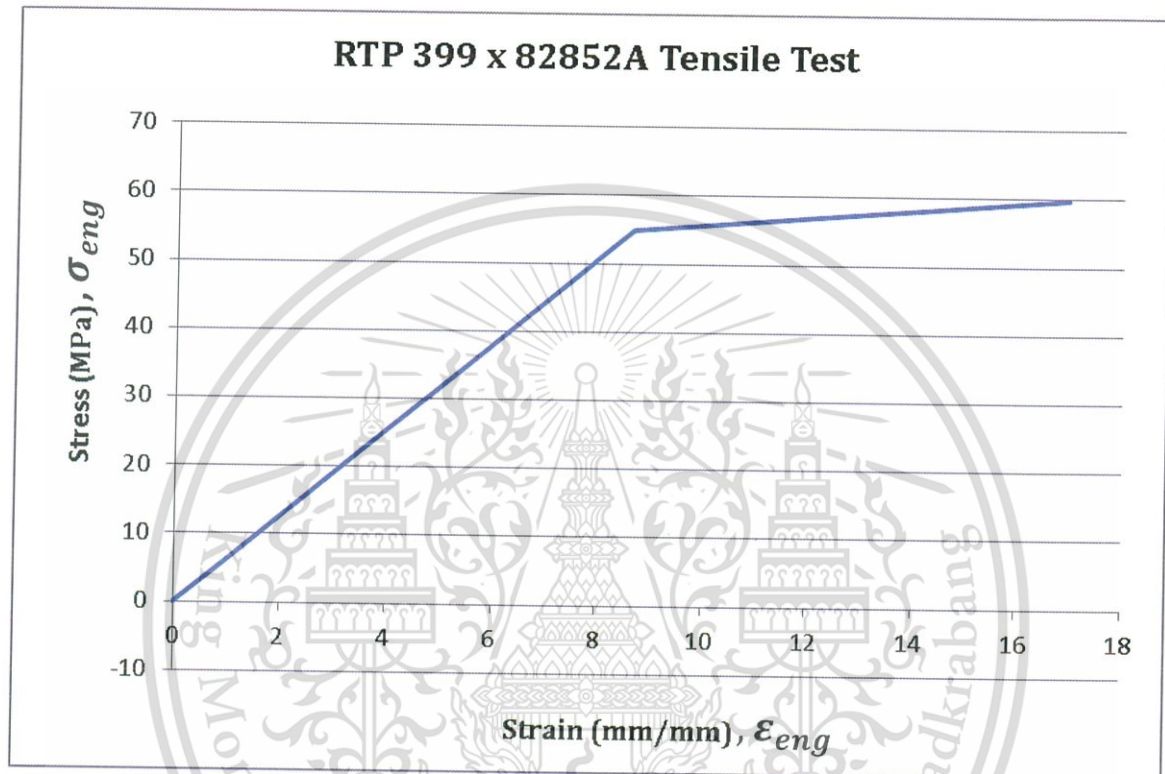


Figure 5.2 True Stress-Strain curve of shipping comb material

5.3 Model Validation Result

The insertion force is represented by pulling force from force gauge and the removal force is represented by pushing force from force gauge as illustrated in Figure 5.3.

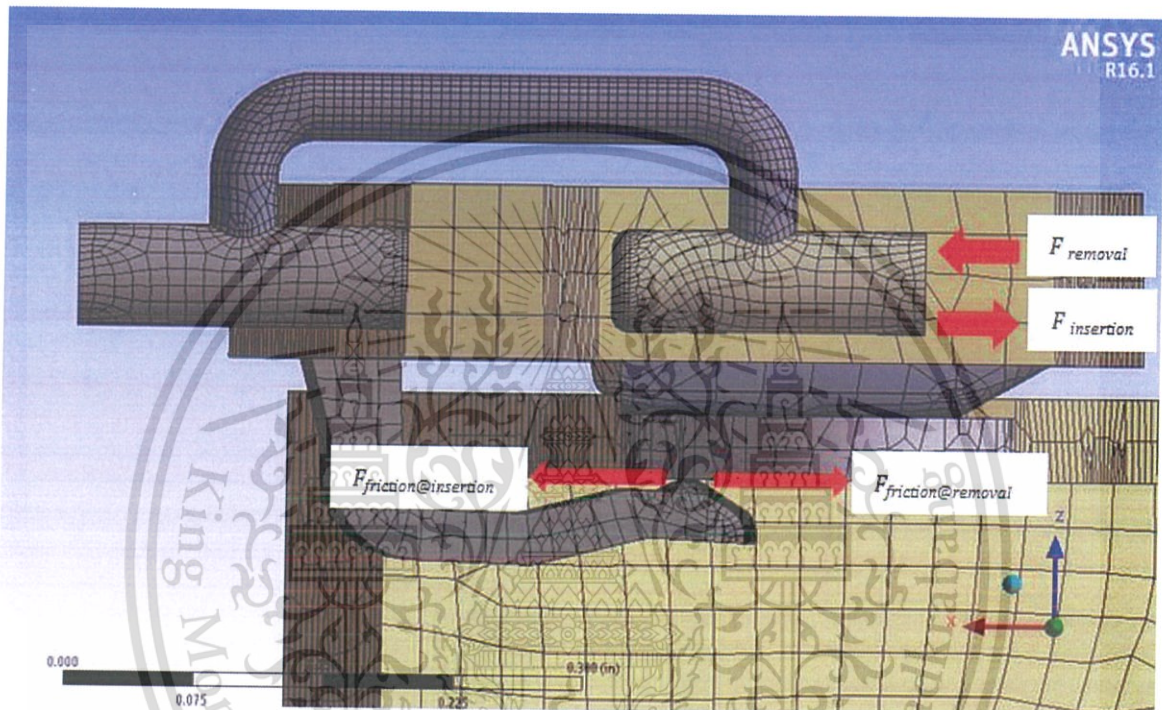


Figure 5.3 Direction of force

The results from simulation are plotted along the time of shipping comb moving as show in Figure 5.4. Forces occur in both of negative and positive region which the negative force during time 0-9 second is the force when insertion the shipping comb and the positive force during time 9-15 second is the force when removal the shipping comb.

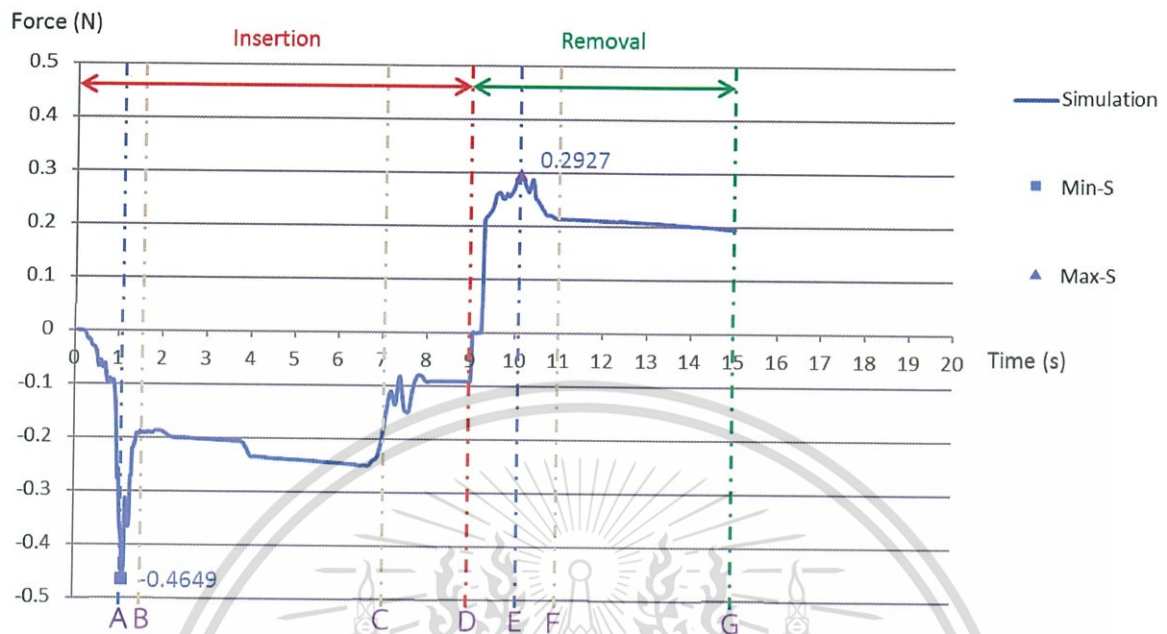


Figure 5.4 Probe reaction force in x direction variation from simulation

From Figure 5.4, at time 0-1 second, the reaction force starts from zero and ramps down to a peak at -0.4649 N at time about 1 second, point A in Figure 5.4. The behavior of the shipping comb at this time is shown in Figure 5.5-5.8. From Figure 5.7, the lowest force occurs when the edge of the actuator moves over the highest of the bump in the normal direction. At this situation, the friction between the actuator and the comb is highest; then this force represents the shipping comb insertion force. After passing the negative peak, the reaction force increases and trends to steady at -0.2 N and continues to steady until time 7 seconds, point B-C in Figure 5.4. The behavior of the shipping comb in this period is shown in Figure 5.9-5.12. During time 7 – 9 seconds, the force increases and changes to zero at time 9 seconds, point D in Figure 5.4.

After 9 seconds, the reaction force switches to the positive region because the direction of the friction force is the same as the direction of the sensor and ramps up to a peak at 0.2927 N at time nearly 10 seconds, point E in Figure 5.4. The behavior of the shipping comb at this time is shown in Figure 5.13-5.16. From Figure 5.15, the edge of the actuator is moved at the peak of the bump in the normal direction; the reaction force at this point is the highest, which represents the removal force. After passing the positive peak, the reaction force starts to decrease and trends to steady at 0.2 N from time 11 seconds until time is 15 seconds, point F-G in Figure 5.4.

This material is reserved for educational use only, not allowed for commercial use.

Forbidden to modify the content, and cite the document when use.

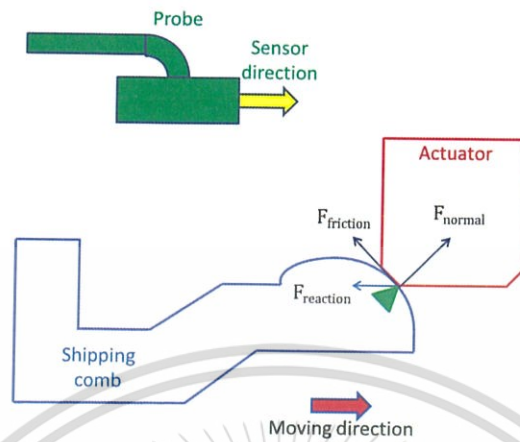


Figure 5.5 Force diagram between shipping comb and actuator at first contact state

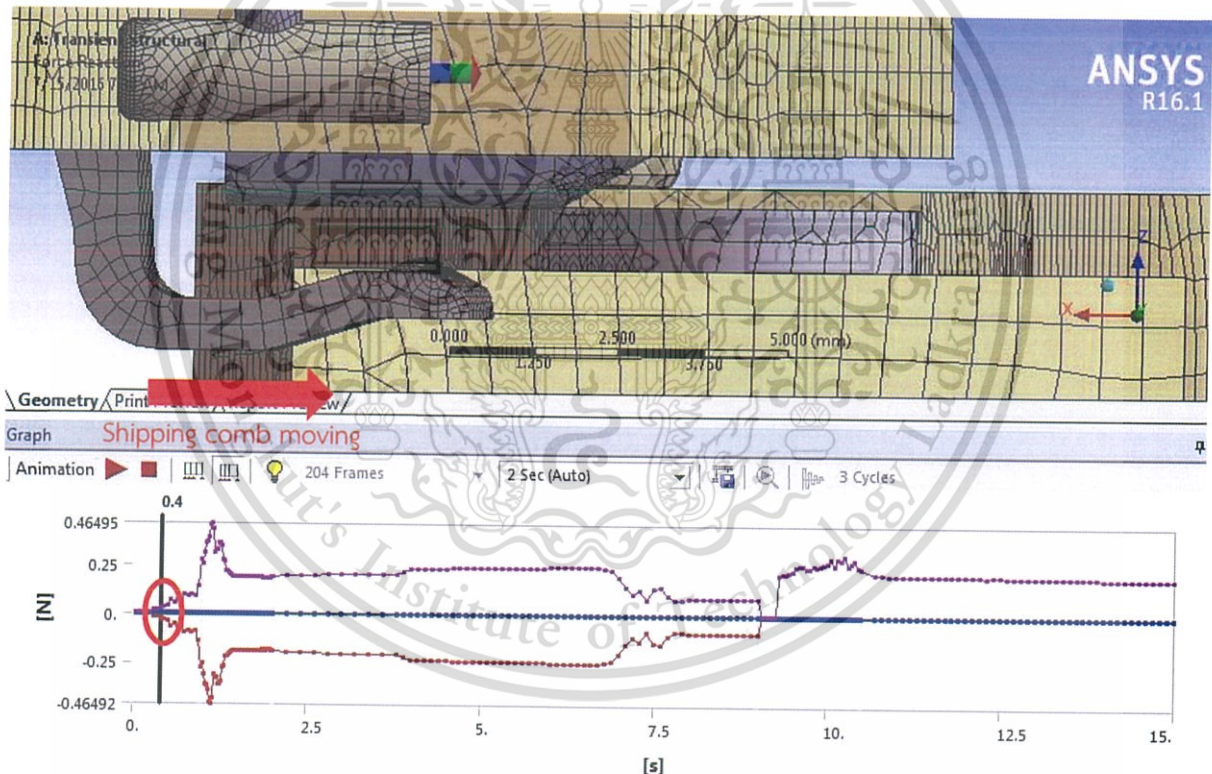


Figure 5.6 Simulation model at first contact state

Figure 5.5 shows diagram of shipping comb when the latch start to contact the actuator, point A in Figure 5.4. At this state, the reaction force occurs and increases the magnitude as shown in Figure 5.6. The violet graph in Figure 5.6 is automatically changed the reaction force to be positive value in order to compare all data point in term of magnitude.

This material is reserved for educational use only, not allowed for commercial use.

Forbidden to modify the content, and cite the document when use.

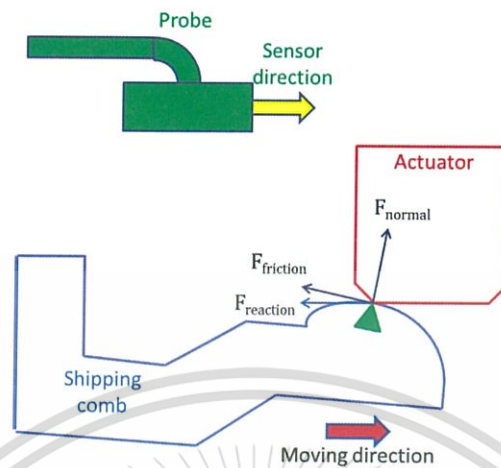


Figure 5.7 Force diagram between shipping comb and actuator at negative peak

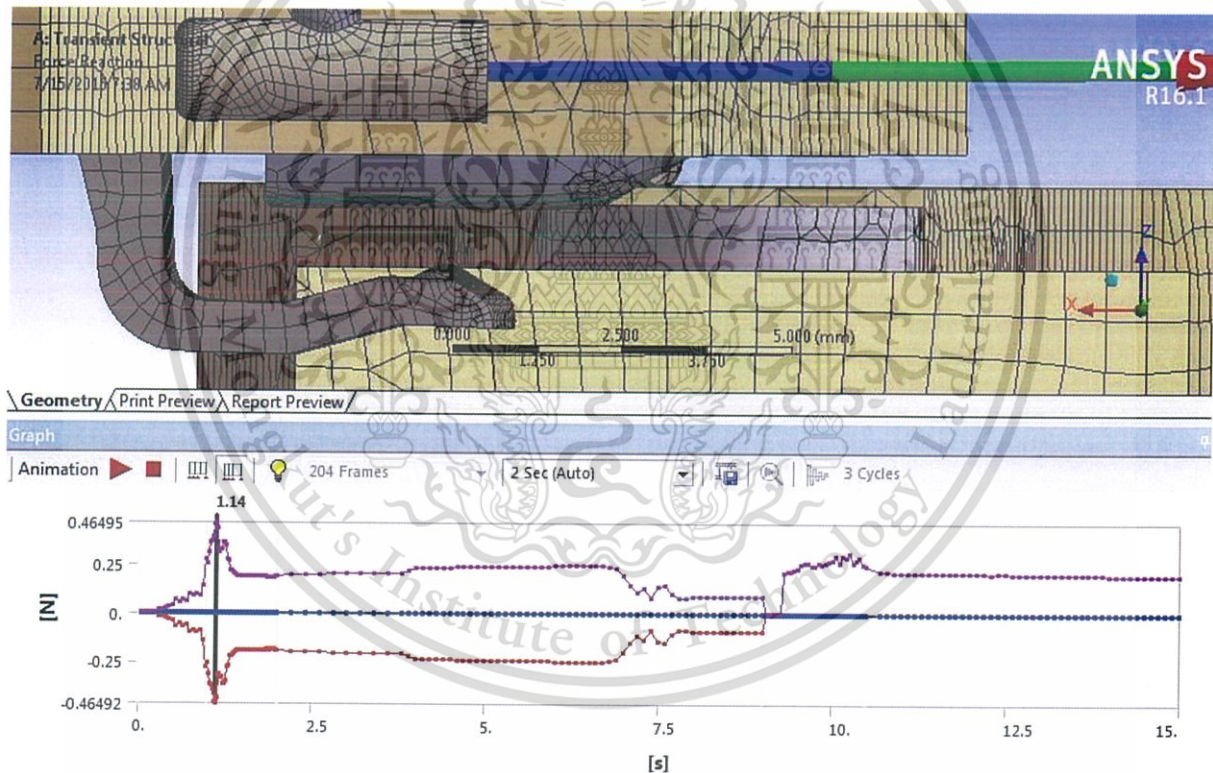


Figure 5.8 Simulation model at negative peak

Diagram in Figure 5.7 shows the shipping comb behavior at peak force when insert the shipping comb, point B in Figure 5.4. At this state the normal force from the latch is highest then the friction force or magnitude the reaction force also highest as shown in Figure 5.8.

This material is reserved for educational use only, not allowed for commercial use.

Forbidden to modify the content, and cite the document when use.

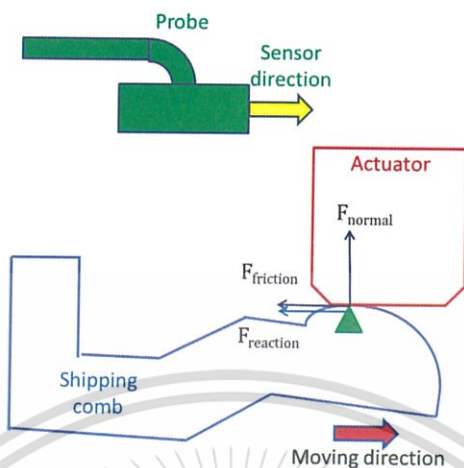


Figure 5.9 Force diagram between shipping comb and actuator at steady in negative

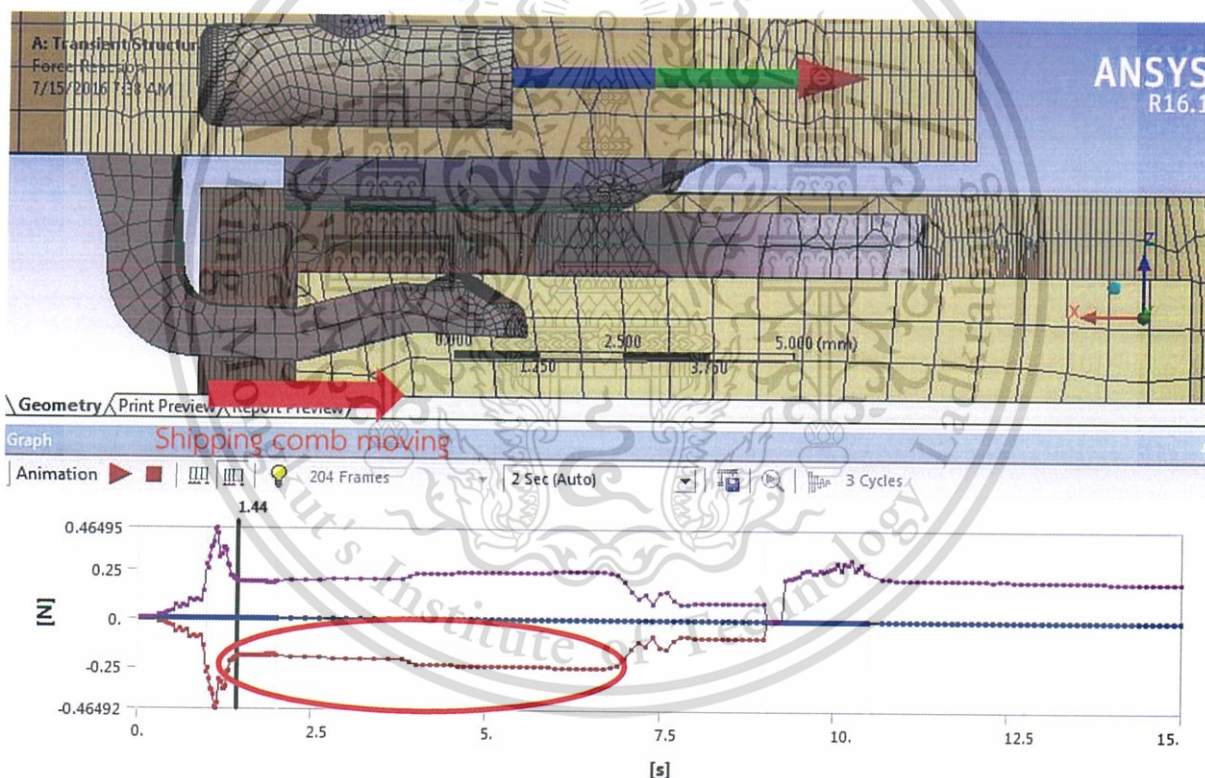


Figure 5.10 Simulation model at steady in negative zone

Diagram in Figure 5.9 shows the behavior of shipping comb when the reaction forces steady in insertion period, between point B-C in Figure 5.4. During this step, the friction force quite constant because the latch contact and move on flat surface of actuator.

This material is reserved for educational use only, not allowed for commercial use.

Forbidden to modify the content, and cite the document when use.

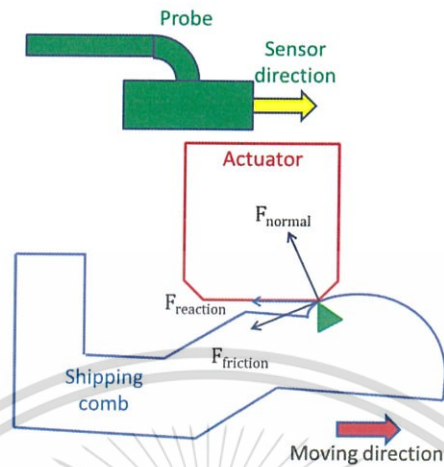


Figure 5.11 Force diagram between shipping comb and actuator at force trends to zero

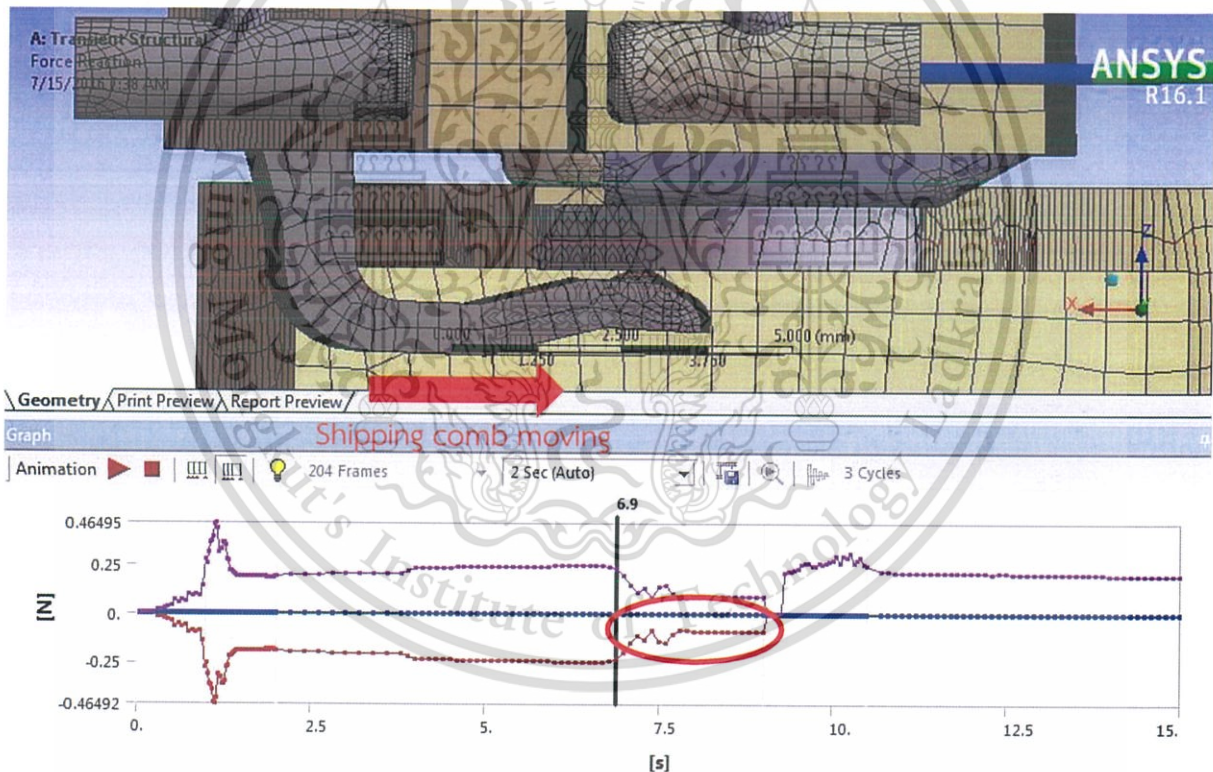


Figure 5.12 Simulation model at force trends to zero

Graph in Figure 5.12 trends to decrease the magnitude of reaction force as shown at point C in Figure 5.4. Diagram in Figure 5.11 shows the latch of shipping comb passed the flat surface and step into hole in actuator. The normal force is decreased because the latch bending is reduced.

This material is reserved for educational use only, not allowed for commercial use.

Forbidden to modify the content, and cite the document when use.

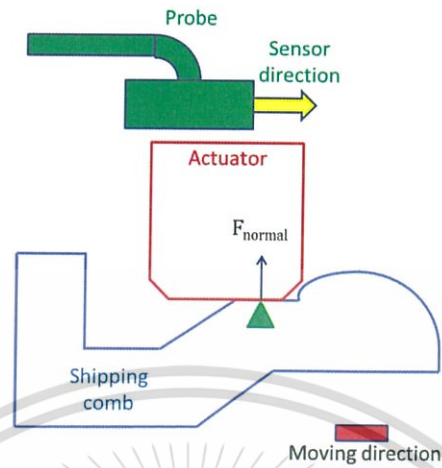


Figure 5.13 Force diagram between shipping comb and actuator at zero force

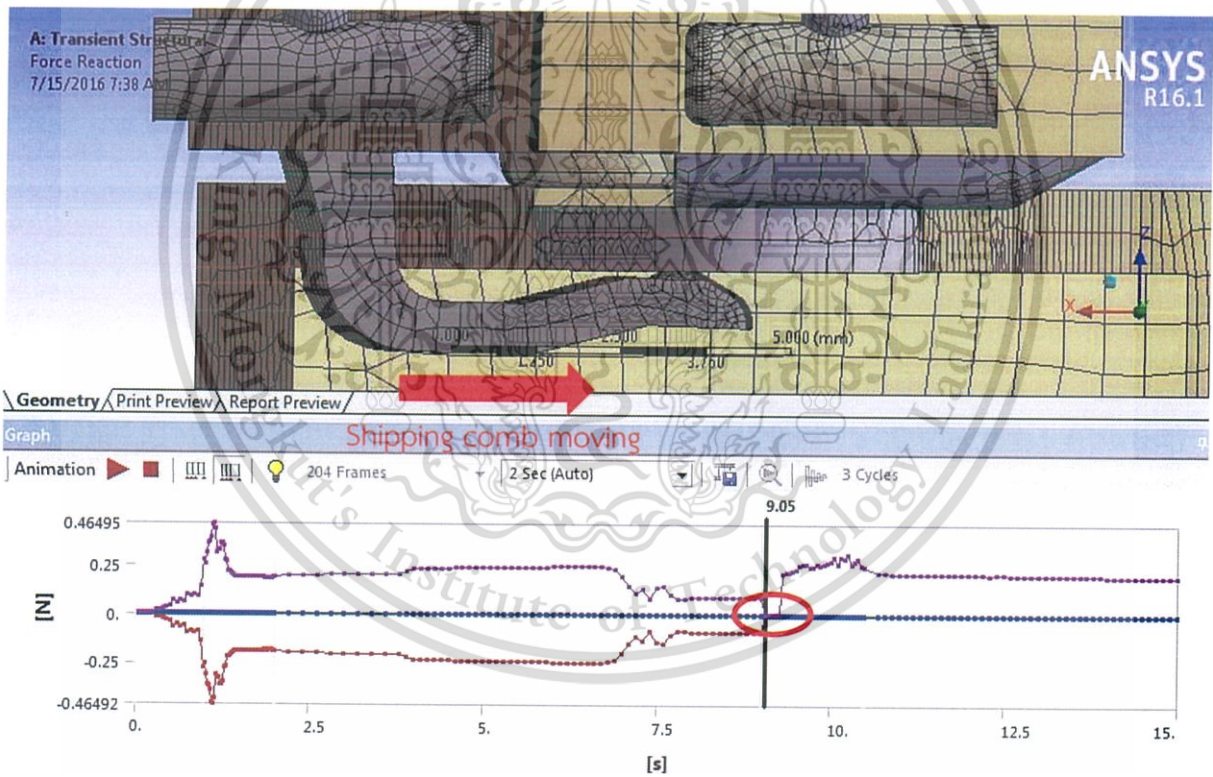


Figure 5.14 Simulation model at zero force

At the zero force, point D in Figure 5.4, the latch of shipping is not bended as shown in Figure 5.13 and 5.14 then the normal force is very small so the friction force and the reaction force are closed to zero.

This material is reserved for educational use only, not allowed for commercial use.

Forbidden to modify the content, and cite the document when use.

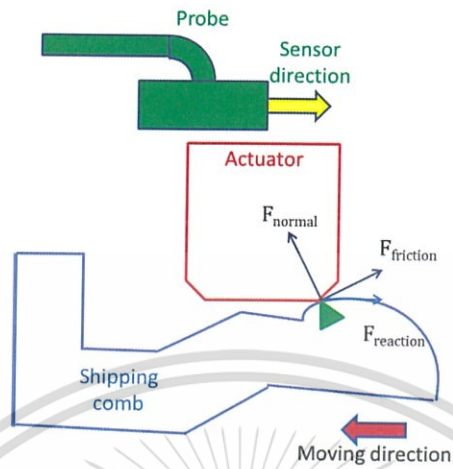


Figure 5.15 Force diagram between shipping comb and actuator at positive peak

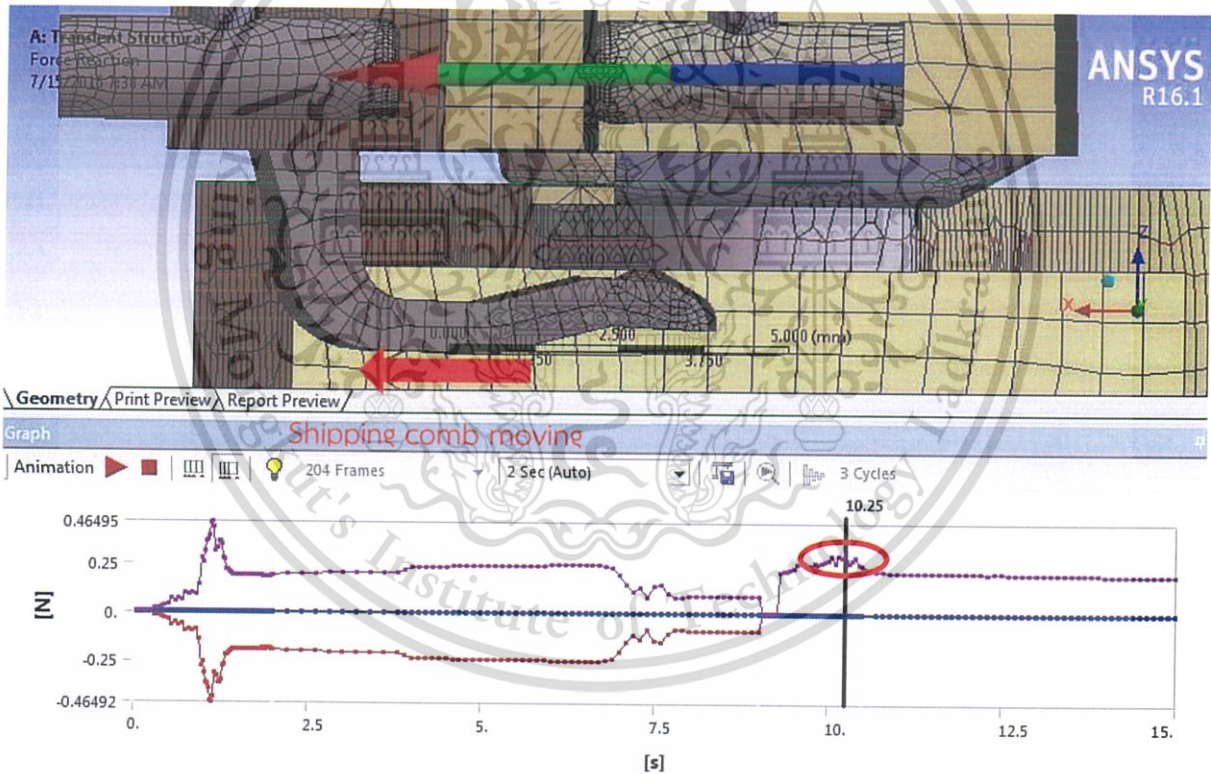


Figure 5.16 Simulation model at positive peak

The positive peak force at point E in Figure 5.4 occurs when the shipping comb move out of the actuator and the latch is in maximum bending as shown in figure 5.15 and 5.16 then the friction force between actuator edge and the latch will be highest.

This material is reserved for educational use only, not allowed for commercial use.

Forbidden to modify the content, and cite the document when use.

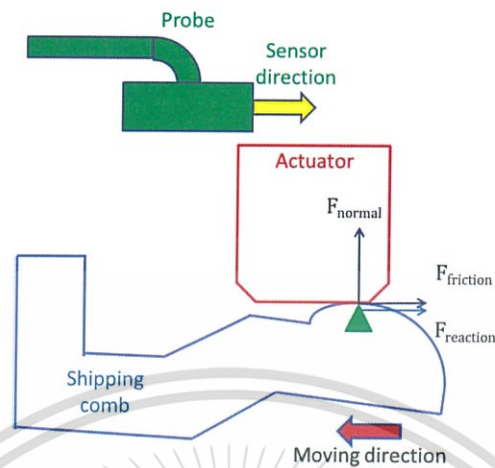


Figure 5.17 Force diagram between shipping comb and actuator at steady in positive

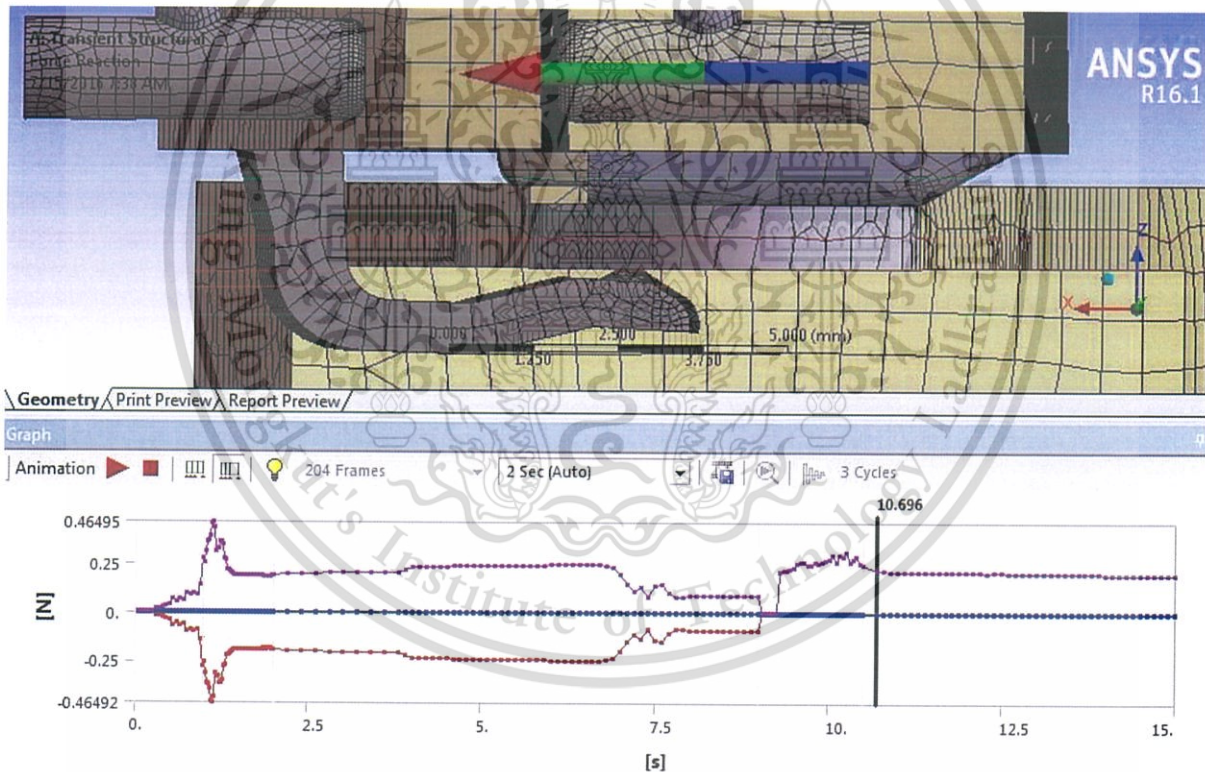


Figure 5.18 Simulation model at force steady in positive

The steady force in positive region at point F-G in Figure 5.4 occurs when the latch is moved on the flat surface while removing the shipping comb, as shown in Figure 5.17 and 5.18. It is similar to the steady force when inserting the shipping comb.

This material is reserved for educational use only, not allowed for commercial use.

Forbidden to modify the content, and cite the document when use.

The measurement data from experiment are recorded from the force gauge and plotted along the shipping moving time as shown in Figure 5.19.

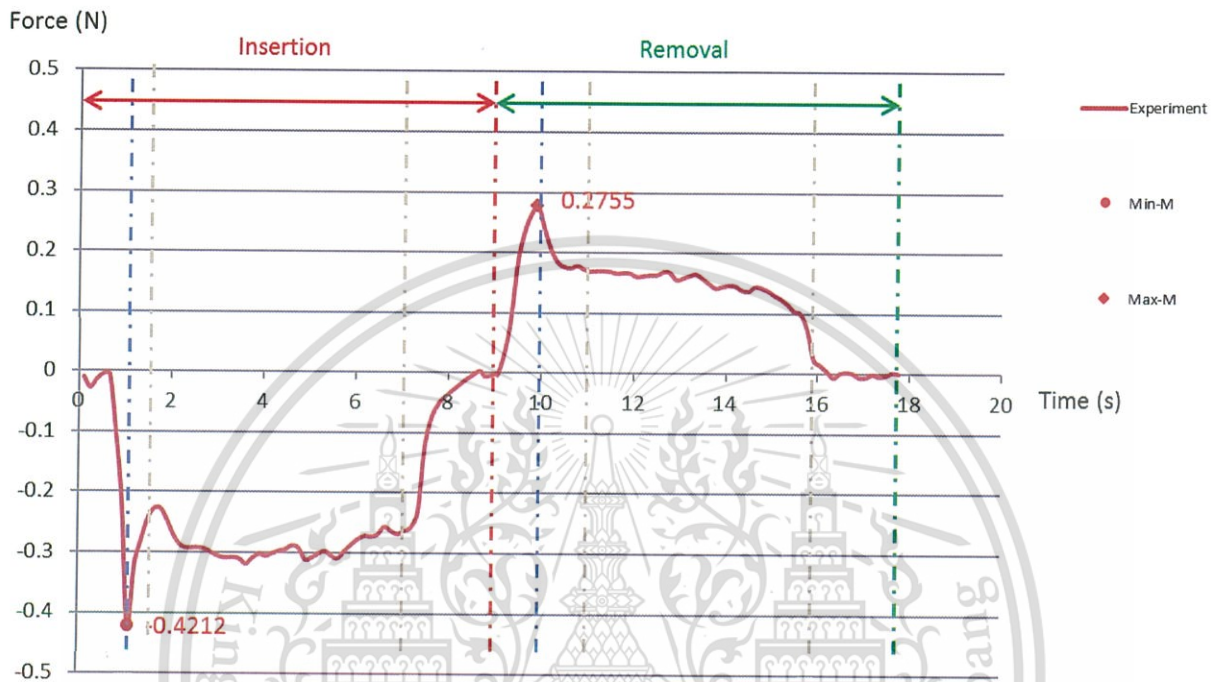


Figure 5.19 Force from experiment

From graph in Figure 5.19, force start from zero and ramp down to negative zone then peak at -0.4212 N at time about 1 second, point A in Figure 5.19. After that, the force ramp up and tend to fluctuate at -0.3 N until time 7 second, point B-C in Figure 5.19. Force ramp up again to zero at time 9 second, point D in Figure 5.19. Force in negative zone, time 0-9 second represent reaction force from insertion and the negative peak represent the insertion force. After time 9 second, the shipping comb move reverse to out of the actuator, force start from zero and ramp up to peak at 0.2755 N at time 10 second, point E in Figure 5.19. After the peak, force ramp down to fluctuate at 0.15 N, point E-F in Figure 5.19, until time 15 second then force tend to zero after time 16 second, point G in Figure 5.19.

To validate the simulation model, result from simulation and experiments are plotted in same graph and same time frame as shown in Figure 5.20.

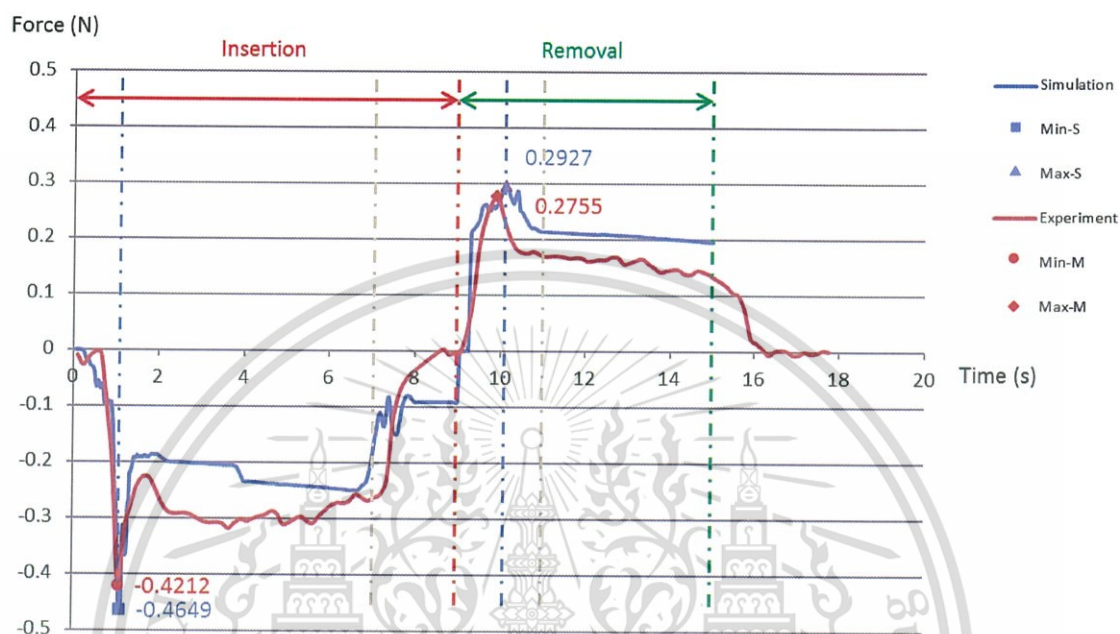


Figure 5.20 Comparison of simulation result and measurement result

From Graph in Figure 5.20, behavior of force from simulation and experiment are similar. In period time 0-1 second, forces start from zero and ramp down to peak at time about 1 second, negative peak force are -0.4649 for simulation and -0.4242 N for experiment.. In period time 1-7 second, forces start to increase to maintain at some value, -0.2 N for simulation and -0.4649 N for experiment. Then forces tend to zero at time 9 second. After that forces switch to positive zone. In period time 9-10 second, force ramp up from zero and increase to peak at time 10 second, positive peak force for are 0.2927 N for simulation and 0.2755 N for experiment. After peak, forces decrease to maintain during time 11–15 second, the maintenance force is 0.2 N for simulation and 0.15 N for experiment. The simulation time is end at 15 second because we know that after this time force is decreased to zero as shown in experiment result.

As comparison result, the behavior of force from simulation is similar to force behavior from experiment. It means simulation model can act as experiment. This model is accepted to use to study the sensitivity of shipping comb parameter.

This material is reserved for educational use only, not allowed for commercial use.

Forbidden to modify the content, and cite the document when use.

5.4 Experimental Result

5.4.1 Effect of the bump height

Result from increasing the bump height by 0.02 mm. shows lowest force -0.5153 N and highest force 0.3310 N per Figure 5.21. It means that the insertion and removal force are increased from the nominal, as shown in Figure 5.23.

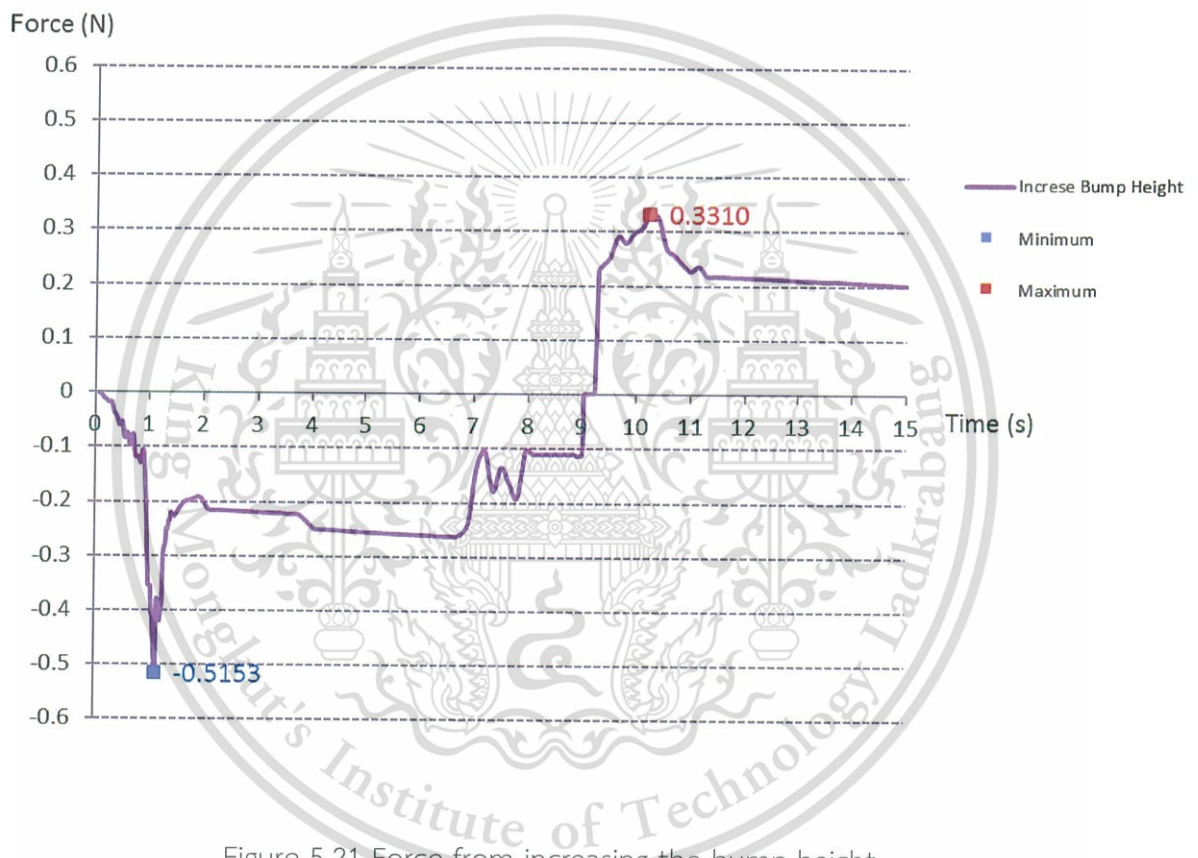


Figure 5.21 Force from increasing the bump height

Result from decreasing the bump height by 0.02 mm. shows lowest -0.3671 N and highest force 0.2558 N per Figure 5.22. It means that the insertion and removal force are decreased from the nominal, as shown in Figure 5.23.

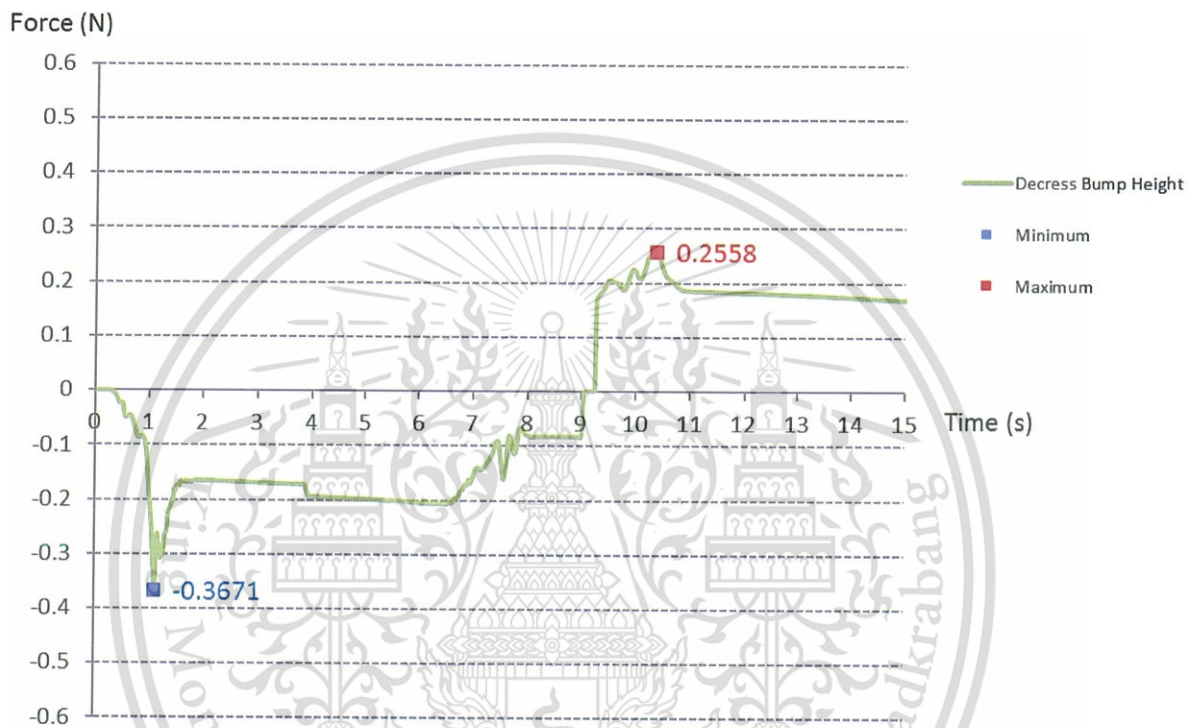


Figure 5.22 Force from decreasing the bump height

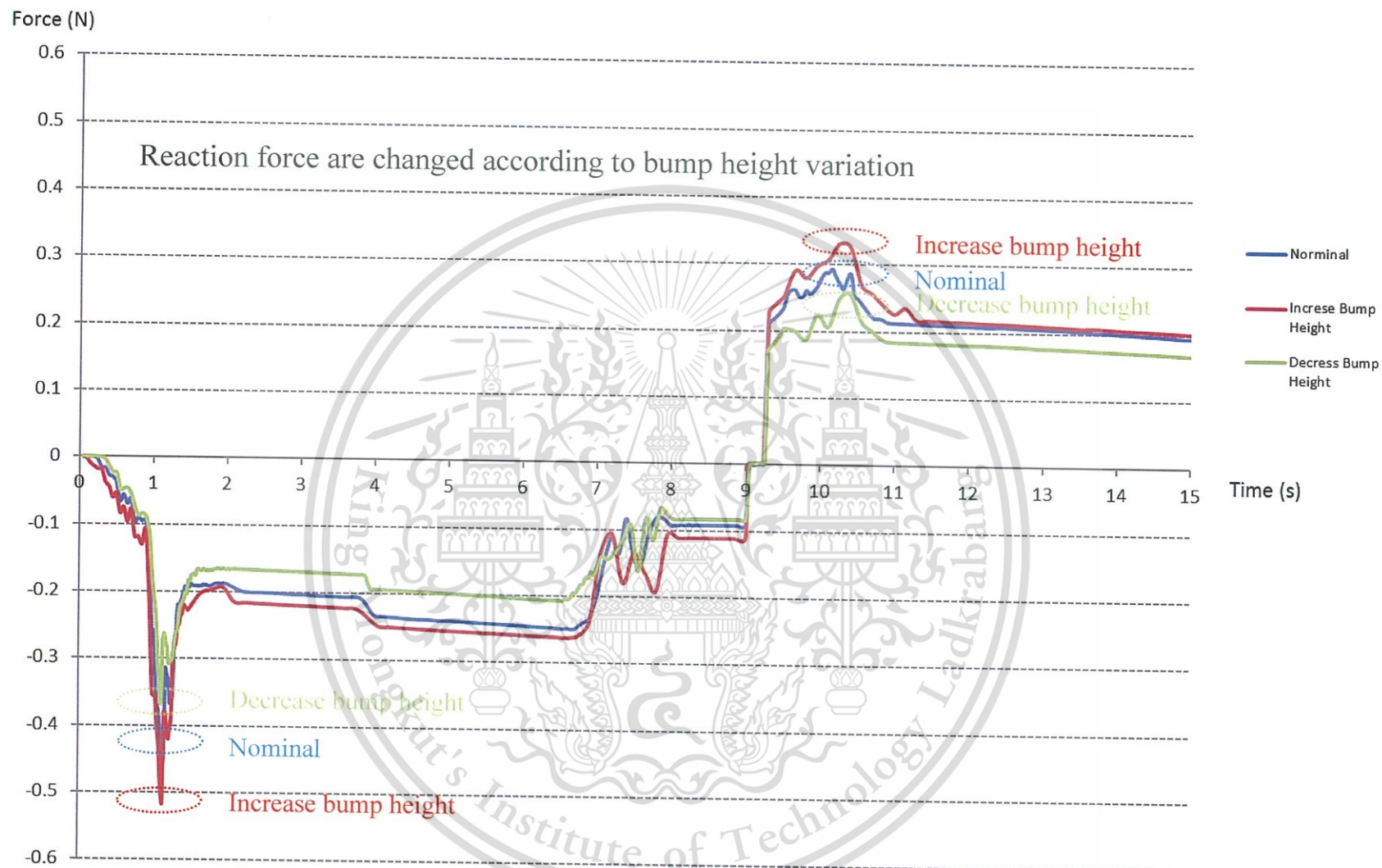


Figure 5.23 Simulation result of bump height variation

Data of insertion and removal force from Figure 5.21 and 5.22 are plotted along the height varying in order to calculate the sensitivity, as shown in Figure 5.24. From linear regression analysis, slope of insertion force is 3.7055 with R^2 of 0.967 and slope of removal force is 1.8805 with R^2 of 0.999.

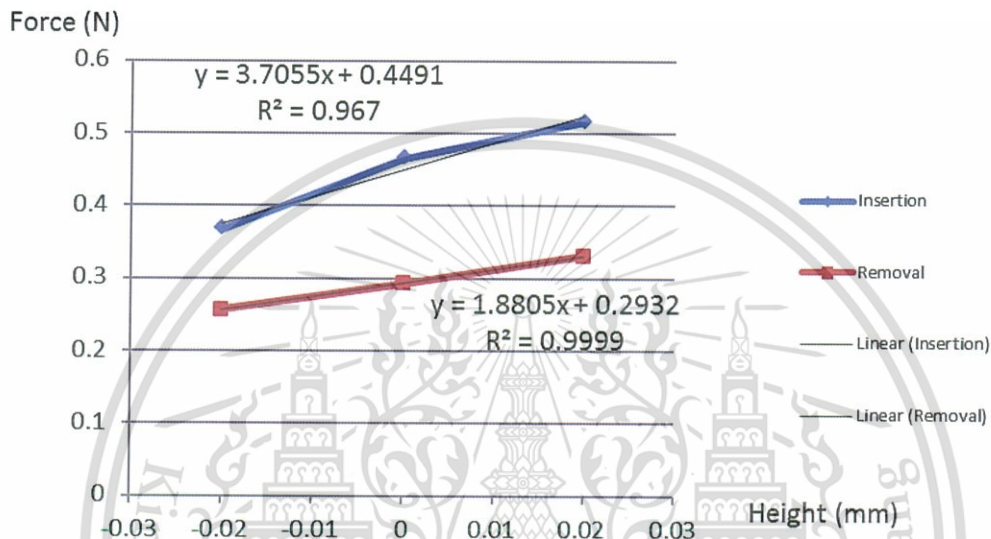


Figure 5.24 Linear regression of bump height

From sensitivity of bump height on insertion 3.7055 N/mm, it means if the bump height was changed by 1 mm the insertion force will be changed by 3.7055 N. For removal, the sensitivity of bump height is 1.8805 N/mm, it means if the bump height was changed by 1 mm the removal force will be changed by 1.8805 N. And according to the sensitivity of bump height on insertion is greater than removal, it means when the bump height was changed the insertion force will be effected greater than the removal force.

5.4.2 Effect of the base width

Result from increasing the base width by 0.12 mm. shows lowest force -0.5006 N and highest force 0.2968 N per Figure 5.25. It means that the insertion and removal forces are increased from the nominal, as shown in Figure 5.27.

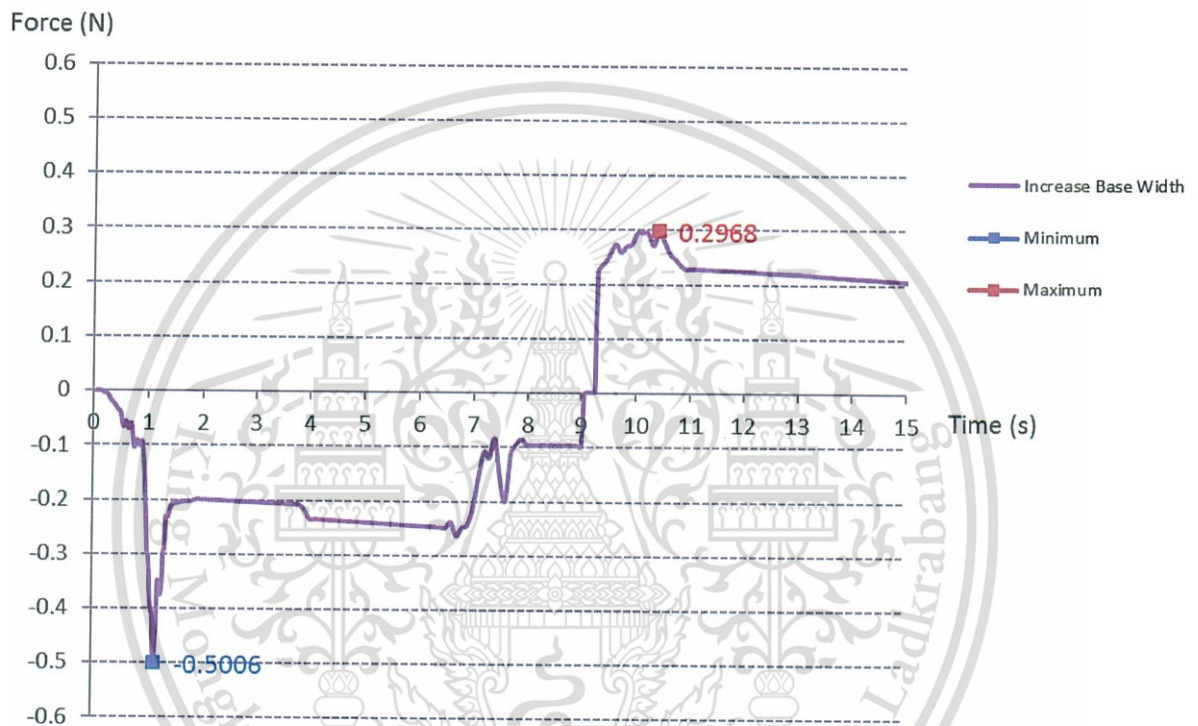


Figure 5.25 Force from increasing the base width

Result from decreasing the base width by 0.14 mm. shows lowest force -0.4277 N and highest force 0.275 N per Figure 5.26. It means that the insertion and removal forces are decreased from the nominal, as shown in Figure 5.27.

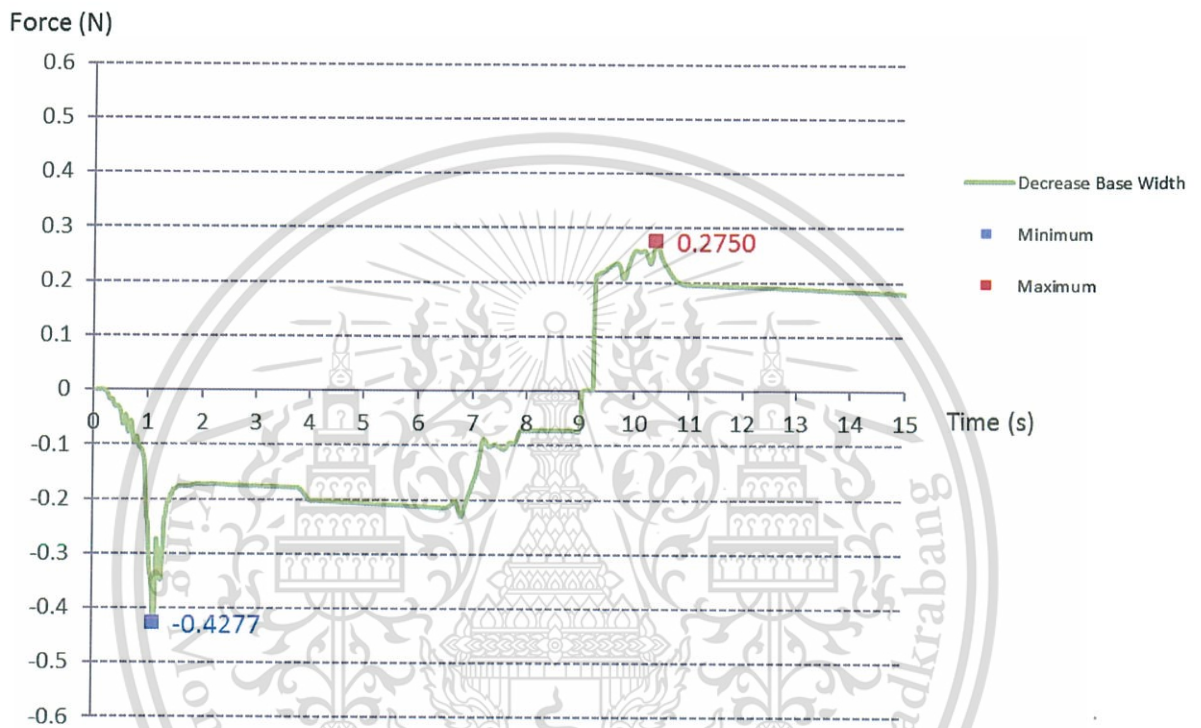


Figure 5.26 Force from decreasing the base width

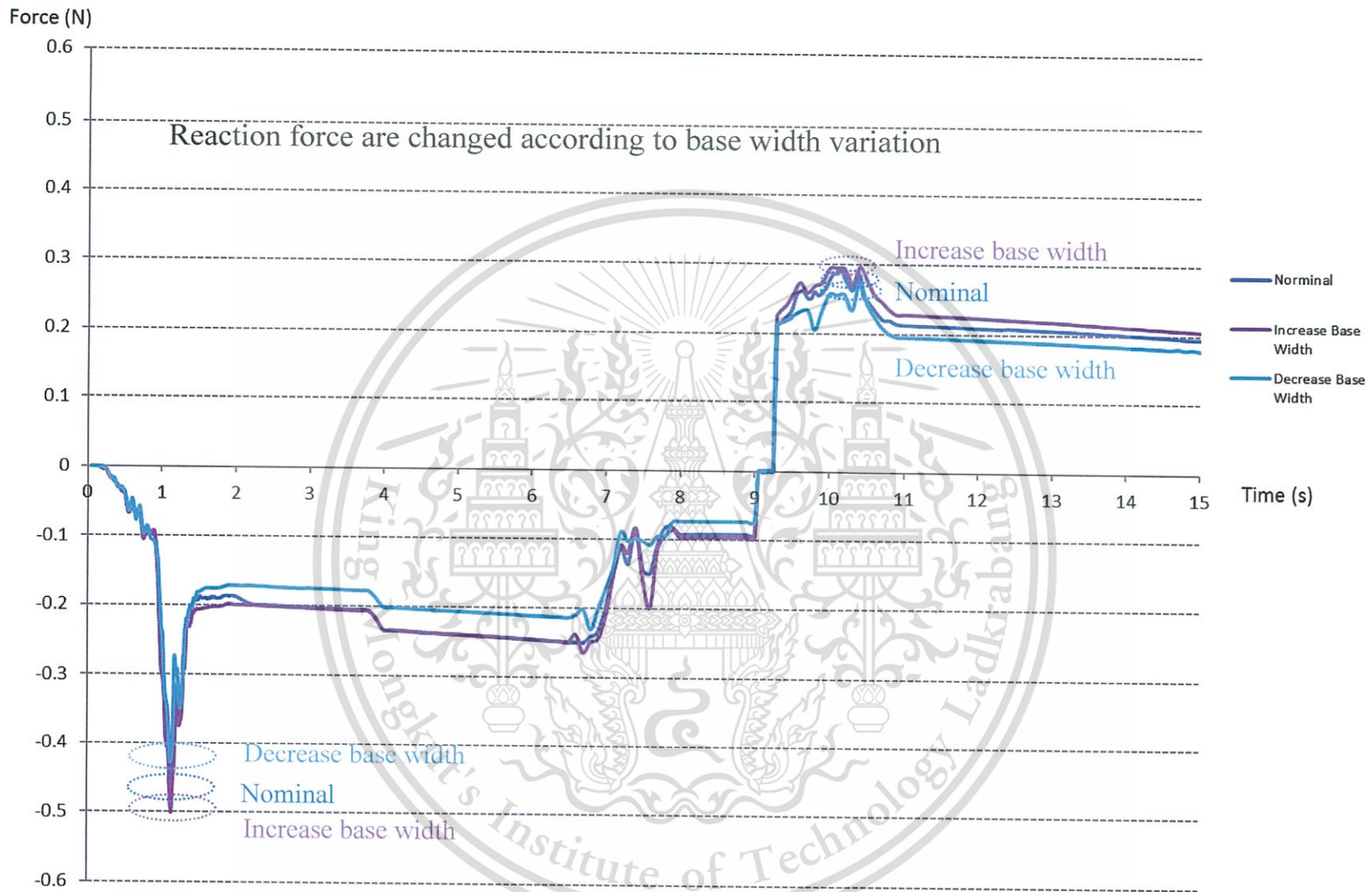


Figure 5.27 Simulation result of base width variation

Data of insertion and removal force from varying the base width are plotted along the height varying in order to calculate the sensitivity, as shown in Figure 5.28. From linear regression analysis, slope of insertion force is 0.2802 with R^2 of 0.999 and slope of removal force is 0.085 with R^2 of 0.913.

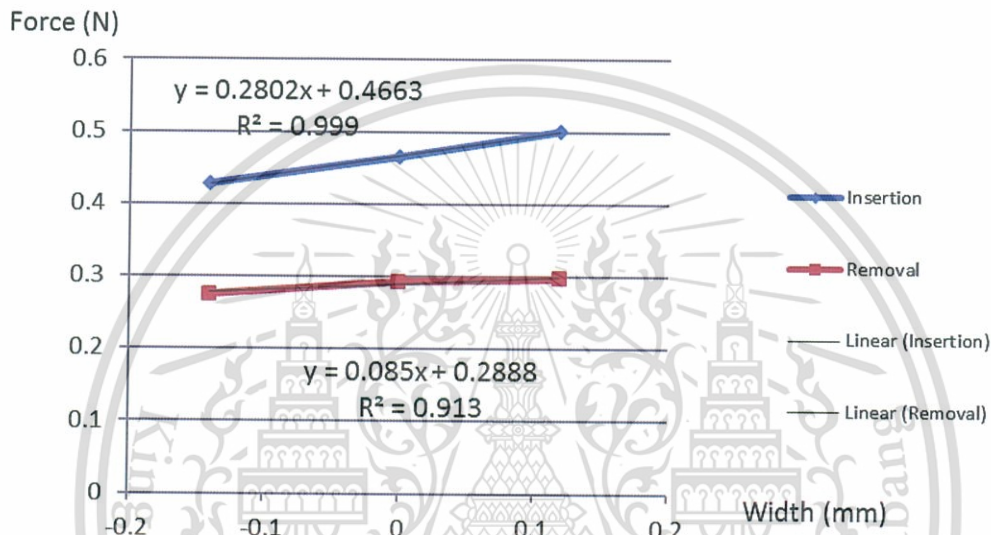


Figure 5.28 Linear regression of base width

From sensitivity of base width on insertion 0.2802 N/mm, it means if the base width was changed by 1 mm the insertion force will be changed by 0.2802 N. For removal, the sensitivity of base width is 0.085 N/mm, it means if the base width was changed by 1 mm the removal force will be changed by 0.085 N. And according to the sensitivity of base width on insertion is greater than removal, it means when the base width was changed the insertion force will be effected greater than the removal force.

5.4.3 Effect of the bar thickness

Result from increasing the bar thickness by 0.1 mm. shows lowest force -0.4982 N and highest force 0.3538 per Figure 5.29. It means that the insertion and removal forces are increased from the nominal, as shown in Figure 5.31.

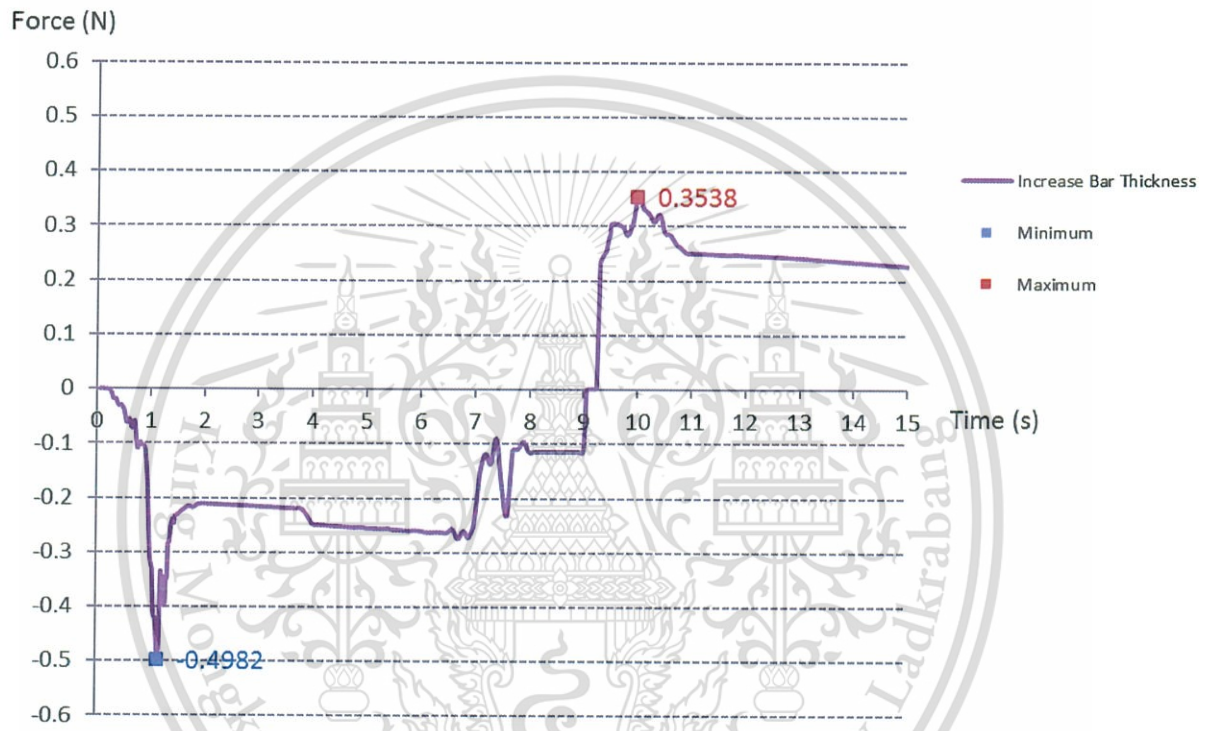


Figure 5.29 Force from increasing the bar thickness

Result from decreasing the bar thickness by 0.1 mm. shows lowest force -0.4414 N and highest force 0.2595 N per Figure 5.30. It means that the insertion and removal force are decreased from the nominal, as shown in Figure 5.31.

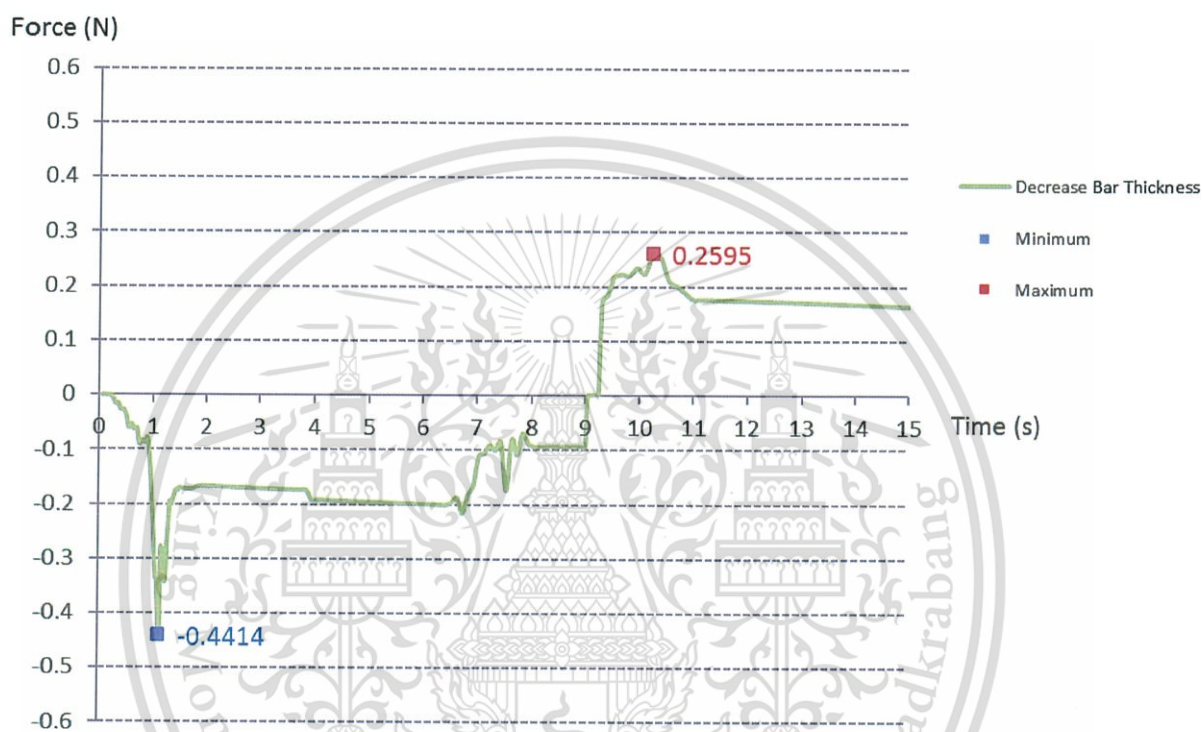


Figure 5.30 Force from decreasing the bar thickness

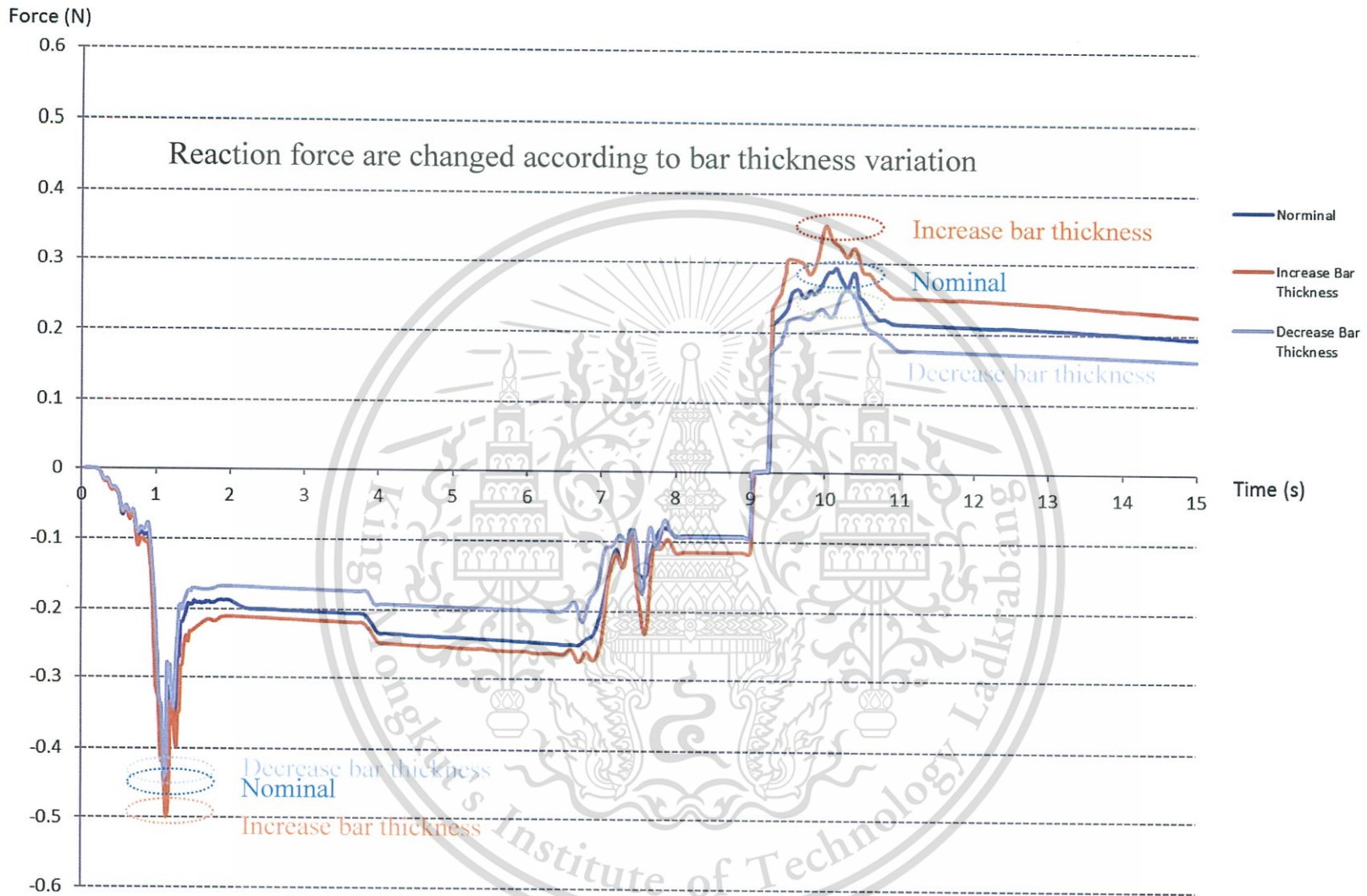


Figure 5.31 Simulation result of bar thickness variation

Data of insertion and removal force from varying the bump height are plotted along the height varying in order to calculate the sensitivity, as shown in Figure 5.32. From linear regression analysis, slope of insertion force is 0.284 with R^2 of 0.9904 and slope of removal force is 0.414 with R^2 of 0.9716.

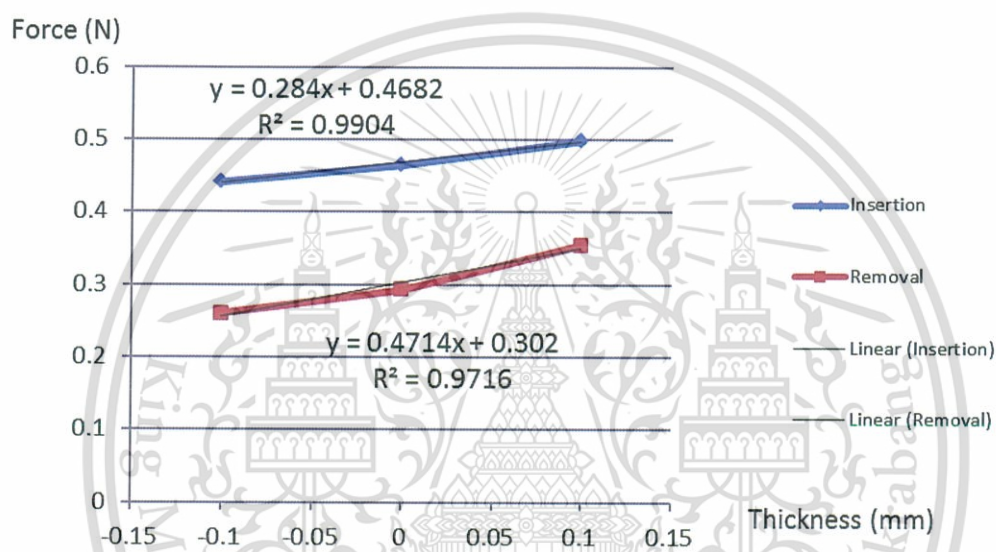


Figure 5.32 Linear regression of bar thickness

From sensitivity of bar thickness on insertion 0.284 N/mm, it means if the bar thickness was changed by 1 mm the insertion force will be changed by 0.284 N. For removal, the sensitivity of bar thickness is 0.4714 N/mm, it means if the bar thickness was changed by 1 mm the removal force will be changed by 0.4714 N. And according to the sensitivity of base width on removal is greater than insertion, it means when the bar thickness was changed the removal force will be effected greater than the insertion force.

To compare the insertion force in same dimension unit, the normalized data of insertion force are plotted as Figure 5.33 and the normalized data of removal force are plotted as shown in Figure 5.34.

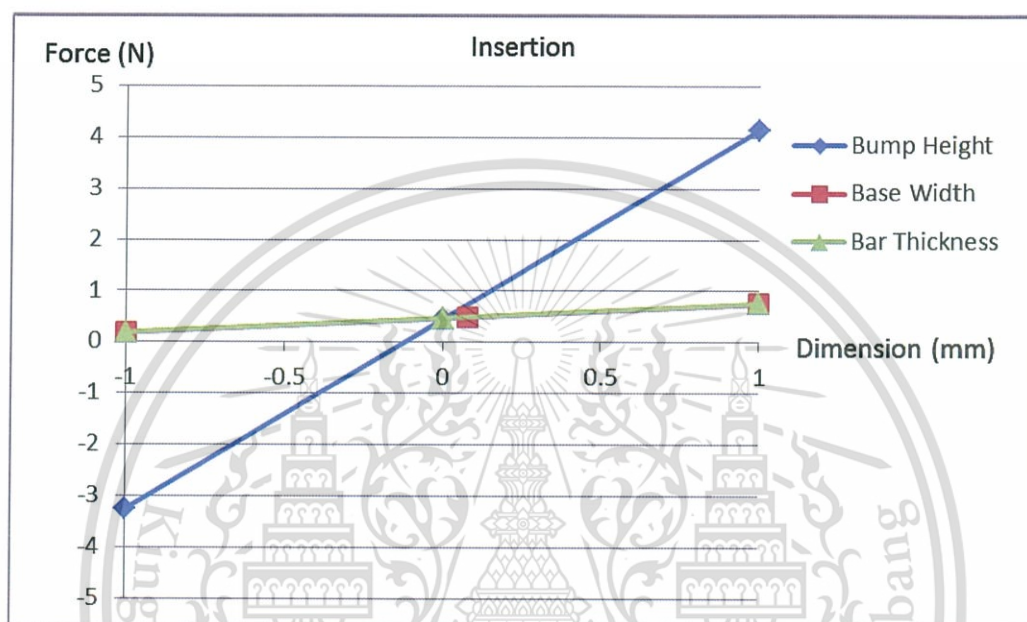


Figure 5.33 Normalized data of insertion forces

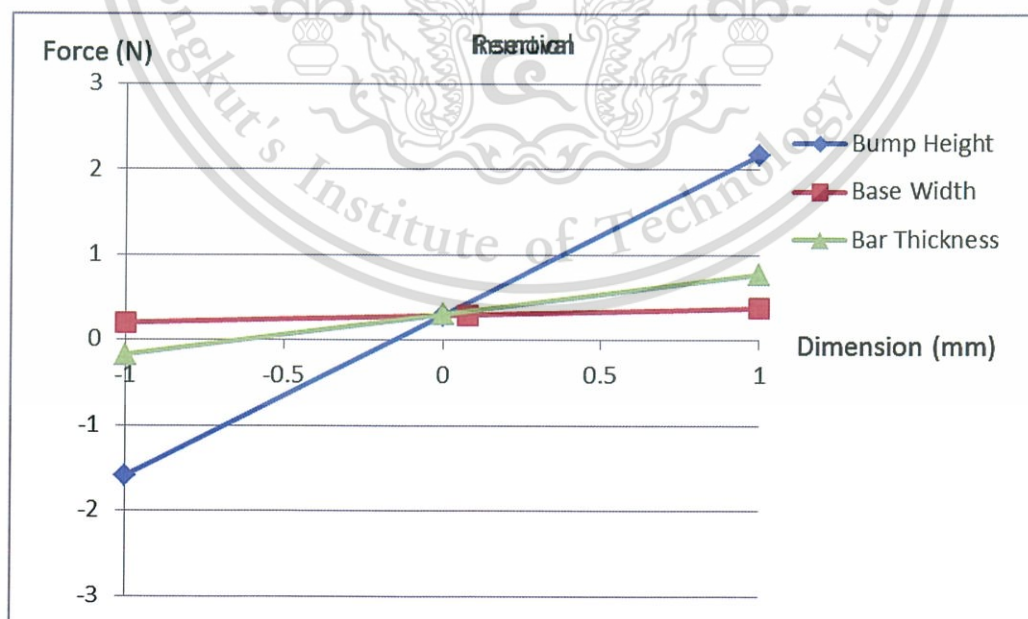


Figure 5.34 Normalized data of removal forces

5.5 Discussion

From model validation, the values of force from simulation are a bit difference from the experiment. This error is occurred from many reasons such as, the imperfect model, definition of material properties, accuracy of measurement, etc.

The model in simulation is a simplified model which not the copy of actual part. The actual part is cannot measured the dimension on some feature due to complexity and limit of measuring tool. The error when program calculate on mass or force is general issue.

In this study we assume all surface of part are smooth but in the actual model all surfaces are rough as shown in Figure 5.34. As graph in Figure 5.19, during time 1.5-7 second, the force from experiment is fluctuate while force from simulation is smooth.

In experiment, the measurement tool is the force gauge, Chatillon DFS II, which has accuracy error at 0.1% or about ± 0.001 N. It means fluctuation of force from experiment may be occurred from error of the gauge.

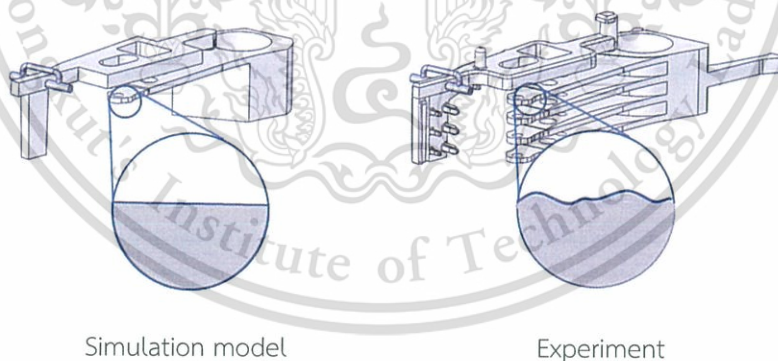


Figure 5.35 Surface of simulation model and experiment

Although the forces from simulation and experiment are a bit difference but if we focus on the behavior, the force behavior from simulation is similar to the force behavior from experiment. It means that the simulation model can be accepted to use for parametric study.

To compare the sensitivity of each parameter, the slope of all parameters are plotted and divided into insertion and removal cases as shown in Figure 5.36

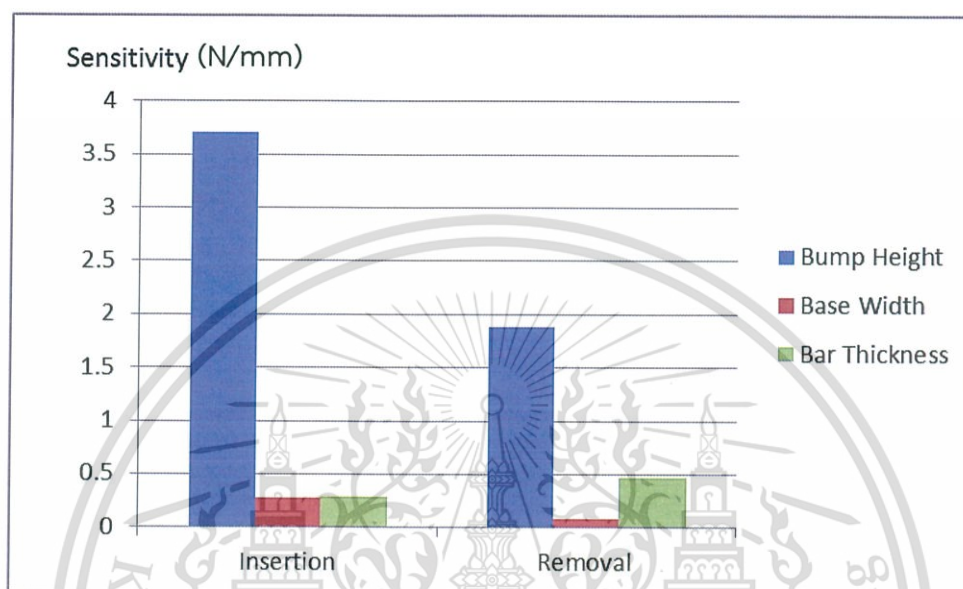


Figure 5.36 Sensitivity of all parameters

From the graph in Figure 5.36, the bump height shows highest sensitivity to the insertion force while the base width and the bar thickness are less sensitivity. The reason of this result is the bump is the main feature of the latch that is resistive to the actuator arm movement and the bump height is the parameter that affects to the deformation of the bar latch.

For the removal, the bump height still shows highest sensitivity to the removal force while bar thickness is the next contributor to the removal force and the base width is the lowest contributor to the removal force.

CHAPTER 6

CONCLUSIONS AND SUGGESTIONS

6.1 Conclusions

As the aim of the thesis are to study the behavior of shipping comb insertion and removal forces from simulation and validate with experimental result, to study the parameters that effect to the shipping comb insertion and removal forces and to identify the most effected parameter on those force. This study is achieved to find out material properties for analysis by ANSYS program, then study shipping comb insertion and removal force behavior by using finite element method and validate result with actual data from the experiment. The sensitivity of shipping comb latch parameters to shipping comb insertion and removal force was investigated.

The simulation model can represent the behavior of shipping comb insertion and removal process. The simulation result is a bit higher than the measurement result but it is still acceptable.

From the parametric study, the bump height is major contributor to insertion and removal forces, but if we focus on mold modification to get shipping comb insertion and removal forces to meet the specification, the bump height is quite difficult to modify the shipping comb mold to meet specification. Otherwise, the base width and the bar thickness are easy to modify to meet specification. Shipping comb designer has to review it carefully case by case to modify on which parameter.

For example, if bump height of shipping comb first lot is lower than nominal design and force also lower than specification. The bump height can be selected to modify. The electrical discharge machining (EDM) is a method to modify surface of bump on core insert because of the surface of bump is complex then the modification cost is very high. For another case, the bump height of shipping comb first lot is equal to nominal design. The base width or bar thickness should be selected to modify instead of bump height. The process to modify dimension of bar thickness is easy because the EDM process can be applied on the surface of bottom plan of latch which is very simple.

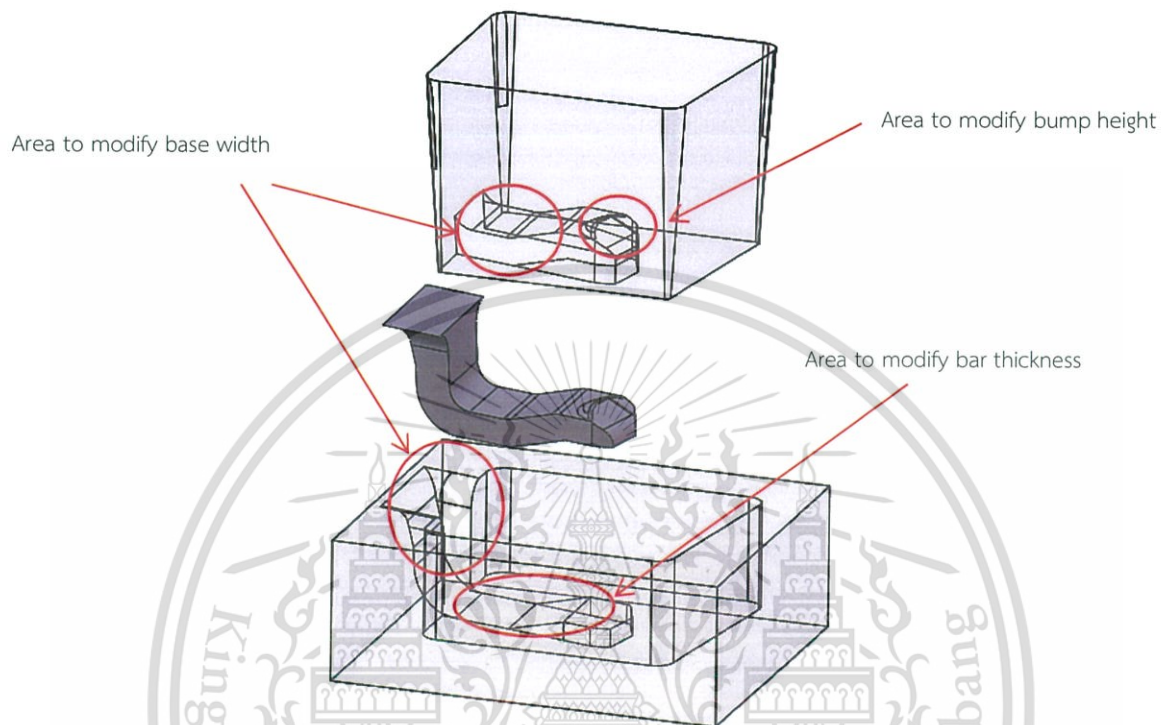


Figure 6.1 Mold insert of shipping comb latch

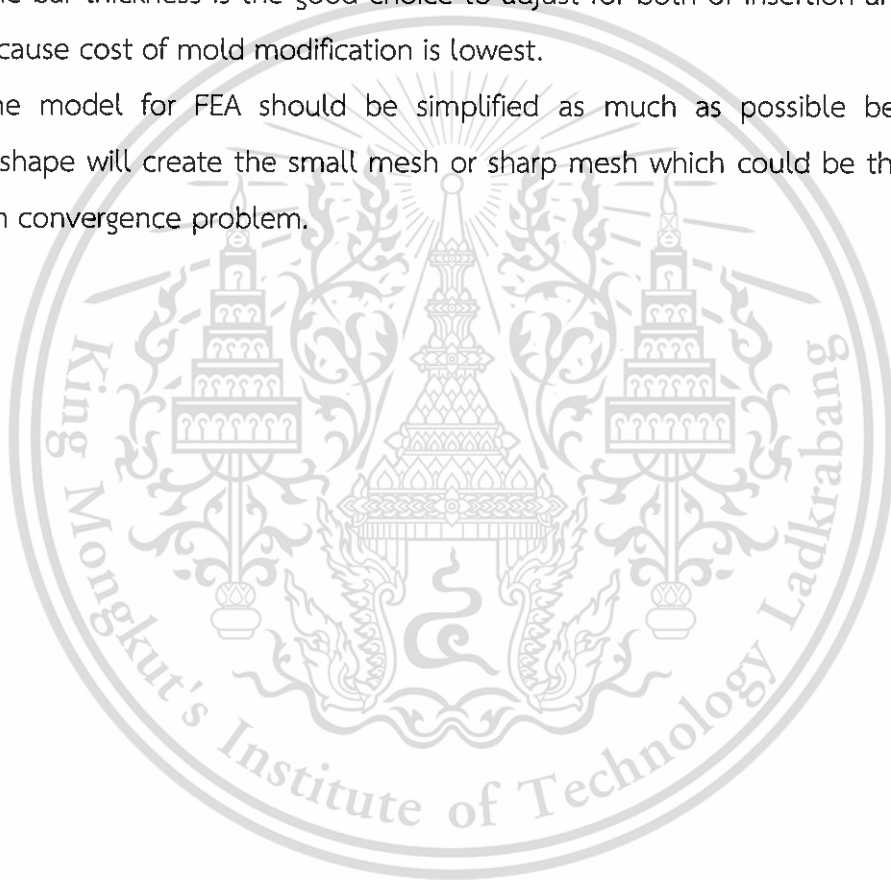
Benefits of this study are to reduce time to design and to develop the shipping comb to meet the requirement and save cost of the mold modification. The modification cost of bar thickness can be cheap to quarter of cost to modify the bump height.

6.2 Suggestion

The bump height is chosen to modify if dimension of the bump height from shipping comb first lot is in lower zone of specification but not recommended because cost of mold modification will be high.

The bar thickness is the good choice to adjust for both of insertion and removal forces because cost of mold modification is lowest.

The model for FEA should be simplified as much as possible because the complex shape will create the small mesh or sharp mesh which could be the cause of simulation convergence problem.



REFERENCES

- [1] ANSYS® Mechanical Premium, Release 16.1, ANSYS, Inc., 2015
- [2] Kajornsak J. and Wisawat A., “A Study of HGA Behaviors after Mounted with Shipping Comb”, the 23rd Conference of the Mechanical Engineering Network of Thailand, 2009.
- [3] Chalermchai C., “Effect of Heat on Properties of Polycarbonate Composites”, the 2nd International Conference on Mechanical Engineering, 2010.
- [4] Thawisanee P., Failure analysis of Polycarbonate part by using Finite Element Simulation, KKU Engineering Journal Vol 38, 2011, pp.421-431.
- [5] Suriya S., Somsak S., “FEA Simulation Study of Shipping Comb Removal and Insertion in HDD Manufacturing”, the 4th International Data Storage Technology Conference (DST-CON2011), 2011.
- [6] Oberoi H.S., “Using actual production runs of components to teach implementation of statistical process control techniques”, Frontiers in Education Conference, USA 1996.
- [7] CAD-IT, ANSYS Mechanical Linear and Nonlinear Dynamics, Training manual to ANSYS Release 15.0, Thailand. 2014
- [8] Nishihata N., “New ESD control material based on special carbon”, Electrical Overstress/Electrostatic Discharge Symposium, Japan 2001.
- [9] Steven B., Ernest P., Karl M., Brett C. A “Comparison of All Hexagonal and All Tetrahedral Finite Element Meshes for Elastic and Elasto-plastic Analysis”, Brigham Young University, Greg Sjaardama Sandia Nation Laboratories Albuquerque, NM, 2009
- [10] B.N.J. Persson, “*Sliding Friction Physical Principles and Applications*”, Second Edition, NanoScience and Technology, 2000.
- [11] Wu Y. Wang F., Ma cb., “*Nonlinear Finite Element Buckling Analysis of Arm Stand of Dynamic Compaction Machinery*”, the 7th International Conference on Computer Science & Education (ICCSE), Australia 2012.
- [12] Beng S.L., “Proactive Performance Optimization Model for EDM Operation”, Industrial Information, IEEE International Conference, Singapore 2006.

This material is reserved for educational use only, not allowed for commercial use.

Forbidden to modify the content, and cite the document when use.

APPENDIX A

PUBLICATION

This study has been published and presented in The 2nd International Conference on Engineering Science and Innovative Technology (ESIT 2016), Phuket



The 2nd International Conference on
**Engineering Science
and Innovative Technology**
April 21-23, 2016
Angsana Laguna Phuket
PHUKET, THAILAND
<http://esit.cit.kmutnb.ac.th>

- Automotive Engineering
- Mechatronics & Mechanical Engineering
- Electrical, Electronic and Automation Engineering
- Energy & Environmental Engineering
- Computer Science / Signal and Image Processing
- Construction Technology

KMUTNB



The image shows a promotional banner for the 2nd International Conference on Engineering Science and Innovative Technology (ESIT 2016). The banner is blue and white, featuring the conference title, dates (April 21-23, 2016), location (Angsana Laguna Phuket, Phuket, Thailand), and a list of six engineering fields: Automotive Engineering, Mechatronics & Mechanical Engineering, Electrical, Electronic and Automation Engineering, Energy & Environmental Engineering, Computer Science / Signal and Image Processing, and Construction Technology. The banner also includes the KMUTNB logo and a globe icon. Below the banner, the KMUTNB logo is displayed in red, and a globe icon is shown in blue and white. The background of the entire page features a large, faint watermark of the Mongkut's University of Technology Ladkrabang seal.

This material is reserved for educational use only, not allowed for commercial use.

Forbidden to modify the content, and cite the document when use.

Parametric Study of Shipping Comb Insertion and Removal Force

Wiriyu Yupensuk¹, Monsak Pimsarn² and Chalothorn Thumtae^{3,*}

Abstract

Shipping comb is a component in Head Stack Assembly (HSA) which is assembled in HSA until the HSA is merged into a hard disk drive. The insertion and removal force of shipping comb is critical for automation tooling. The variation of latch dimension from different mold results in force varying and sometimes also leads to out of specification. Thus, this paper aims to study the sensitivity of shipping comb latch dimensions, namely, bump height, base width and bar thickness, and to predict appropriate dimensions for mold modification in order to meet insertion and removal force requirement. The transient structural of Finite Element Analysis (FEA) is employed to simulate the behavior of the shipping comb model. From the simulated results, it is found that the bump height is provided highest sensitivity for both of insertion and removal force, but before making decision to modify the mold, shipping comb designer must review on dimension of shipping comb from first lot. If the bump height is equal to nominal design, the bump height should be maintained and select to adjust on base width or bar thickness instead. Benefits of this study are to reduce design process time and to save cost of the mold modification.

Keywords: Shipping comp, Head stack assembly, Insertion and removal force

¹ Graduate Student, Department of Data Storage Technology, College of Data Storage Innovation, King Mongkut's Institute of Technology Ladkrabang.

² Assistant Professor, Department of Mechanical Engineering, Faculty of Engineering, King Mongkut's Institute of Technology Ladkrabang.

³ Faculty Members, Department of Mechanical Engineering, Faculty of Engineering, Suranaree University of Technology.

* Corresponding author, E-mail: Wiriyu.Yupensuk@seagate.com

1. Introduction

Shipping comb is a component in Head Stack Assembly (HSA) which is assembled in HSA until the HSA is merged into a hard disk drive. In many HSA operations, the shipping comb is inserted and removed in order to measure the HSA parameters. The insertion and removal force of shipping comb are critical property for many machines because HSA will be damaged if the machine cannot remove the shipping comb before measurement or immobile it back into the HSA. These forces are complex properties that are contributed from many parameters such as shape, material property, contact condition etc. In recent years, some researchers have studied shipping comb properties. Pattamapradit [1] reported that the strength of shipping comb is reduced from high temperatures and chemicals in HSA assembly process. The strength of shipping comb will be stable after 7-10 cycles. Supa [2] studied the shape of shipping comb concerning with shipping comb insertion and removal force. The result showed that chamfer on latch is the major contributor to shipping insertion and removal force. He suggested shipping comb designers to focus on the chamfer when they design the shipping comb. However, in case modification, the chamfer is not the good parameter to adjust. The aim of the paper is to study the sensitivity other shape of shipping comb latch and predict optimum dimension for mold modification [3] in order to meet insertion and removal force requirement. The result of this paper will help reduce time and cost for the design of shipping comb.

2. Method

2.1 Finite Element Analysis Model

Finite Element Analysis (FEA) is the numerical method used to simulate and analyze the behavior of the physics problems. ANSYS [4] is one of the commercial FEA

programs generally used to simulate the linear and nonlinear problems. In order to analyze the shipping comb insertion and removal force, the transient structural system of nonlinear module in ANSYS program must be adopted because the actual process time is very short, about 50 milliseconds. Thus, this paper studies the shipping comb movement when it is inserted and removed on the actuator arm. The reaction force on the measurement probe in Figure 1 is the model that represented the shipping comb insertion and reaction force.

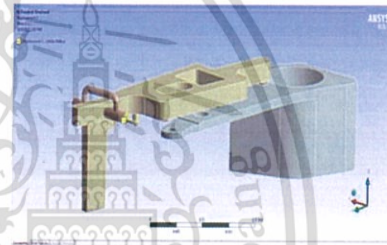


Fig.1. Model shipping comb and actuator

The model of shipping comb and actuator is simplified by removing non touching arm and the shipping comb finger in order to reduce number of elements. The fillet and the chamfer are also removed in order to reduce errors from the sharp mesh element when the program calculates the mass and momentum conservation. The Hex Dominant method [5] is selected to create mesh for the mode. The model with hexagonal elements is enabled to deform in a lower strain energy state, thus it produced lower error than tetrahedron elements. Figure 2 shows the hexagonal and tetrahedron element and Figure 3 is the mesh model of shipping comb and actuator

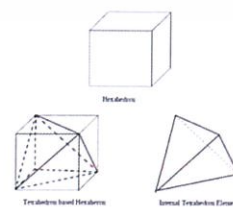


Fig.2 Element Type

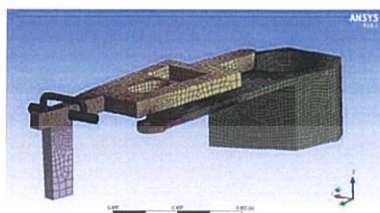


Fig.3. Discretized model of shipping comb and actuator

The transient structural analysis in ANSYS is selected to simulate the action of shipping comb insertion and removal because it can determine the dynamic response of the model under action of time-dependent loads. The movement of shipping comb is split into small time steps to capture the reaction force on the measurement probe in each time steps.

2.2 Material Property

Polycarbonate is material of shipping comb that is developed to support specific requirement such as high wear resistant, ESD safe and low particle shading [6]. Some properties may not provide in public such as friction coefficient and stress-strain curve which are important properties for FEA.

2.2.1 Friction Coefficient

A simple method to find out friction coefficient [7] is calculated from force which is defined to push static mass. Figure 4 shows equipment for push force measurement.

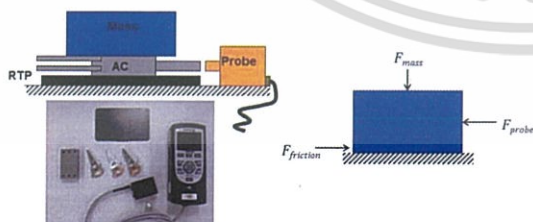


Fig.4. Tool and force diagram

From force diagram in Figure 4, the friction coefficient can be calculated from Eq. (1)

$$\mu = \frac{F_{probe}}{F_{mass}} \tag{1}$$

Table 1 Measurement data and friction coefficient

	HSA1	HSA2	HSA3
	0.658	0.763	0.716
	0.615	0.807	0.705
	0.654	0.764	0.781
	0.709	0.722	0.713
	0.681	0.773	0.824
	0.688	0.668	0.668
	0.597	0.860	0.688
	0.628	0.736	0.727
	0.656	0.749	0.710
	0.613	0.772	0.707
Average	0.650	0.761	0.724
Weight (N)	2.331	2.354	2.382
Friction	0.279	0.323	0.304

From the obtained data, the average friction coefficient is 0.31.

2.2.2 Stress-Strain curve

One important material property for FEA in non-linear is stress-strain curve [8]. The Universal Testing Machine 5560 is chosen to generate stress-strain curve for shipping comb material.

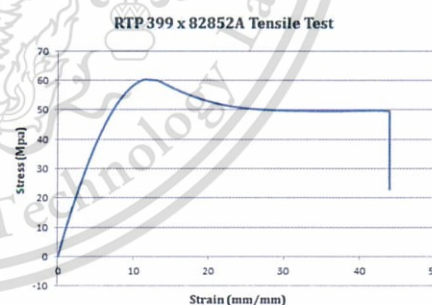


Fig.5. Stress-Strain curve of shipping comb material

2.3. Model validation

The results from simulation are plotted along the time and compared with the results from experiment to make sure the model is appropriate. The comparison of results is shown in Figure 6.

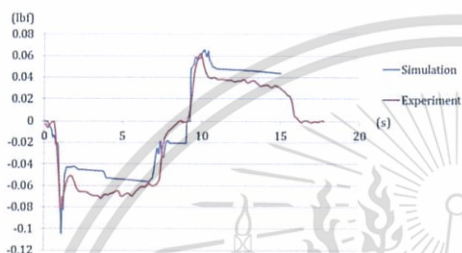


Fig.6. Simulation result compare with experiment

The result from simulation is show behavior of force similar to the result from experiment. This model is acceptable.

2.4 Parametric Study

In order to study parametric of shipping comb, the dimensions on latch are defined and considered critical dimensions to study the sensitivity of each dimension to the shipping comb force. The dimensions shown in Figure 7 are the interesting dimensions. However, the latch position is dependent on HSA design that is rarely changed. The slope angle is difficult to control and measure. This parameter should be maintained once shipping comb has been injected. The bump height, the base width, and the bar thickness are always varied from different mold cavity. The bump height, the base width and the bar thickness are selected to study their effect on the insertion and removal force.

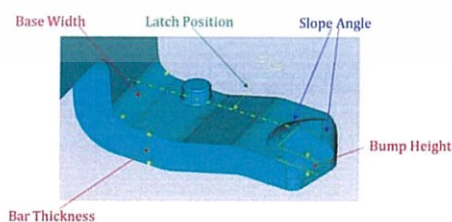


Fig.7. Interesting parameters on shipping comb

3. Result

The nominal FEA model is replicated to two models for each parameter by the one model is increased the dimension and another model is reduced the dimension. According to the variation range of each parameter is quite narrow and the simulation time for each model is quite long, three times varies, included the nominal, is enough to represent the behavior of each parameter. The r-square of all experiment are over than 0.9, the prediction is confidence.

3.1 Effect of the bump height

Result from varying the bump height by +/-0.02mm showed slope 0.833N/mm for insertion force and slope 0.423 N/mm for removal force.

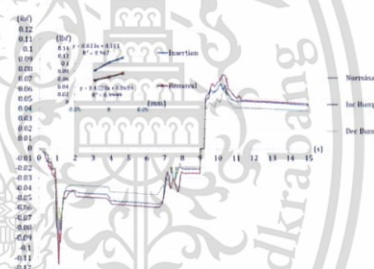


Fig.8. Result from varying the bump height

3.2 Effect of the base width

Result from varying the base width by +/-0.1mm showed slope 0.061 N/mm for insertion force and slope 0.019 N/mm for removal force.

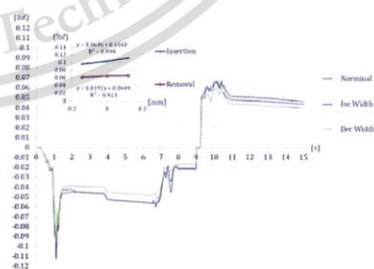


Fig.9. Result from varying the bump height

3.3 Effect of the bar thickness

Result from varying the bar thickness by $\pm 0.1\text{mm}$ showed slope 0.064 N/mm for insertion force and slope 0.106 N/mm for removal force.

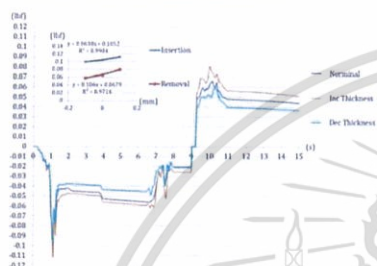


Fig.10. Result from varying the bump height

In summary, the bump height provided highest sensitivity to both of insertion and removal force.

4. Discussion

From the validation results, the graph in Figure 6 shows behavior of insertion and removal force which the force starts from zero and ramps down to negative zone then ramps up across x-axis to positive zone. That graph showed cycle of the shipping comb force measurement, the insertion force is represented by negative force or pulling force from force gauge and the removal force is represented by positive force or pushing force from force gauge.



Fig.11. Tool for force measurement.

The insertion force is occurred when the latch contacts to the actuator arm and the value is increased to maximum when the bump is passed thru the edge of actuator. After that the a few value of force still maintain during the bump is moved on the bottom plane of actuator arm. Then the force will be dropped to zero when the shipping comb is completely inserted to actuator arm.

The removal force is occurred when the bump contacts to the chamfer of hole on actuator arm and shoot up very fast according to slope of removal side steeper than insertion side. Then the force is maintained a few value when the bump is moved on flat plane.

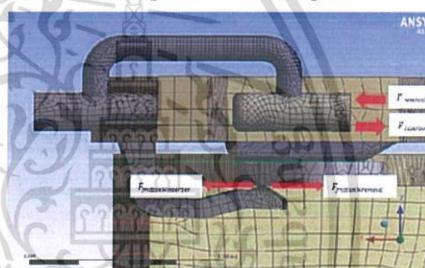


Fig.12. Direction of force.

From the parametric study, the bump height is major contributor to insertion and removal force, but if we focus on mold modification to get dimension per model, the bump height is quite difficult to modify to meet specification. Otherwise, the base width and the bar thickness are easy to modify to meet specification. Shipping comb designer has to review it carefully case by case to modify on which parameter. For example, if bump height of shipping comb first lot is lower than nominal design and force also lower than specification, the bump height can be selected to modify. The Electrical discharge machining (EDM) is method to modify surface of bump on core insert because of the surface of bump is complex then the modification cost is very high [9]. For another case, the bump height of shipping comb first lot is equal to nominal

design, the base width or bar thickness should be selected to modify instead of bump height. The process to modify dimension of bar thickness is easy because the EDM process can be applied on the surface of bottom plan of latch which is very simple. Benefits of this study are to reduce time to design and to develop the shipping comb to meet the requirement and save cost of the mold modification. The modification cost of bar thickness can be cheap to quarter of cost to modify the bump height.

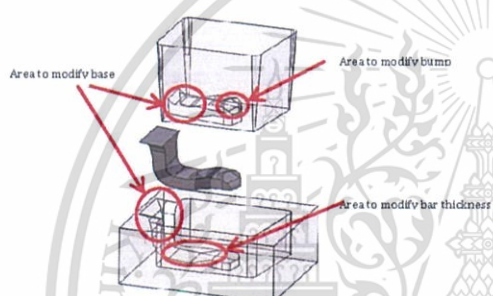


Fig.13. Mold insert of shipping comb latch

5. Concluding Remarks

- The sensitivity of the bump height is highest when compare with the base width and the bar thickness.
- The bump height is chosen to modify if dimension of the bump height from shipping comb first lot is lower than specification.
- The bar thickness is the good choice to adjust for both of insertion and removal force because cost of mold modification is lowest.

6. Reference

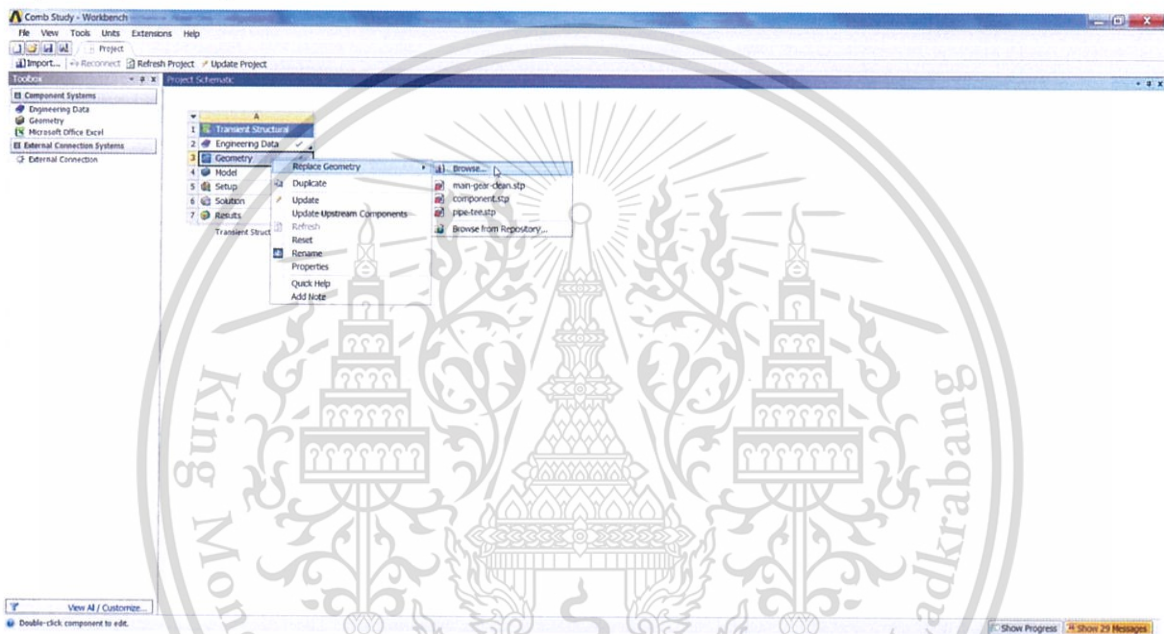
- [1] Thawisanee P.,Chalearmchai C.,Somsak S., Product Development Process Improvement by Using Finite Element Simulation, Master Thesis of Suranaree University of Technology, Thailand. 2011
- [2] Suriya S., Somsak S., FEA Simulation Study of Shipping Comb Removal and Insertion in HDD Manufacturing, Master Thesis of Suranaree University of Technology, Thailand. 2011
- [3] Oberoi H.S., Using actual production runs of components to teach implementation of statistical process control techniques, Frontiers in Education Conference, USA 1996.
- [4] CAD-IT, ANSYS Mechanical Linear and Nonlinear Dynamics, Training manual to ANSYS Release 15.0, Thailand. 2014
- [5] Steven B., Ernest P., Karl M., Brett C. A Comparison of All Hexagonal and All Tetrahedral Finite Element Meshes for Elastic and Elasto-plastic Analysis, Brigham Young University, Greg Sjaardama Sandia Nation Laboratories Albuquerque, NM, 2009
- [6] Nishihata N., New ESD control material based on special carbon, Electrical Overstress/Electrostatic Discharge Symposium, Japan 2001.
- [7] B.N.J. Persson, "Sliding Friction Physical Principles and Applications", Second Edition, NanoScience and Technology, 2000
- [8] Wu Y. Wang F., Ma cb., "Nonlinear Finite Element Buckling Analysis of Arm Stand of Dynamic Compaction Machinery", The 7th International Conference on Computer Science & Education (ICCSE), Australia 2012.
- [9] Beng S.L., Proactive Performance Optimization Model for EDM Operation, Industrial Information, IEEE International Conference, Singapore 2006.

APPENDIX B

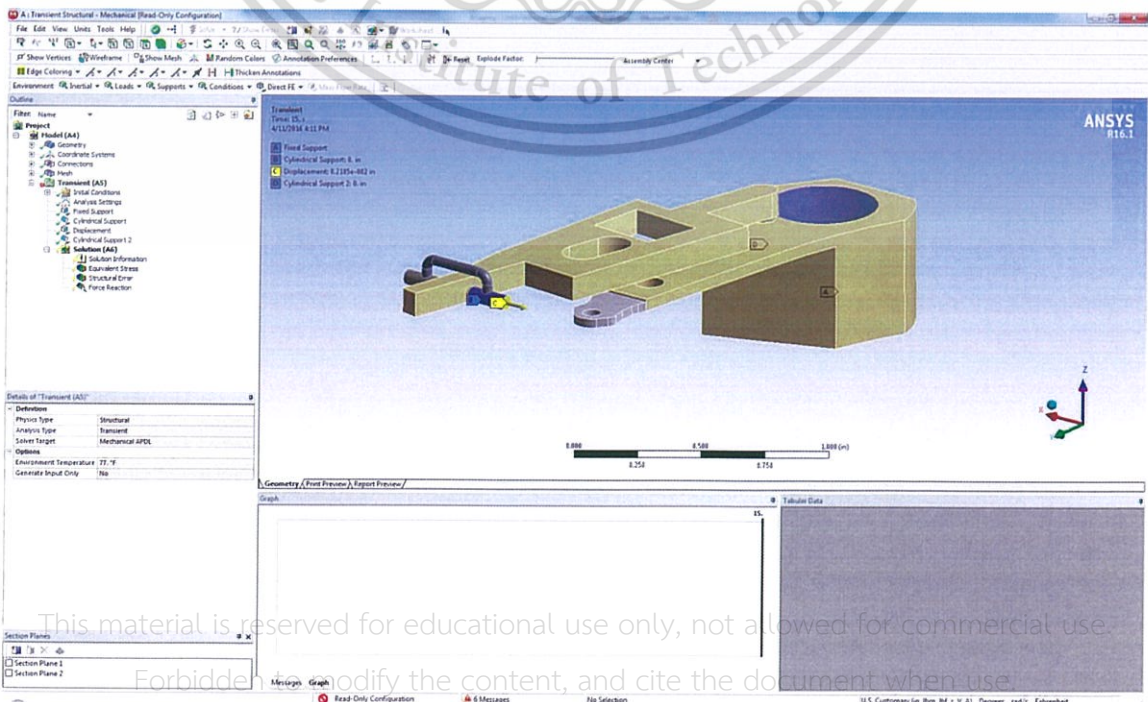
ANSYS Setting

Model Input

In workbench window, right clicks on geometry in project schematic, selects replace geometry and browse to new 3D model.



New model will appear geometry window in transient structural window.



This material is reserved for educational use only, not allowed for commercial use.

Forbidden to modify the content, and cite the document when use.

Material properties

Input material properties in engineering data tab on workbench window.

Aluminum SG

The screenshot displays the ANSYS Workbench Engineering Data environment. The central pane shows the 'Outline of Schematic A2: Engineering Data' with a table of material sources:

Row	Material	Source	Description
1	Contents of Engineering Data		
2	Material		
3	Aluminum SG	E:(Data)\W\...	
4	Polycarbonate SG	E:(Data)\W\...	
5	Structural Steel	General_Mate	Fatigue Data at zero mean stress comes from 1998 ASME BPV Code, Section 8, Div-2, Table S-110.1

The 'Properties of Outline Row 3: Aluminum SG' table is shown below:

Row	Property	Value	Unit
1			
2	Density	2724	kg m ⁻³
3	Isotropic Elasticity		
4	Derive from		
5	Young's Modulus	7.1001E+10	Pa
6	Poisson's Ratio	0.33	
7	Bulk Modulus	5.9609E+10	Pa
8	Shear Modulus	2.6692E+10	Pa
9	Field Variables		
10	Temperature	Yes	
11	Shear Angle	No	
12	Degradation Factor	No	
13	Bilinear Isotropic Hardening		
14	Yield Strength	2.75E+08	Pa
15	Tangent Modulus	9E+08	Pa

The 'Table of Properties Row 2: Density' shows a single data point:

Row	Temperature (C)	Density (kg m ⁻³)
1		2724
2		2724

The 'Chart of Properties Row 2: Density' displays a plot of Density (kg m⁻³) versus Temperature (C), showing a constant density of 2724 kg m⁻³ across the temperature range from -1 to 1.

Polycarbonate SG

Comb Study - Workbench

File View Tools Units Extensions Help

Project / A2:Engineering Data X

Filter Engineering Data Engineering Data Sources

Toolbox

- Physical Properties
 - Isotropic Secant Coefficient of Thermal Exp
 - Orthotropic Secant Coefficient of Thermal Exp
 - Isotropic Instantaneous Coefficient of Thermal Exp
 - Orthotropic Instantaneous Coefficient of Thermal Exp
 - Constant Damping Coefficient
 - Damping Factor (a)
 - Damping Factor (B)
- Linear Elastic
 - Orthotropic Elasticity
 - Anisotropic Elasticity
- Hyperelastic Experimental Data
 - Hyperelastic
 - Chaboche Test Data
- Plasticity
 - Multilinear Isotropic Hardening
 - Bilinear Kinematic Hardening
 - Multilinear Kinematic Hardening
 - Chaboche Kinematic Hardening
 - Anand Viscoplasticity
- Creep
- Life
- Strength
 - Tensile Yield Strength
 - Compressive Yield Strength
 - Tensile Ultimate Strength
 - Compressive Ultimate Strength
 - Orthotropic Stress Limits
 - Orthotropic Strain Limits
 - Tsai-Wu Constants
 - Puck Constants
 - LaRC3/04 Constants
- Gasket
- Viscoelastic Test Data
- Viscoelastic
- Shape Memory Alloy
- Damage
- Cohesive Zone
- Fracture Criteria

Outline of Schematic A2: Engineering Data

	A	B	C	D
1	Contents of Engineering Data			
2	Material	Source Description		
3	Aluminum SG			
4	Polycarbonate SG			
5	Structural Steel	Fatigue Data at zero mean stress comes from 1998 ASME BPV Code, Section 8, Div 2, Table S-110.1		
*	Click here to add a new material			

Table of Properties Row 14: Bilinear Isotropic Hardening

	A	B
1	Temperature (C)	Yield Strength (Pa)
2		5.9E+07
*		

Properties of Outline Row 4: Polycarbonate SG

	A	B	C	D	E
1	Property	Value	Unit		
2	Density	1190	kg m^-3		
3	Isotropic Elasticity				
4	Derive from	Young's Modulus and...			
5	Young's Modulus	2.413E+09	Pa		
6	Poisson's Ratio	0.3912			
7	Bulk Modulus	5.3745E+05	psi		
8	Shear Modulus	1.2609E+05	psi		
9	Field Variables				
10	Temperature	Yes			
11	Shear Angle	No			
12	Degradation Factor	No			
13	Bilinear Isotropic Hardening				
14	Yield Strength	5.9E+07	Pa		
15	Tangent Modulus	2.413E+08	Pa		

Chart of Properties Row 14: Bilinear Isotropic Hardening

Stress [Pa]

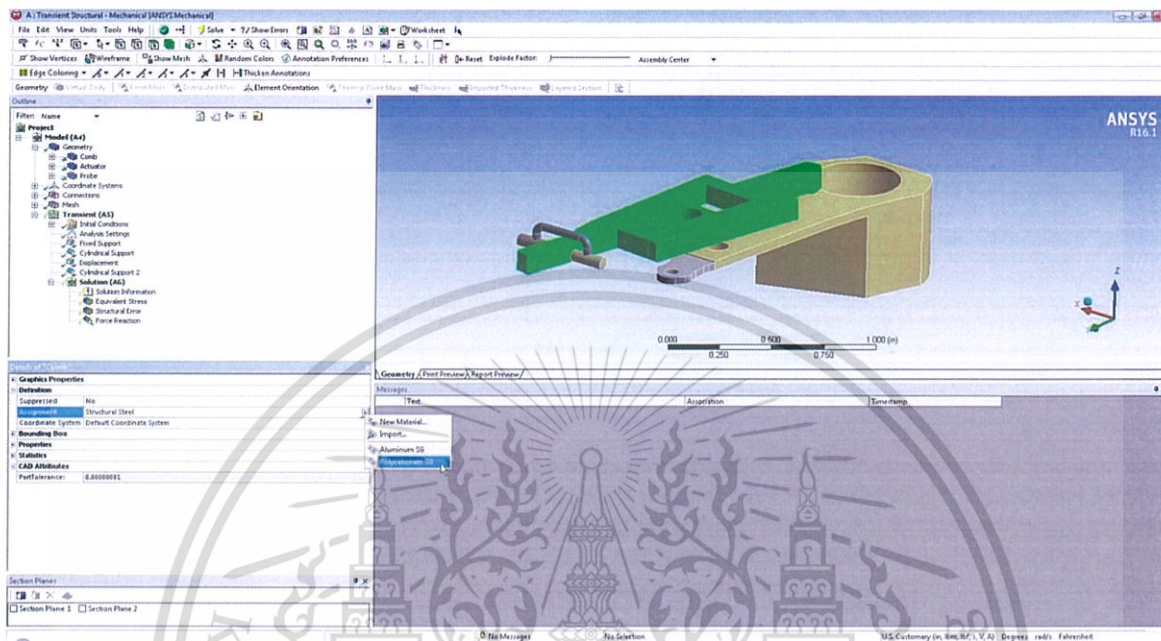
Strain [m m^-1]

Bilinear Isotropic Hardening

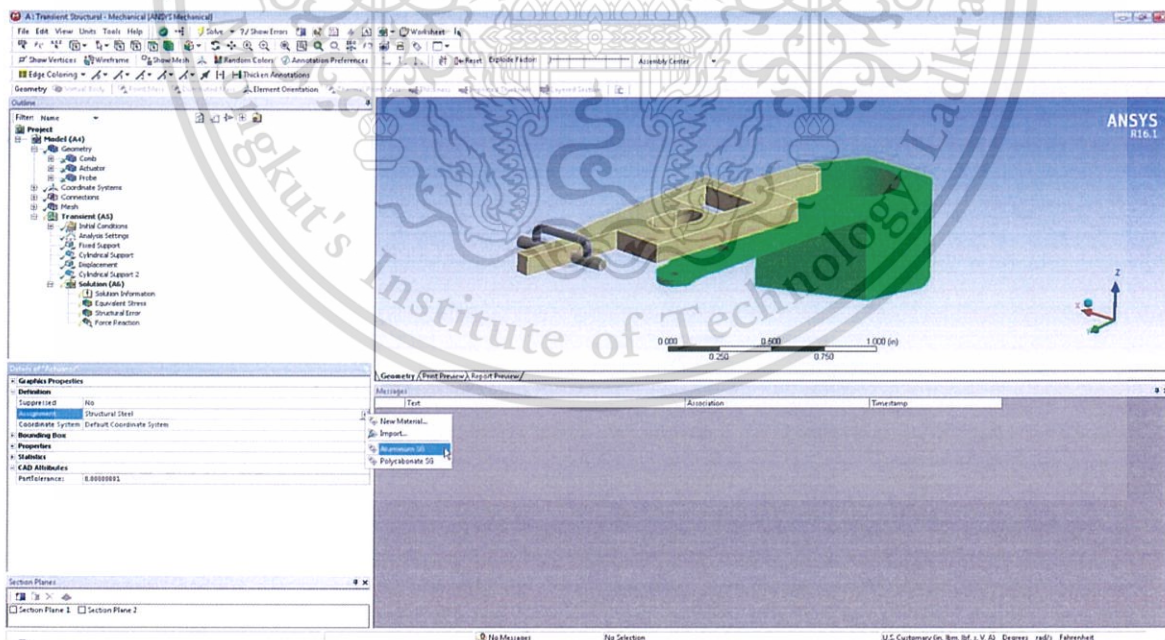
Ready

Show Progress Show 28 Messages

In transient structural window, assign the material name Polycarbonate SG to shipping comb..



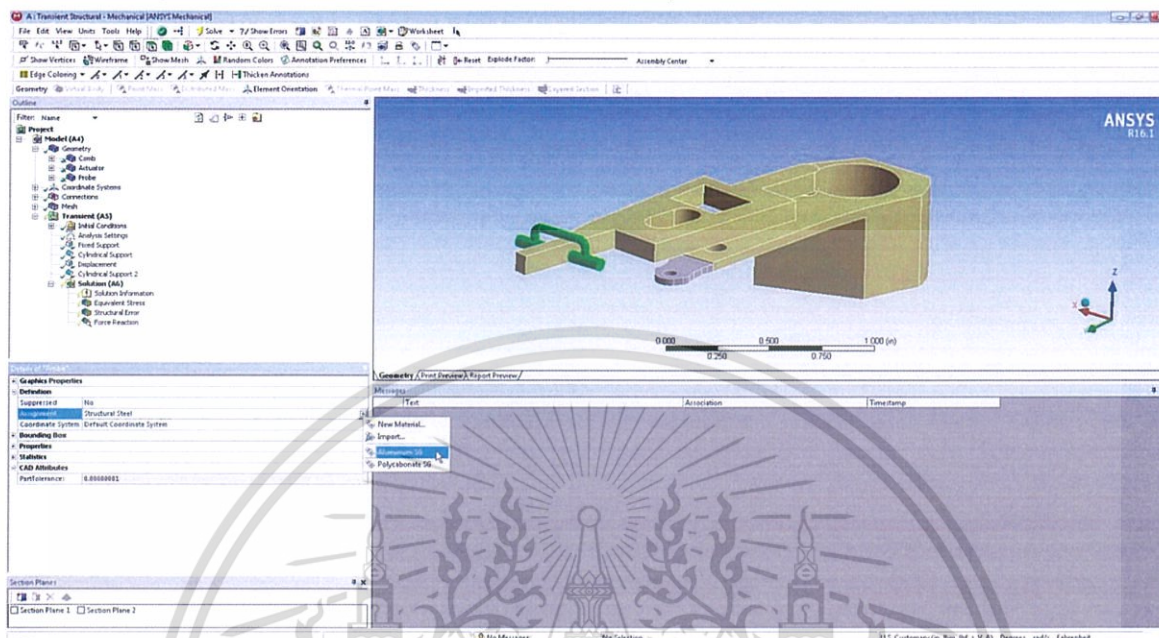
Assign the material name Aluminum SG to actuator..



This material is reserved for educational use only, not allowed for commercial use.

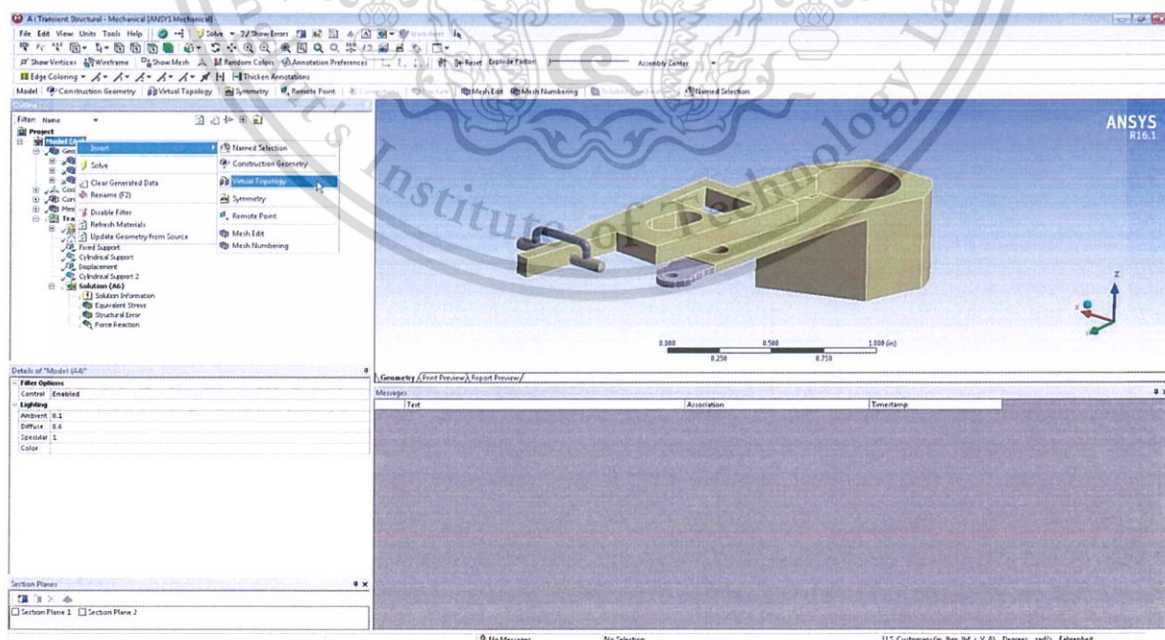
Forbidden to modify the content, and cite the document when use.

Assign the material name Aluminum SG to probe..



Virtual Topology (Optional)

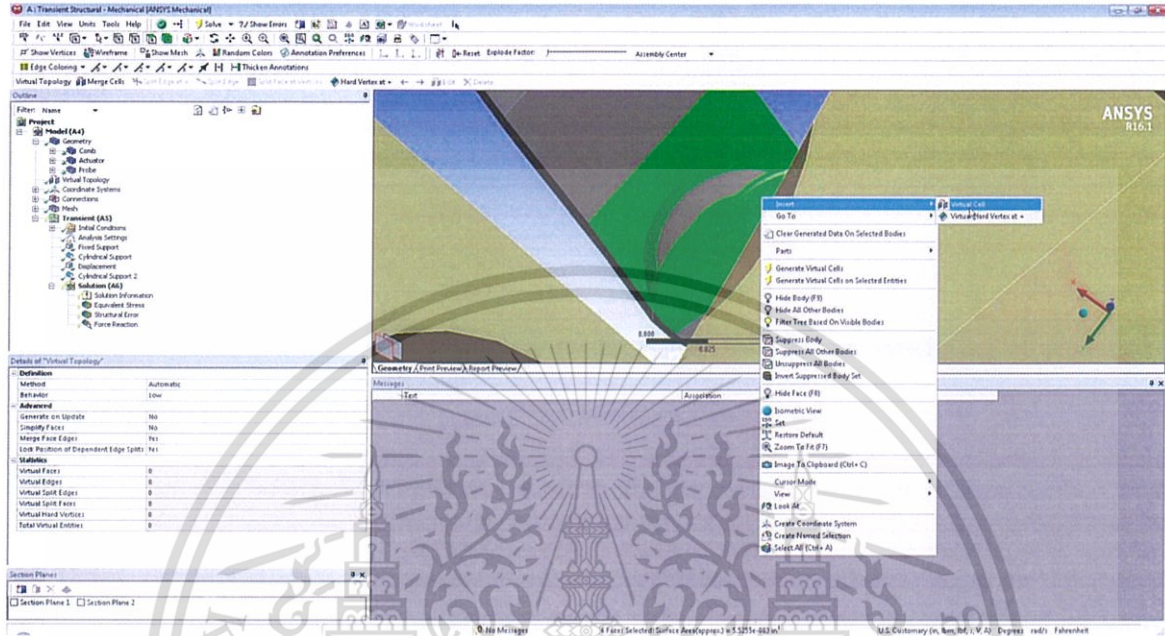
In case model do not simplify enough, the virtual topology should be applied on small surface or sharp feature.



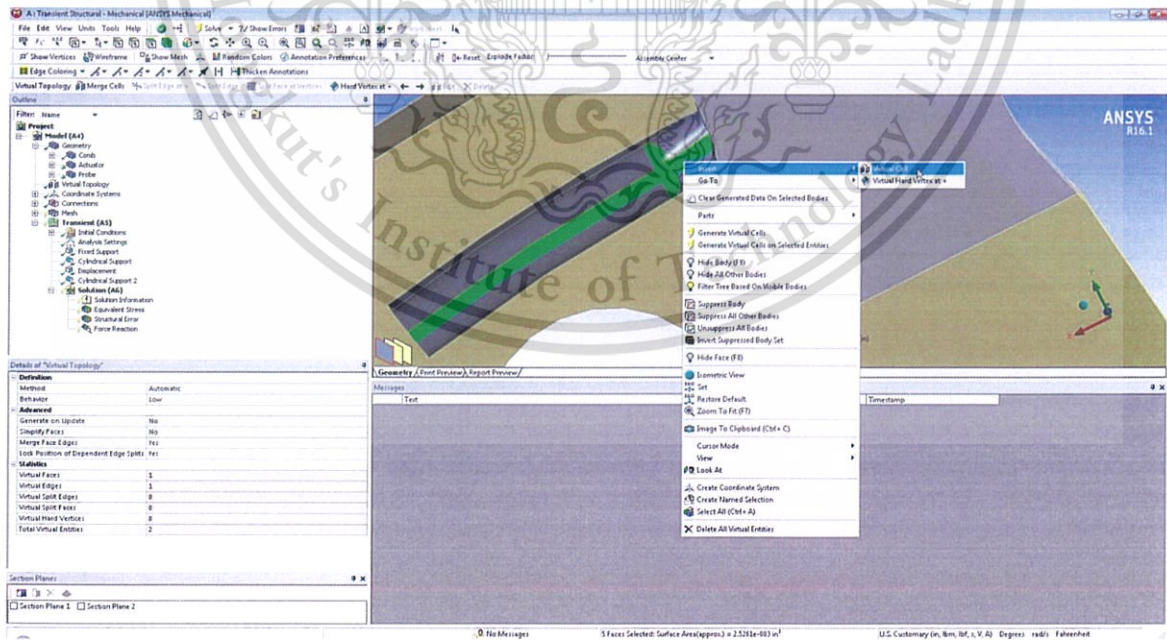
This material is reserved for educational use only, not allowed for commercial use.

Forbidden to modify the content, and cite the document when use.

Apply virtual cell on small surface of latch.



Apply virtual cell on small surface comb ramp.

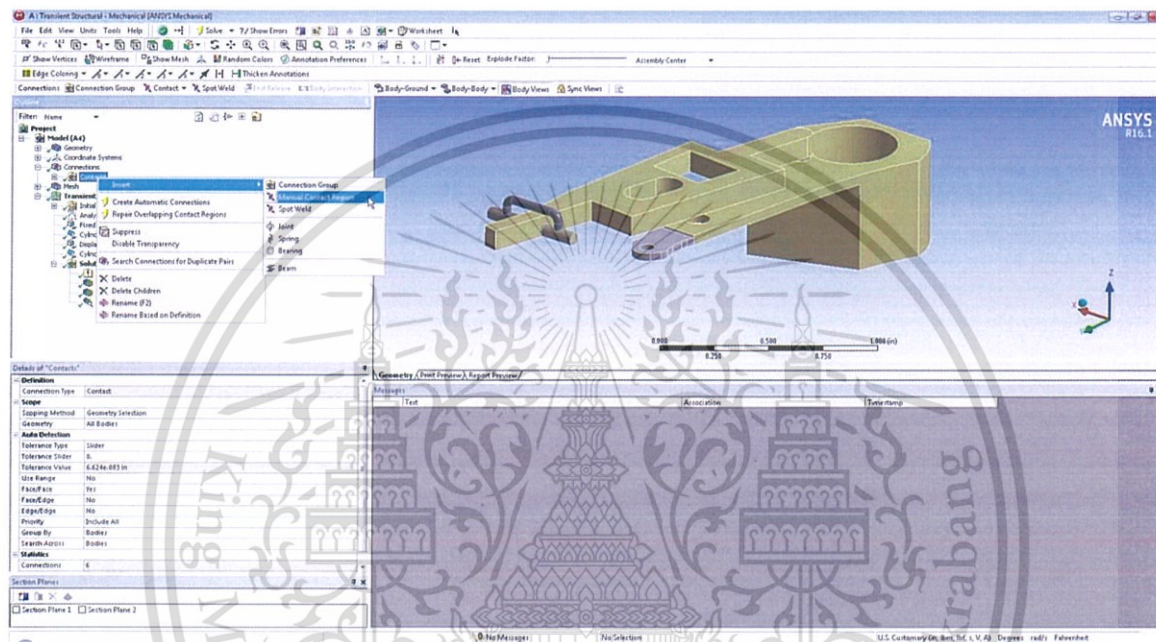


This material is reserved for educational use only, not allowed for commercial use.

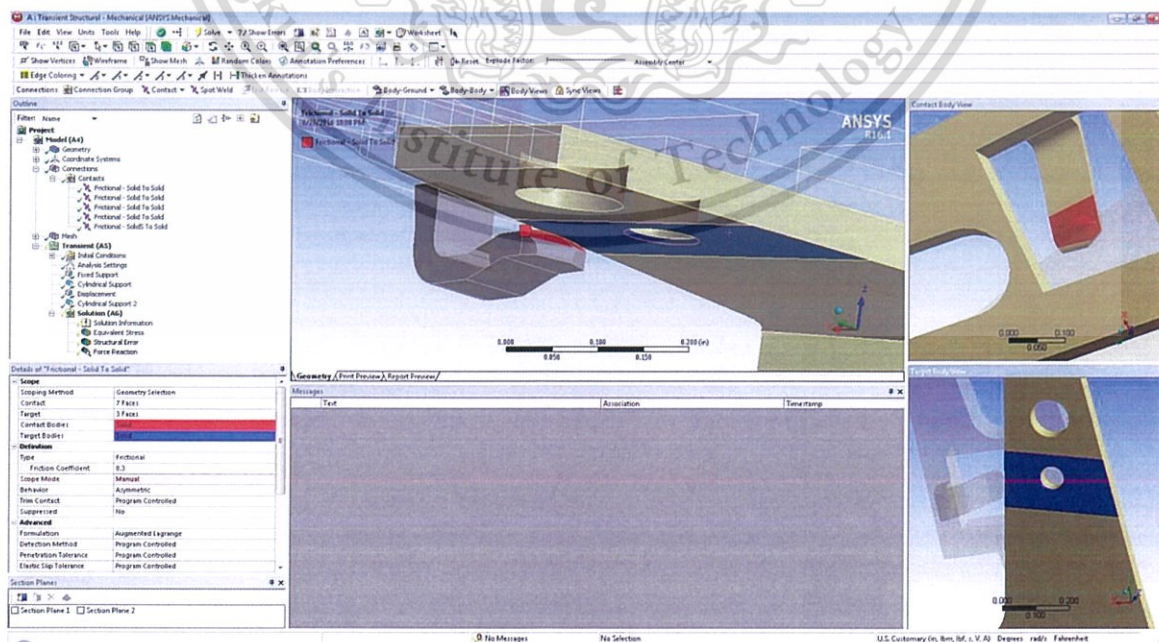
Forbidden to modify the content, and cite the document when use.

Contact

Under connection option, right click on connection then select manual contact region. Create contact for each pair of contact surface. Do not apply contact for two or more contact area. Apply contact type to be frictional and friction coefficient 0.3 for all contacts.



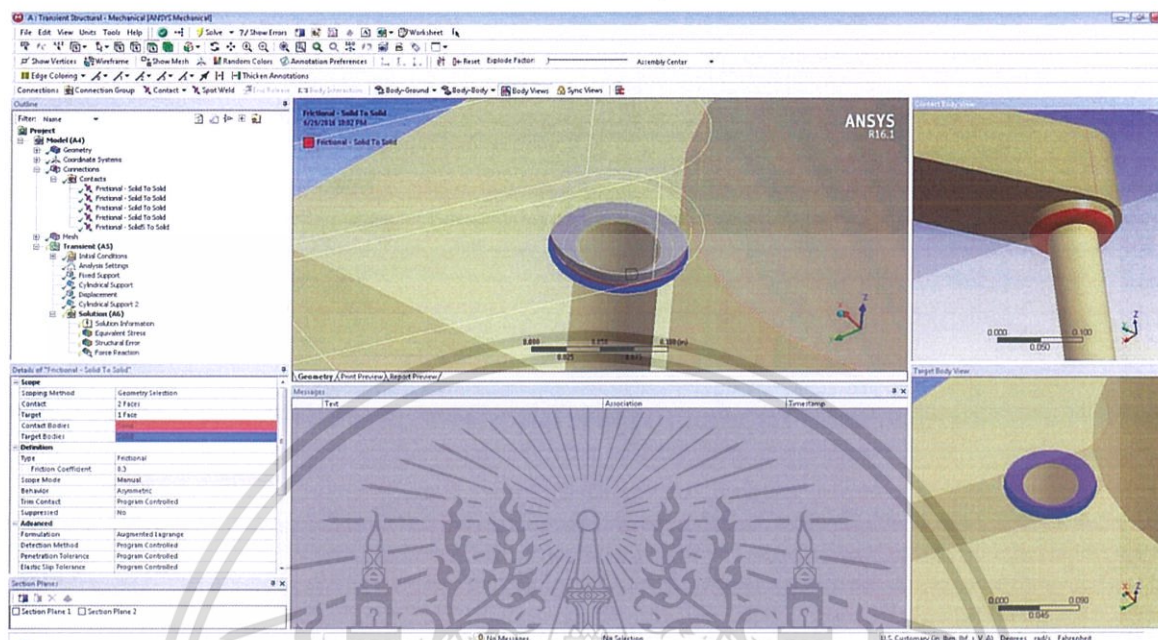
Contact for surface on latch and surface under actuator.



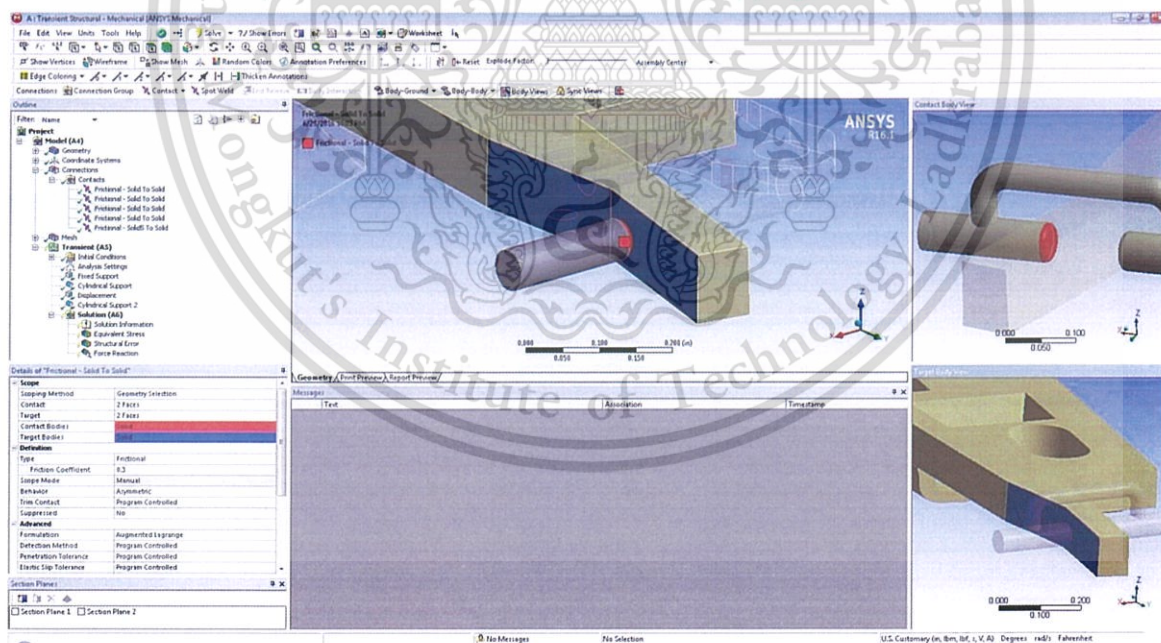
This material is reserved for educational use only, not allowed for commercial use.

Forbidden to modify the content, and cite the document when use.

Contact for surface of comb datum and top surface of actuator.



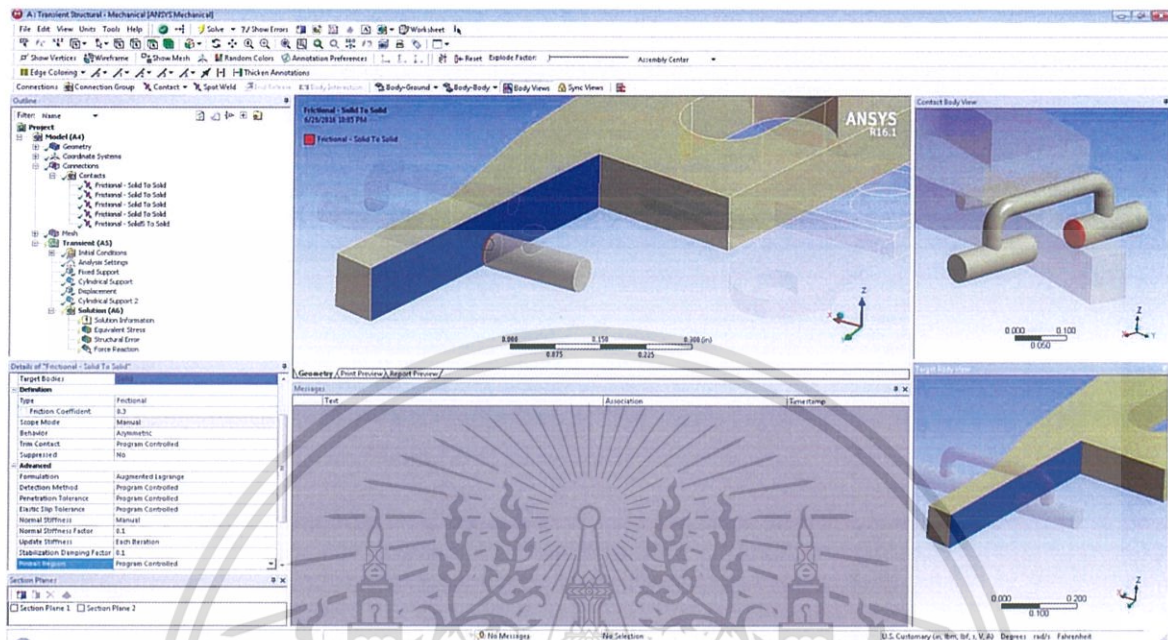
Contact for probe and comb when insert the shipping com



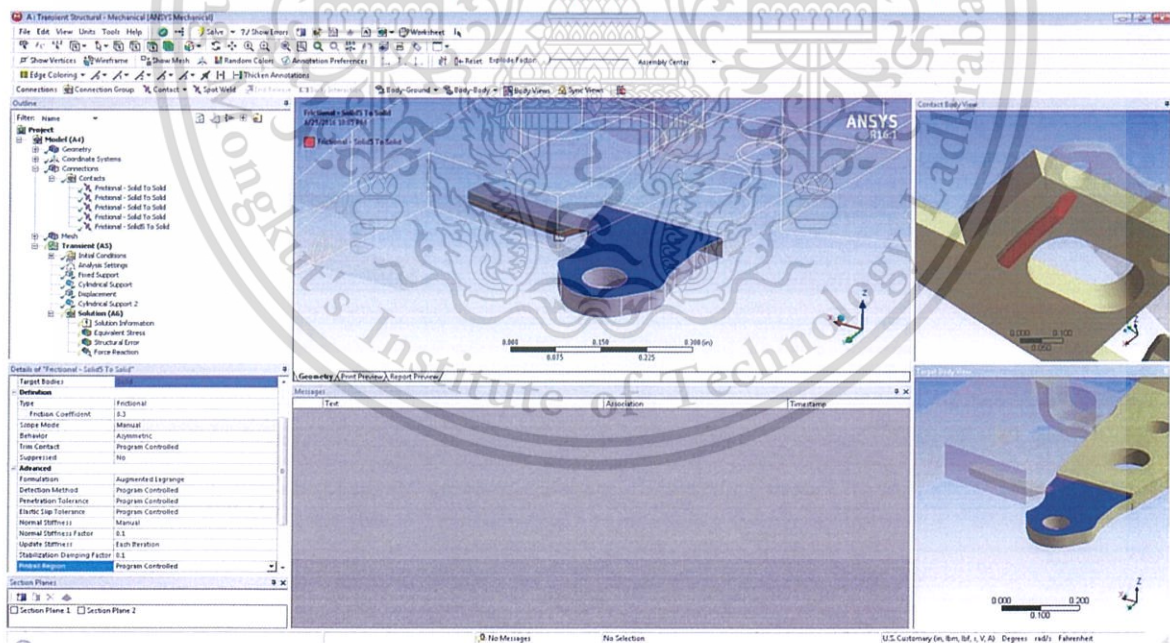
This material is reserved for educational use only, not allowed for commercial use.

Forbidden to modify the content, and cite the document when use.

Contact for probe and comb when remove the shipping com



Contact for surface of ramp on shipping comb and surface of tip on actuator.

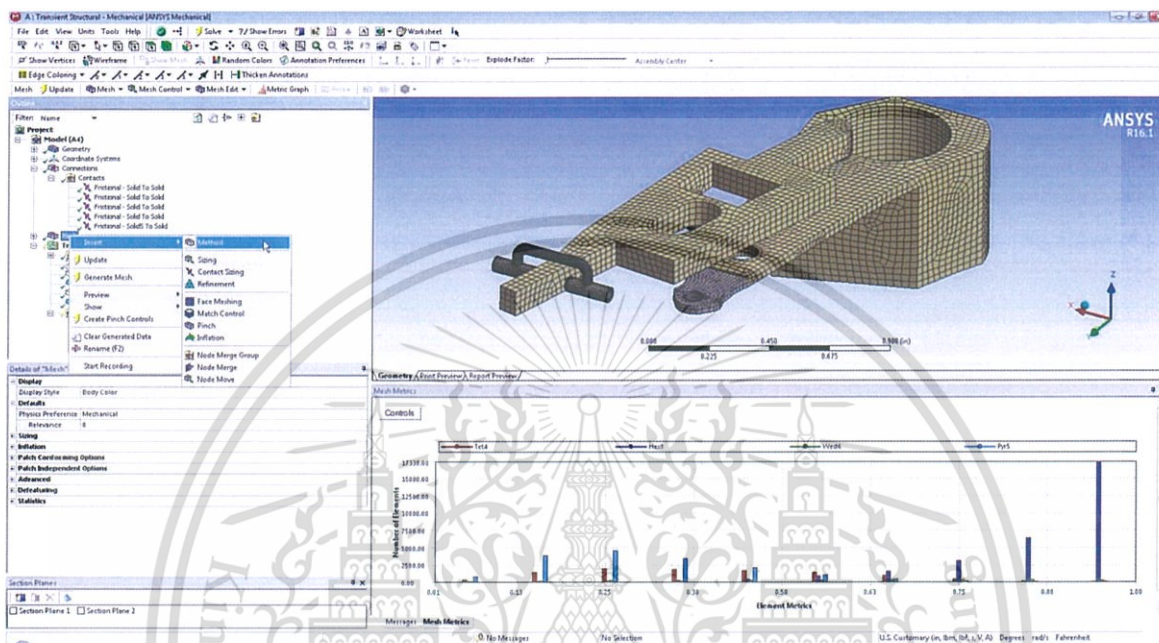


This material is reserved for educational use only, not allowed for commercial use.

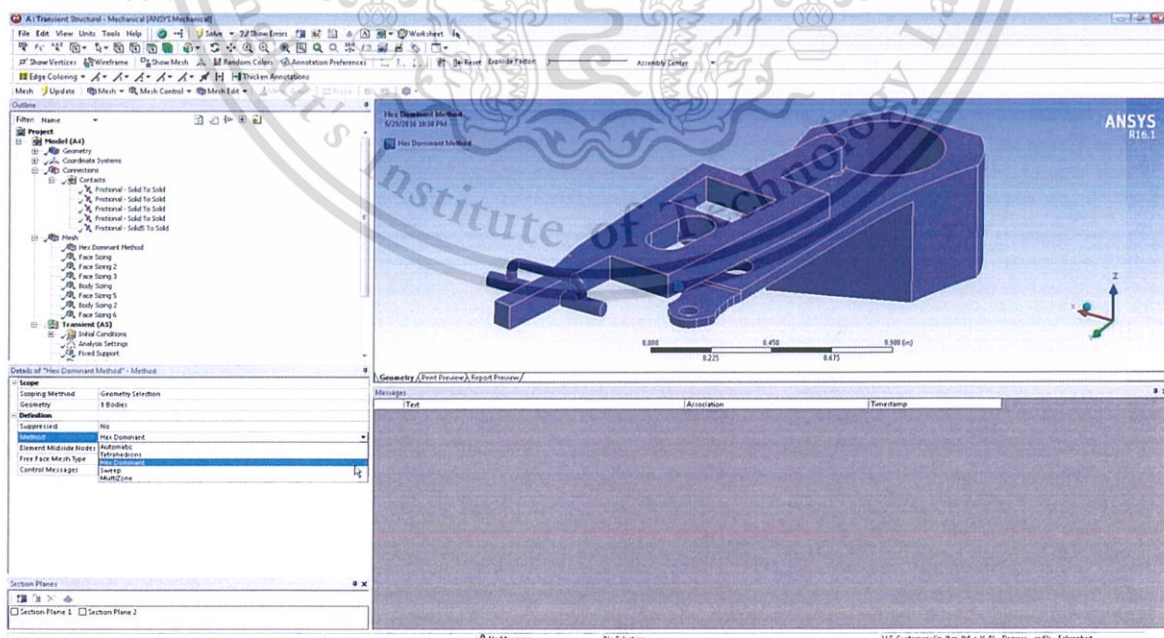
Forbidden to modify the content, and cite the document when use.

Meshing

Right click on option mesh select insert method.

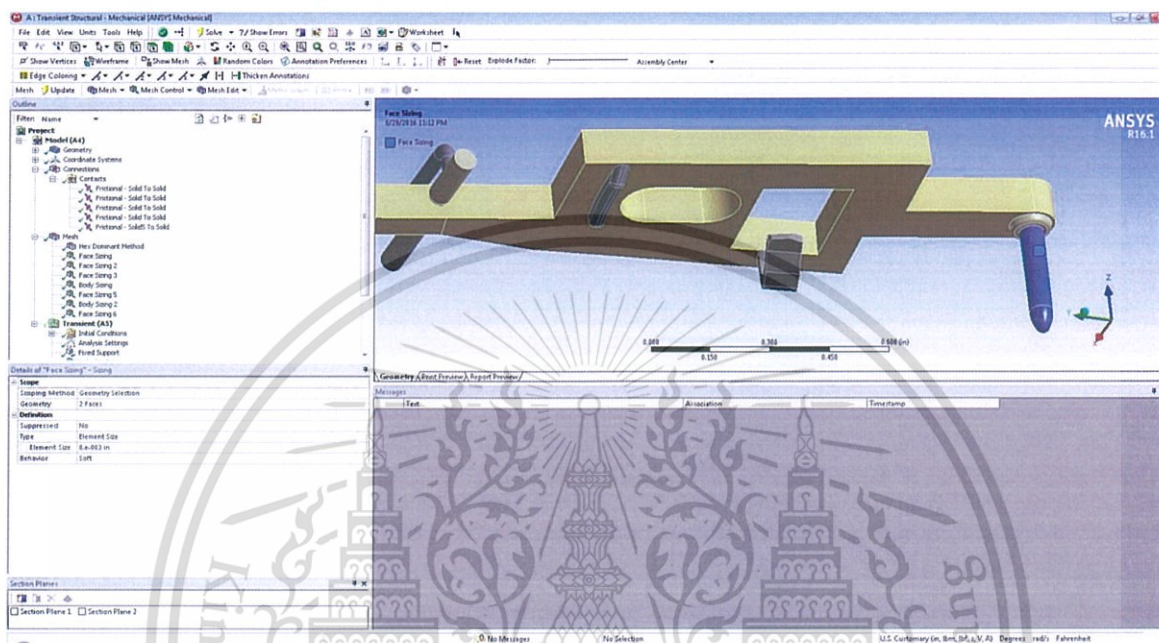


Apply hex dominant method for all body.

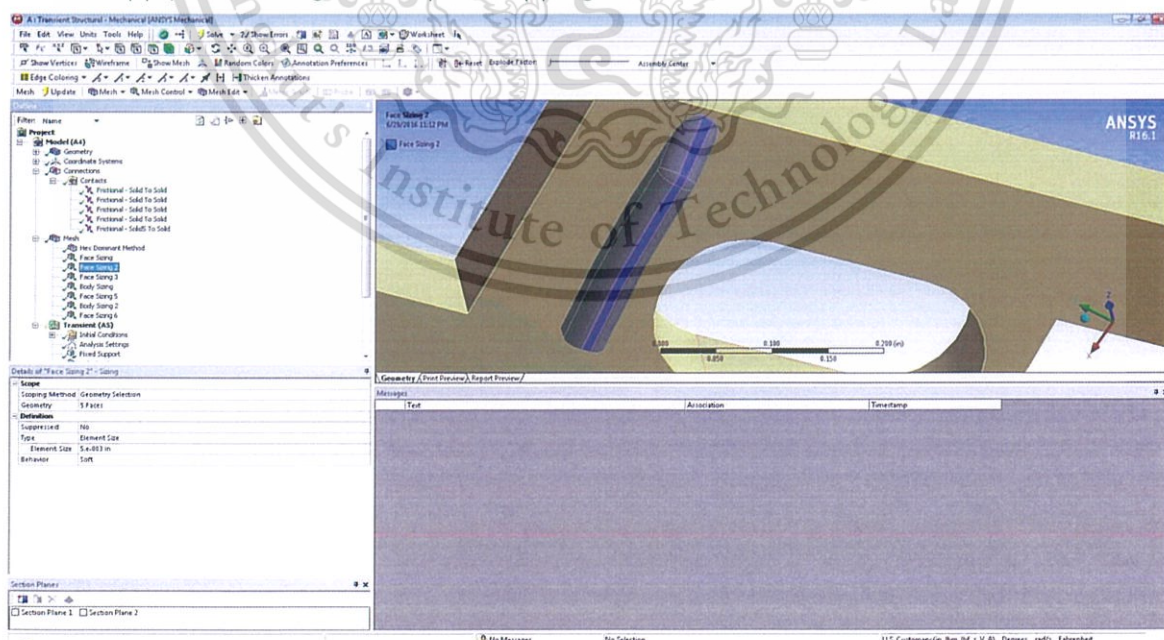


Apply mesh sizing for critical surface for example, contact face or small feature to control mesh size to small enough for program calculation.

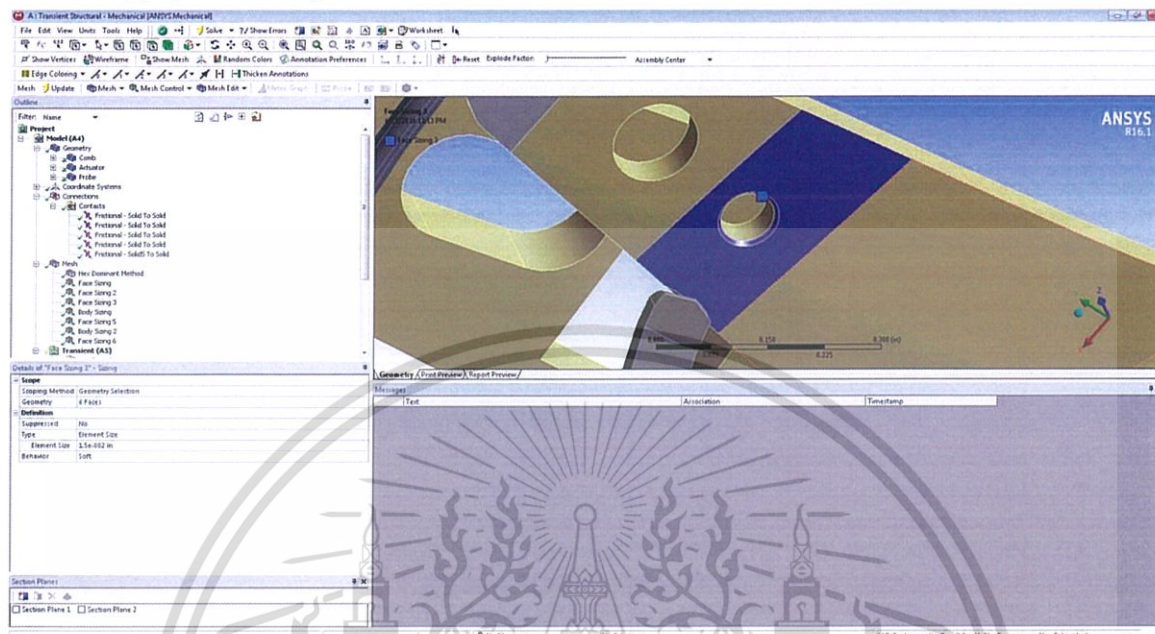
Apply face sizing of pivot pin



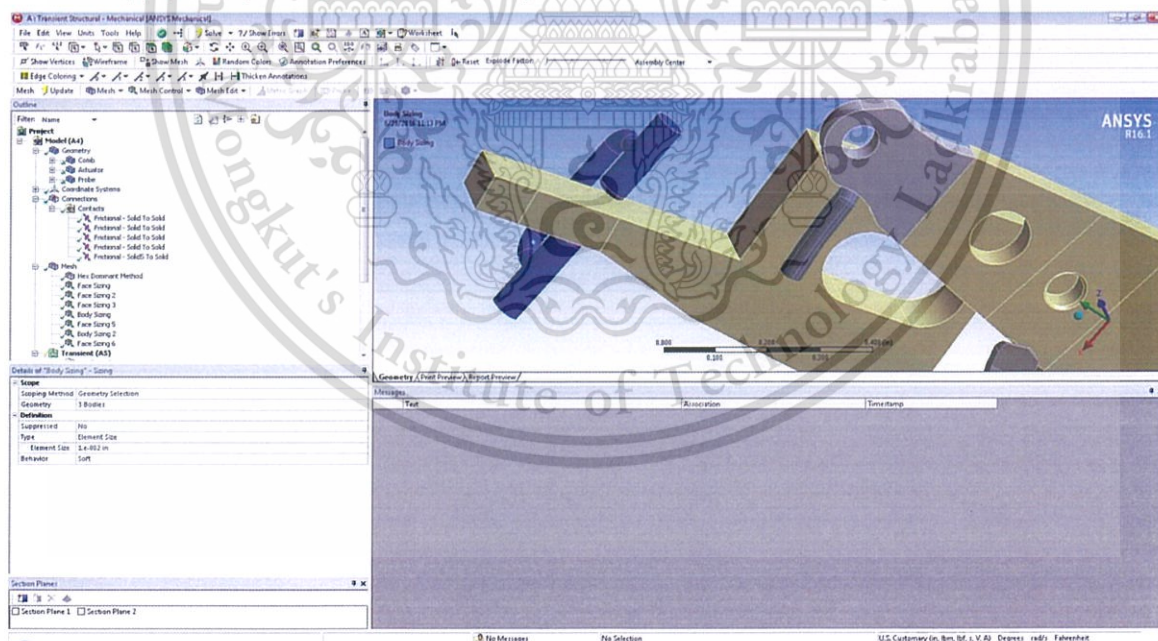
Apply face sizing on ramp of shipping comb



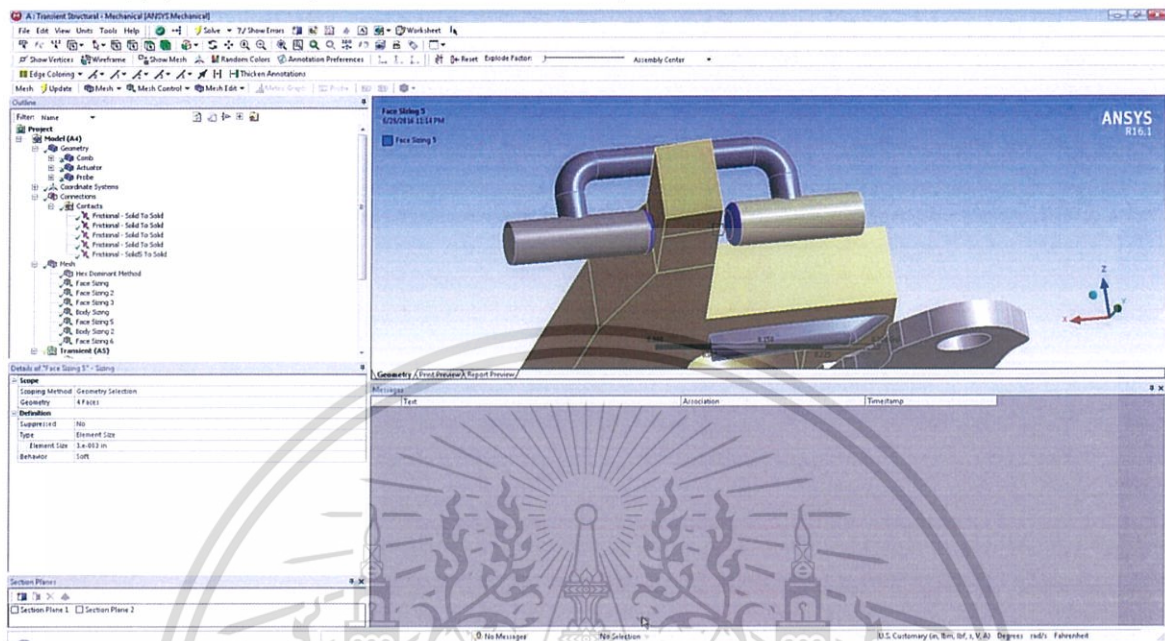
Apply face sizing of under surface of actuator.



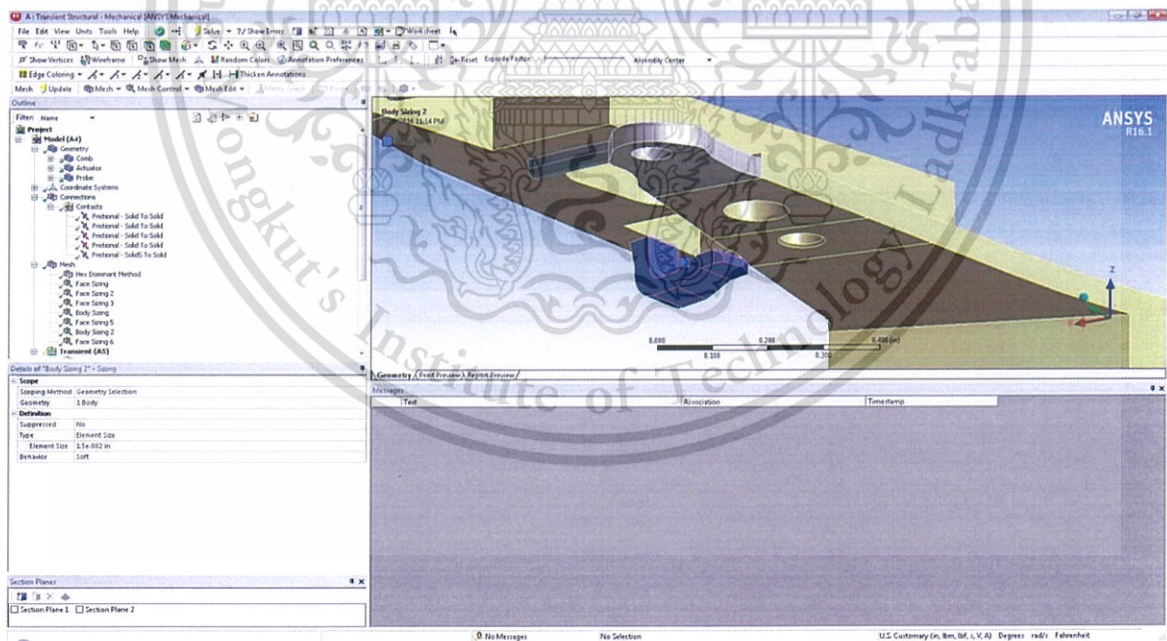
Apply body sizing for probe body.



Apply face sizing on contact surface of probe.



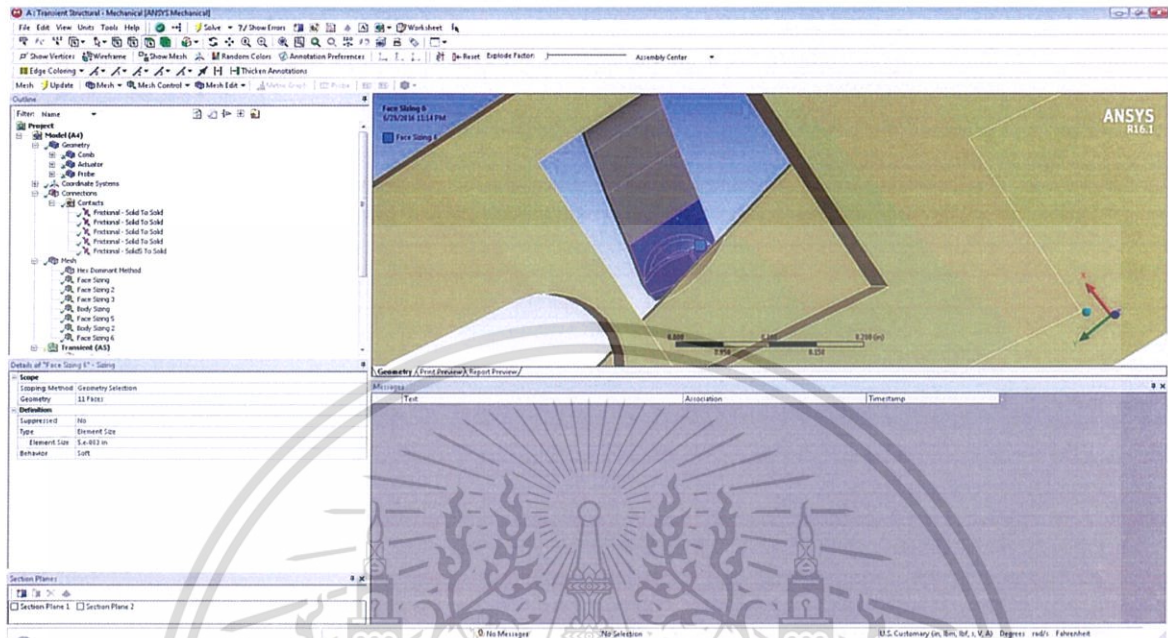
Apply face sizing for side surface and under surface of shipping comb latch.



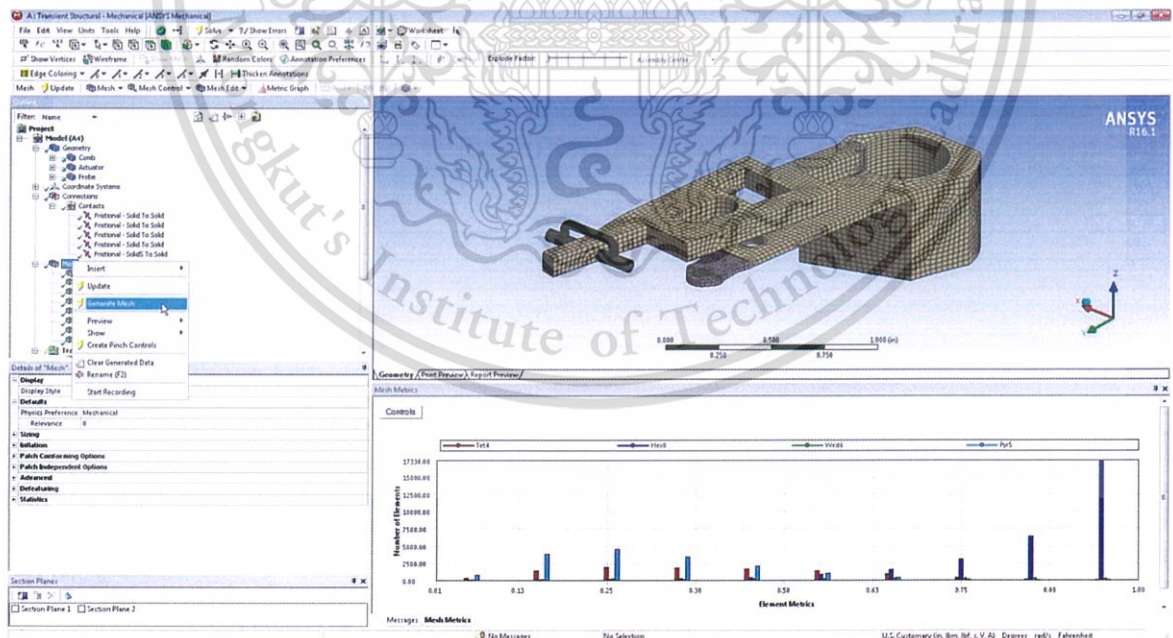
This material is reserved for educational use only, not allowed for commercial use.

Forbidden to modify the content, and cite the document when use.

Apply face sizing for top surface of shipping comb latch.



After apply all face and body sizing, right click on option mesh select generate mesh.

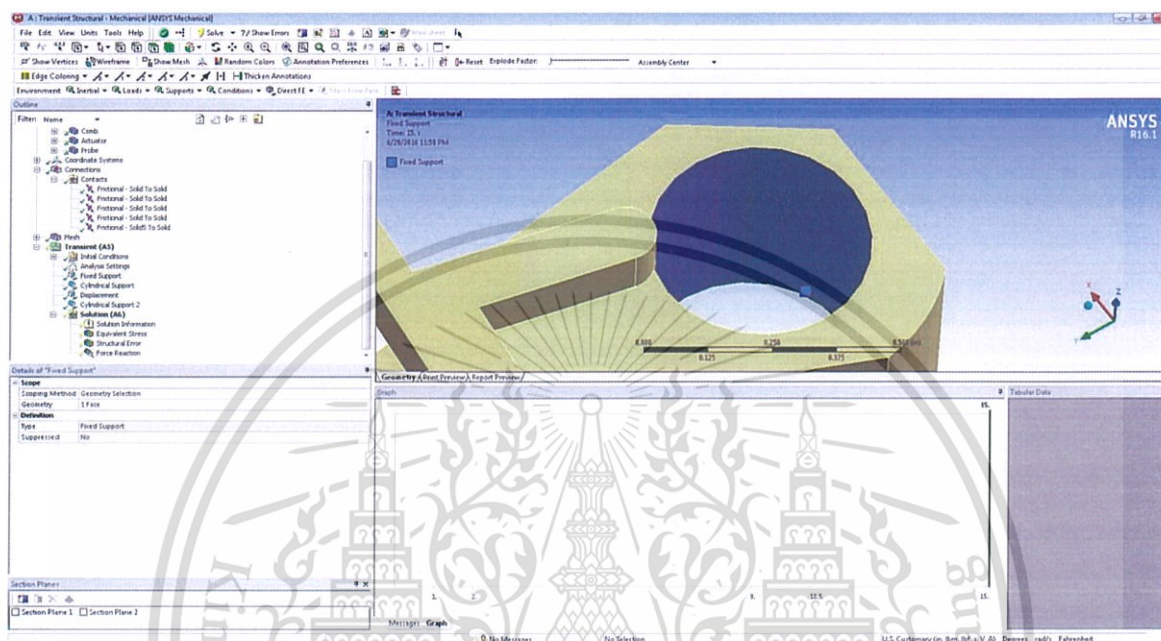


This material is reserved for educational use only, not allowed for commercial use.

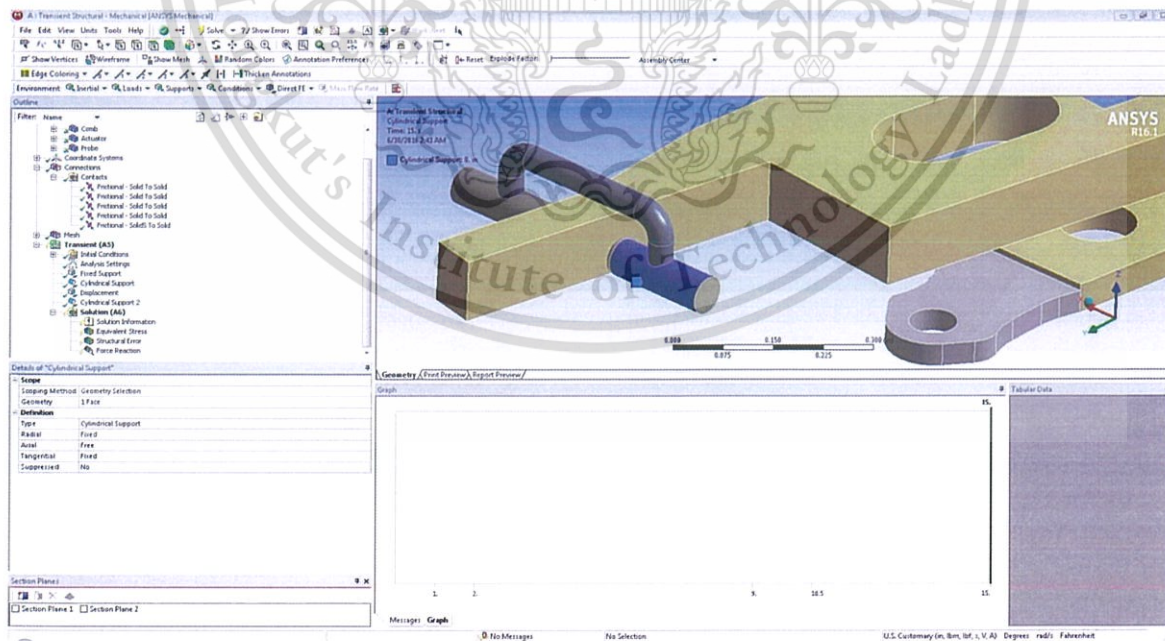
Forbidden to modify the content, and cite the document when use.

Boundary Condition

Right click on transient option then insert fixed support and assign to hole of actuator.



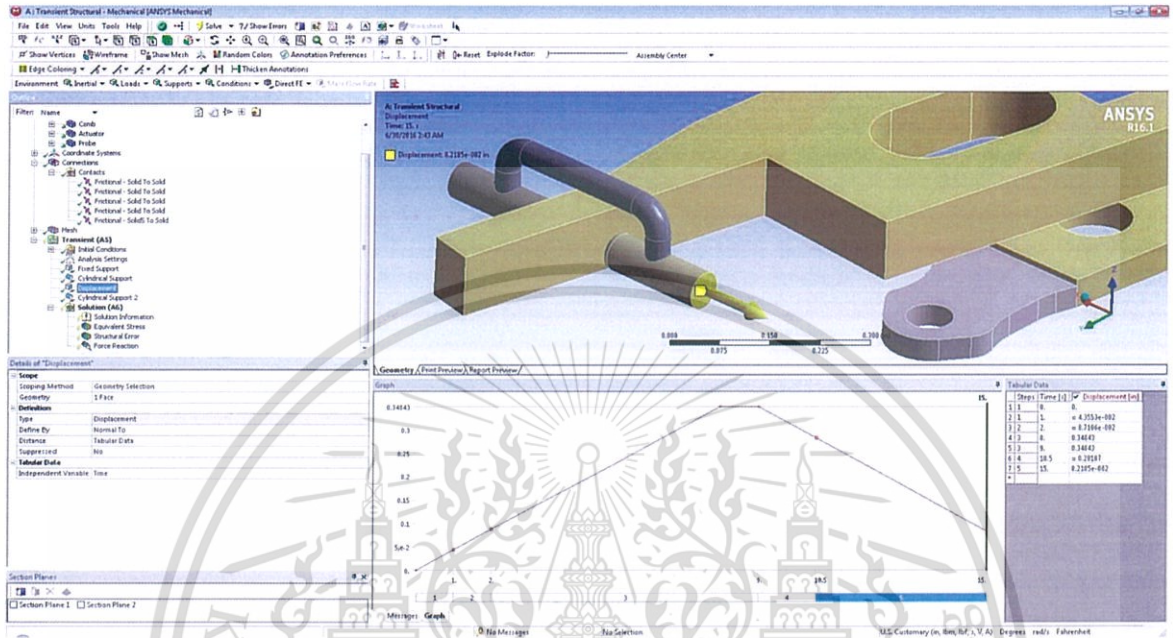
Apply cylindrical support to probe, allow moving in axial only.



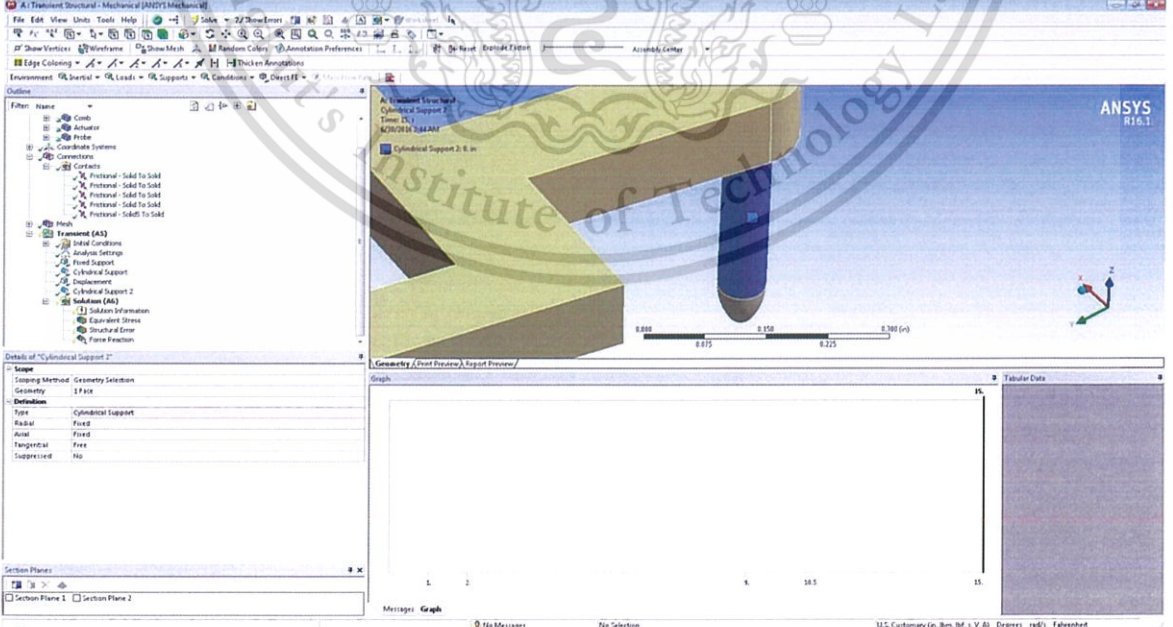
This material is reserved for educational use only, not allowed for commercial use.

Forbidden to modify the content, and cite the document when use.

Apply displacement on surface of probe end, input distance from 0 to 8.85mm and reward to 2.0875mm.

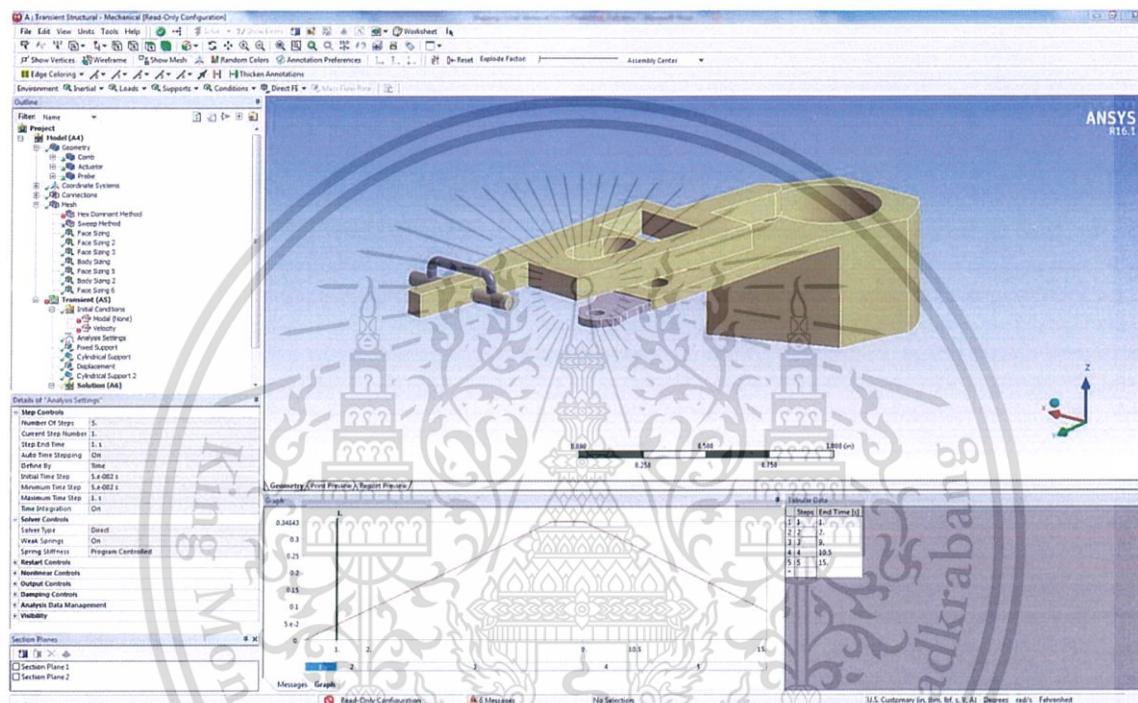


Apply cylindrical support to surface of pivot pin and allow movement in tangential only.



Step Control

In analysis setting, create 5 step of setting by step 1 is start from time 0 to 1 sec, step 2 start from time 1 sec to 2 sec, step 3 start from time 2sec to 9 sec, step 4 start from time 9 sec to 10.5 sec and step 5 start from time 10.5 sec to 15 sec.



Initial time step

Inputs the initial time step per below figure.

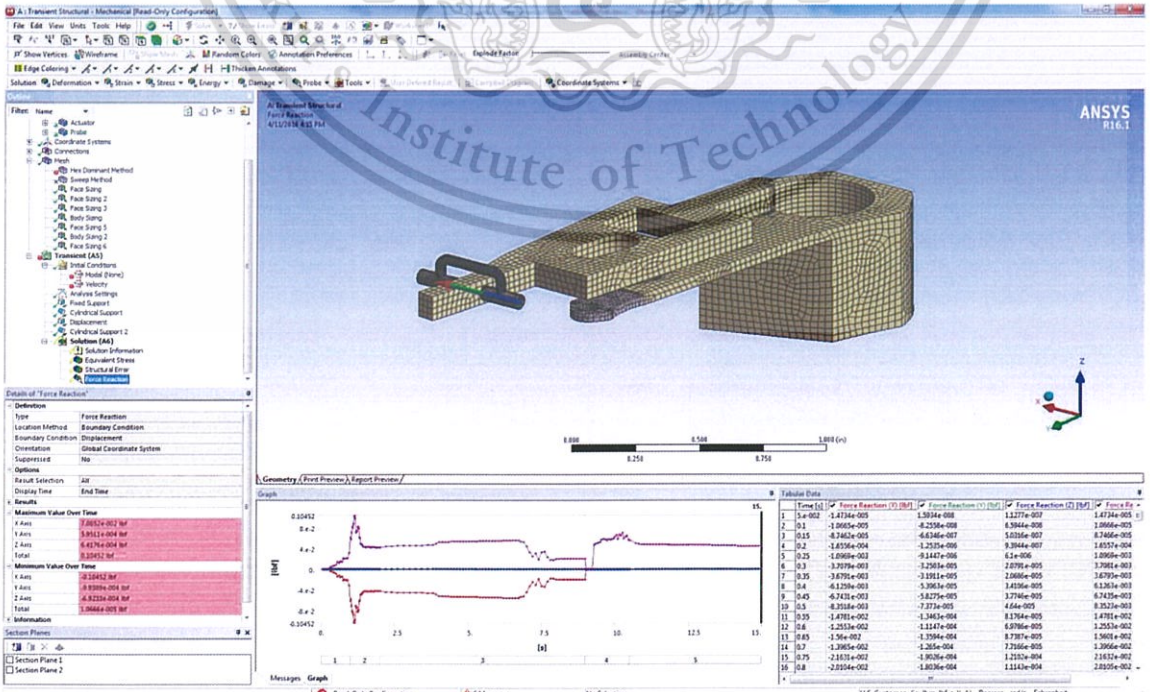
Step Controls					
Number of Steps	5.	5.	5.	5.	5.
Current Step Number	1.	2.	3.	4.	5.
Step End Time	1. s	2. s	9. s	10.5 s	15. s
Auto Time Stepping	On	On	On	On	On
Define By	Time	Time	Time	Time	Time
Initial Time Step	5.e-002 s	Off	Off	Off	Off
Minimum Time Step	5.e-002 s	2.e-002 s	0.1 s	5.e-002 s	0.2 s
Maximum Time Step	1. s	2.e-002 s	0.1 s	5.e-002 s	0.1 s
Time Integration	On	1. s	1. s	1. s	1. s
Solver Controls					
Solver Type	Direct				
Weak Springs	On	Direct	Direct	Direct	Direct
Spring Stiffness	Program Controlled	On	On	On	On
Restart Controls					
		Program Controlled	Program Controlled	Program Controlled	Program Controlled
Nonlinear Controls					
Output Controls					
Damping Controls					
Analysis Data Management					
Visibility					
	ment	ment	ment	ment	ment

Numerical damping (γ)

Details of "Analysis Settings"	
Initial Time Step	0.2 s
Minimum Time Step	0.1 s
Maximum Time Step	1. s
Time Integration	On
Solver Controls	
Solver Type	Direct
Weak Springs	On
Spring Stiffness	Program Controlled
Large Deflection	Off
Restart Controls	
Nonlinear Controls	
Output Controls	
Damping Controls	
Stiffness Coefficient Define By	Direct Input
<input type="checkbox"/> Stiffness Coefficient	0.
<input type="checkbox"/> Mass Coefficient	0.
Numerical Damping	Manual
Numerical Damping Value	0.1
Analysis Data Management	
Visibility	

Result

To collect the result of insertion and removal force, the reaction force is select to show the result from solution.



This material is reserved for educational use only, not allowed for commercial use.

Forbidden to modify the content, and cite the document when use.

AUTHOR BIOGRAPHY

Name-Surname: Mr. Wiriya Yupensuk

Date of Birth: October 06th, 1981

Present Address: 33/58, Moo 15, Tambol Sungnoen, Amphur Sungnoen, Nakornratchasima, Thailand 30170

Education: 2001-2004: Bachelor degree in Mechatronics Engineering, King Mongkut's institute of technology Ladkrabang.

Scholarships: 2011-2012 Scholarship for study in Master of Engineering in Data Storage Technology (English program) by NSTDA, KMITL and Seagate Technology (Thailand) Ltd.

Publications: Wiriya Y., Monsak P. and Chalothorn T. "Parametric Study of Shipping Comb Insertion and Removal Force", The 2nd International Conference on Engineering Science and Innovative Technology (ESIT 2016), Phuket, Thailand, April 21 – 23 2016.

Experience:

2006-Present Seagate Technology (Thailand) Ltd.

- Tooling Development and Replication, Tooling Design Engineer